The application of Radon-222 in constraining zones of recent groundwater recharge in the Table Mountain Group aquifer in the City of Cape Town and its surrounding areas.

By Yaa Agyare-Dwomoh

Thesis presented in fulfilment of the requirements for

the degree MSc. Geology in the Department of

Earth Science at Stellenbosch University

Supervisor: Prof J Miller

March 2020

DECLARATION

I, Yaa Agyare-Dwomoh, hereby declare that the work contained in this thesis is my own original work and that I have not previously in its entirety or in part submitted it at any other university for a degree, and that all the sources I have used or quoted have been indicated and acknowledge by complete references.

Yaa Agyare-Dwomoh,

Date: March 2020

ACKNOWLEDGEMENTS

I would like to express my deepest gratitude to the following people for their contribution to this project. Firstly, I would like to thank Prof Jodie A Miller for her continued patience, supervision, support and guidance throughout my MSc. A special thanks to the National Research Foundation (NRF), the iPhakade Earth Stewardship Science and the Water Research Commission (WRC) of South Africa for the bursary and financial project support over these two years. A special thank you to Mr Ryno Botha for your undivided support, supervision and for continuously teaching me new things. I have learnt a lot from you, and I appreciate how you continue to educate and facilitate the understanding of radon in South Africa. To the team at the University of Lausanne - Prof Torsten Vennemann, Laetitia Monbaron, Gabriel Cotte, Zoneibe Luz and Anaël Lehmann - thank you for welcoming and taking care of me during my time there. I appreciate all your assistance in the laboratories and during the data compilation. To all the farmers, municipalities and people at Cape Nature, thank you for giving access to all the borehole and springs I needed to complete this project. A special thank you to Mr Johan Schoeman who helped me in on numerous occasions in getting access to the Stellenbosch boreholes. To Helena Costaras, thank you for helping me in the field and in my times of need. A special thank you my fellow MSc student Zita Harilall, for her continuous support and assistance during these two years. Finally, I would like to thank my parents for giving me the opportunity to persevere in my studies, and for their perpetual support throughout my entire university career.

ABSTRACT

The world's population is expected to increase by 2.14 billion people by the year 2050, and therefore finding sustainable water resources to satisfy humanity's water demand has become one of the most urgent challenges of the 21st century. Due to population growth, poor water management practices and climate change, water scarcity has become a critical issue in arid regions like South Africa. Drought conditions affected the available water resources in the Western Cape during 2015-2018, and groundwater was considered as a sustainable water resource to mitigate recurrent water stresses. The Table Mountain Group (TMG) aquifer that surrounds the City of Cape Town is considered an excellent target for large scale abstraction to supplement the municipal supply. Although the high quality of the water (judged on the basis of very low TDS) makes this aquifer suitable for domestic abstraction purposes, for long term sustainability of abstraction still needs to be evaluated. ^{222}Rn is an inert radioactive noble gas with a half-life of 3.82 days. This isotope is present in very low concentrations in precipitation but much higher concentrations in groundwater. Therefore, changes in the radon activity concentrations in groundwater might reflect dilution due to rapid recharge. Thus radon has the potential to be a means of evaluating groundwater sustainability where sustainable groundwater is defined as groundwater that is regularly recharged by modern precipitation.

Analysis of ^{222}Rn as undertaken in groundwater from different aquifer systems that surround the City of Cape Town in order to understand the groundwater recharge dynamics of each system. The groundwater systems examined were the Table Mountain Group aquifer, the Malmesbury Group aquifer, the Cape Granite Suite aquifer, the Bokkeveld Group aquifer, the Witteberg Group aquifer and the Quarternary sediments aquifer. As the groundwater was not further differentiated into specific formations or rock units within each of these stratigraphic units, they are referred to as aquifer

systems. The hydrochemistry including stable isotopes of each groundwater sample was used to assign each groundwater sample to a host aquifer system. These host aquifer groupings were then used to characterise radon activity concentrations in each aquifer. Radon activity concentrations were variable in each aquifer system and these significant ranges meant that each aquifer system did not have a distinct radon activity concentration character. The two exceptions to this were: (1) the TMG aquifer where the lack of U and Ra in the aquifer host rocks, meant that the activity concentration of radon was lower in this aquifer than the other aquifers; and (2) the Cape Granite Suite aquifer system, where the high concentrations of U and Ra in the host rocks resulted in higher radon activity concentrations in groundwater hosted by these rocks. The radon activity concentration in groundwater in different locations changed as a consequence of groundwater recharge. As rainwater contains negligible radon activities, a dilution effect was noted in response to groundwater recharge in some of the aquifer systems. Three radon activity concentration trends were noted: (1) an immediate dilution in the radon activity concentration was recorded due to direct recharge; (2) a delayed dilution in the radon activity concentration was recorded due to a lag time in the recharge; and (3) radon activity concentrations were stable indicating little or no recharge response within a period of ~ 20-25 days after the recharge event (precipitation event). The radon data was compared with radiocarbon data (collected as part of a separate parallel study) for the same sample locations. The ^{14}C data was consistent with the three radon activity concentration trends above being associated with groundwaters of different ages. The groundwater samples with the stable radon activity concentrations were associated with lower ^{14}C activities, implying older residence times and hence a disconnection from modern recharge.

In utilising the groundwater radon activity concentrations, sites of rapid groundwater recharge were delineated and mixing behaviour between surface water and groundwater was evaluated. This contributed to a better understanding of the groundwater recharge dynamics and allowed assessment of which aquifer systems were more sustainable. Groundwater from the TMG aquifer system has low radon activity concentrations. After precipitation events, these values dropped rapidly implying a direct recharge response. ^{14}C data for the same groundwater samples, indicates the groundwater is typically young (± ≥ 100 pMC) and thus its sustainability is directly linked to current precipitation patterns. Hence, during periods of little or no rain, the aquifer is vulnerable to overexploitation and should be closely monitored and used sparingly. The results presented here introduce new perspectives in the application of groundwater isotopic tracers to understanding the TMG aquifer system and how it is recharged.

Contents

LIST OF FIGURES

LIST OF TABLES

CHAPTER 1: INTRODUCTION

1.1. GENERAL INTRODUCTION

In the last few centuries, the global demand for water has increased 35-fold and continues to grow (Jones, 1999; Kundzewicz and Döll, 2009). Throughout the evolution of human development, water has been a plentiful resource in most areas aiding in population growth, industrialization and energy development. However the situation is now changing to the point where, particularly in the more arid regions of the world, water scarcity has become the single greatest threat to food security, human health and natural ecosystems (Jones, 1999; Seckler et al., 1999). With the world population estimated to increase by an additional 2.14 billion people by the year 2050 (United Nations, 2018), finding new ways to satisfy humanity's water demand while still protecting the environment and its natural ecosystems is now one of the most critical and difficult challenges of the 21st century (Postel, 2000).

A water resource that is managed to contribute to the objectives of society, now and in the future is defined as a sustainable water resource. Sustainable water resources have the capacity to satisfy humanity's water demand, whilst still maintaining ecological, environmental, and hydrological integrity, without the degradation of the resource (Loucks, 2000; UNESCO, 1998). Groundwater makes up approximately 0.76 % of the total water available on Earth, making it the largest freshwater reservoir accounting for a third of available freshwater resources worldwide. Found within soil pore spaces, permeable rocks and rock fractures, groundwater is a relatively clean, reliable and cost-effective water source that has the capacity to be sustainable, if managed correctly (Fig.1) (Calow et al., 1997). Moreover, in regions where water stress is a recurring issue, groundwater is often the only source of water and needs to be managed correctly and sustainably in order to mitigate water stress.

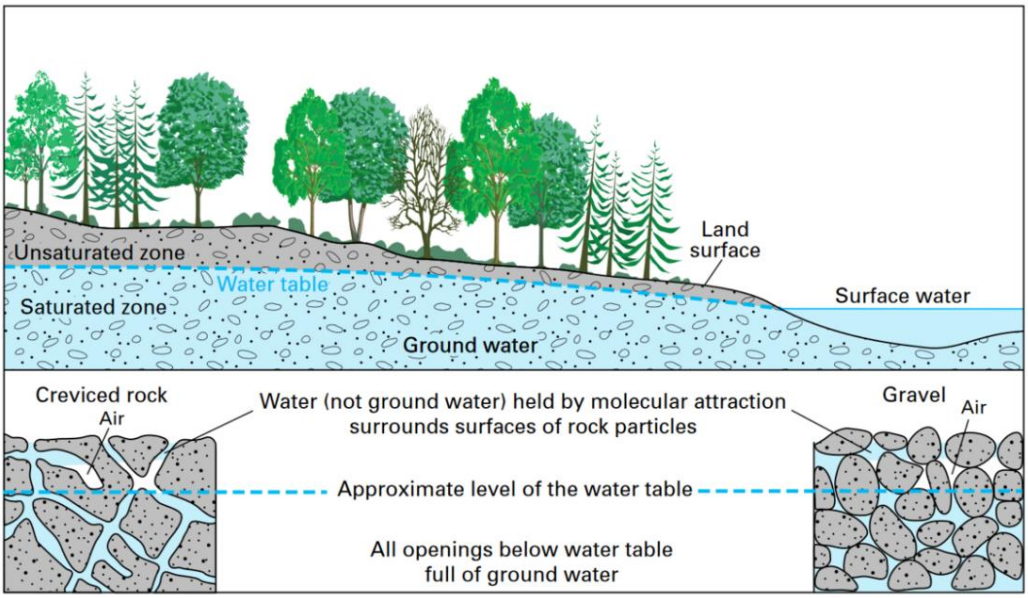

Figure 1 - Diagrammatical illustration of groundwater hosted within an aquifer (internet sourced from https://www.livescience.com/39579-groundwater.html).

Groundwater's role in providing potable water has become more prominent as surface waters are affected by climate change, contaminated by various types of pollution and are in general over exploited to support continuously increasing population and development (Bovolo et al., 2009). Groundwater is often considered to be less vulnerable to direct pollution than surface water (Vaux, 2011). It is generally regarded as more resilient to climate variability because of the way it is stored and in particular is less vulnerable to direct evaporative losses (Vorosmarty et al., 2005). Furthermore, groundwater generally allows for withdrawals even during dry seasons when rivers, lakes and dams may carry little or no water (Vaux, 2011). However, groundwater can still be subject to stress with respect to both quantity and quality. The long-term average groundwater recharge, determines the maximum value of withdrawals without depleting the resource (Kundzewicz and Döll, 2009).

Groundwater depletion occurs when the water table is permanently lowered by non-sustainable pumping practices (Konikow and Kendy, 2005). Once groundwater depletion starts to occur, it can take many years, decades or millennia to replenish the groundwater resource (Gleeson et al., 2015). However, the notion of groundwater recharge should not be explicitly equated with the concept of safe yield, (the amount of water that can be withdrawn from an aquifer without groundwater depletion and producing unacceptable negative effects) (Kundzewicz and Döll, 2009). In order to prevent groundwater depletion, an understanding of the aquifer characteristics, storage capacity, groundwater fluxes and recharge rates are required. In doing so, the residence times and the potential yield may be quantified allowing for the sustainability of this resource to be determined. Additional

contributing factors such as the effect that extraction can have on the surrounding water systems (wetlands, and streams) and ecosystems should also be accounted for (Kundzewicz and Döll, 2009).

Arid countries, like South Africa, are prone to water stress as precipitation is generally low and unevenly distributed throughout the country (Fig. 2) (Benhin, 2015). Generally, the western side of South Africa is drier than the eastern side, as the western part, and particularly the western coastal zone, receives annual precipitation of 200 mm or less per year (Fig. 2). Areas in the eastern highlands can receive more than 500 - 900 mm precipitation per annum, at times exceeding 2000 mm per annum (Botai et al., 2018). The central parts of the country, receive average annual precipitation of 400 mm per annum while large variations can still occur as one traverses to the north eastern coast (Fig. 2). As climate change affects the amount and distribution of precipitation falling across South Africa (Kahinda et al., 2010), water stress could become a recurring issue in South Africa, particularly in the western parts of the country, increasing the dependence on groundwater.

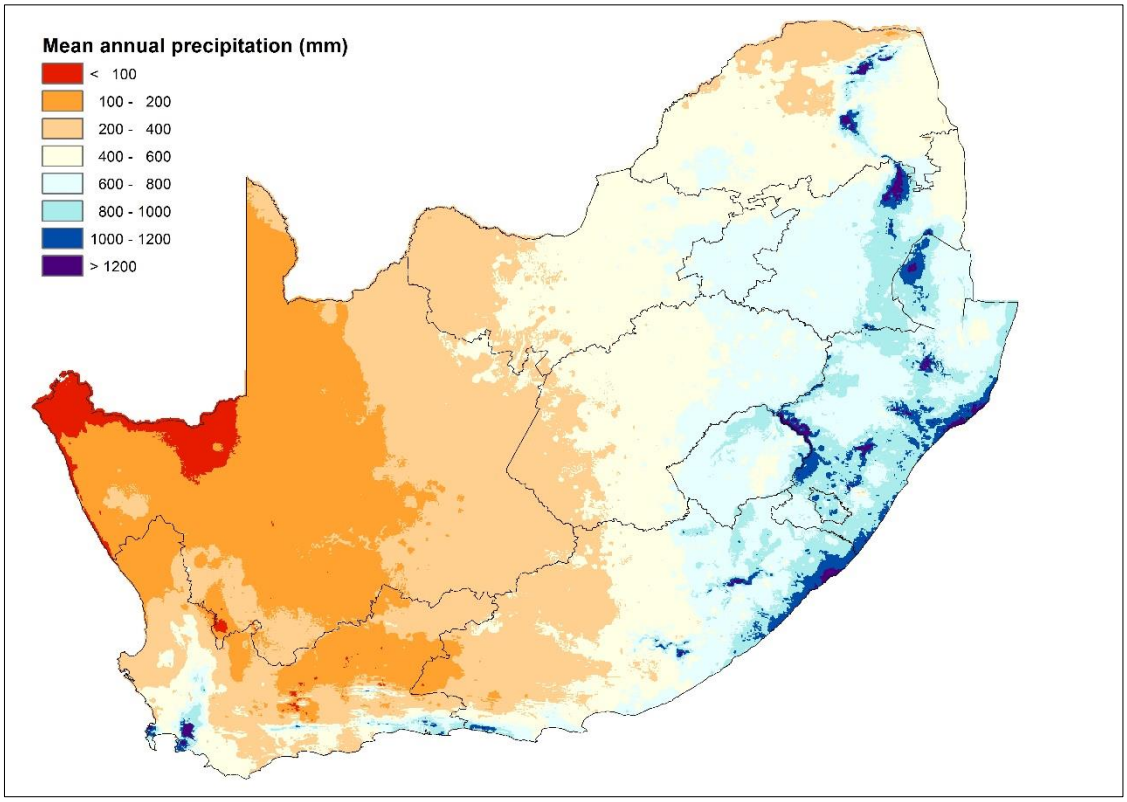

Figure 2 - Rainwater distribution map of South Africa, highlighting how the north eastern regions receive more rain than the western parts of the country, From Lynch (2004)

From 2015 to 2018, elevated atmospheric temperatures and reduced precipitation resulted in severe drought in the Western Cape of South Africa. Combined with poor water management and high population growth, this severely affected the available water resources along the western coast of

South Africa. As drought conditions worsened, cities such as Cape Town were forced to implement strict water restrictions to reduce water consumption. To address the water shortage, serious consideration was given to large-scale groundwater abstraction from aquifers in and around the City of Cape Town. The Table Mountain Group (TMG) aquifer is one of the largest aquifers in South Africa and occurs within the Western Cape and Eastern Cape provinces, extending from just north of Nieuwoudtville to Cape Agulhas and then eastwards to Algoa Bay (Rosewarne, 2002) (Fig. 3). The TMG forms the lower part of the Cape Supergroup (De Beer, 2002) and is composed of various mature and pure sandstones and quartzites with minor shales. The TMG aquifer generally yields high quality water, low in total dissolved solids (TDS), with very low calcium and magnesium because of the generally quartzitic nature of the aquifer host rocks (Smart and Tredoux, 2002). The aquifer is primarily regarded as fractured rock aquifer with low primary porosity because of the high proportion of quartzites relative to sandstones. Thus, flow of water through this aquifer is generally along heterogeneous fracture networks that allow for an interconnected secondary porosity.

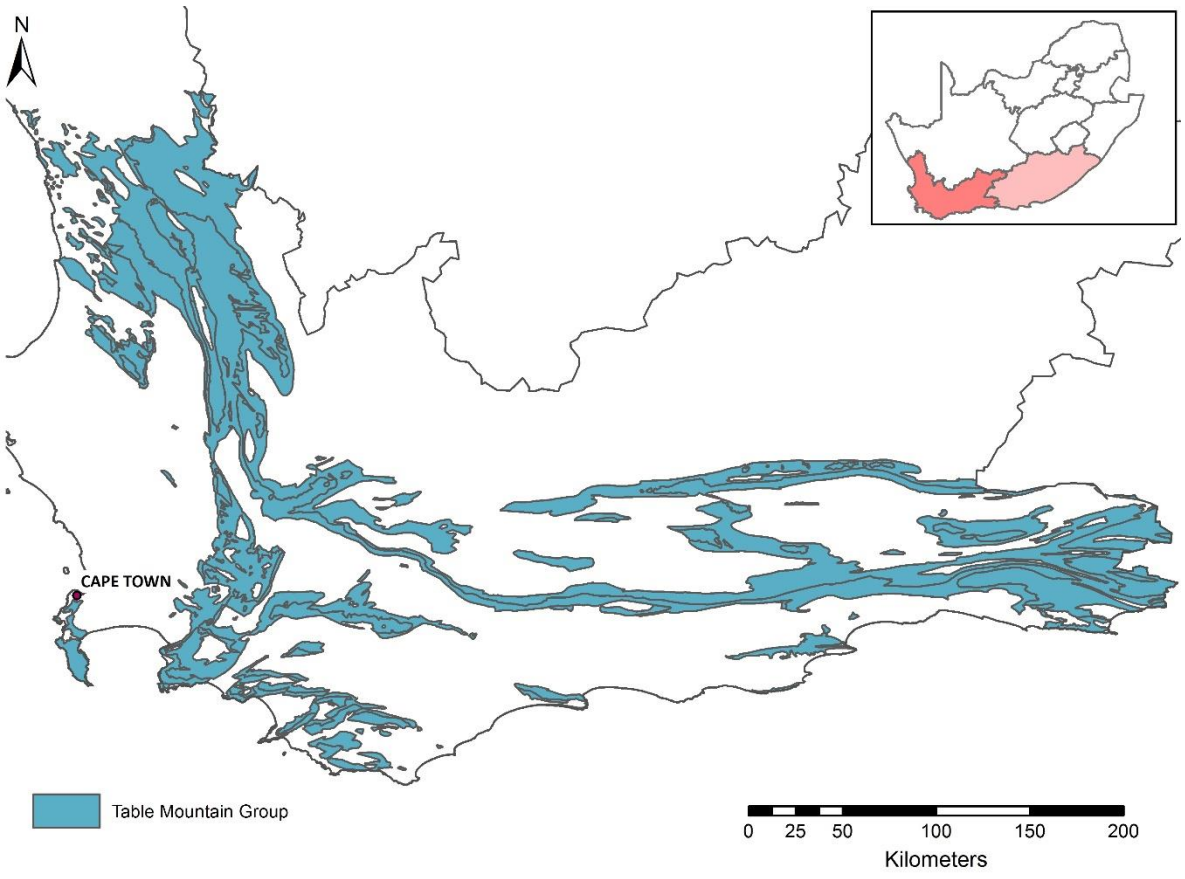

Figure 3 - Table Mountain group outcrop in the Western Cape Province. The TMG continues eastwards into the Eastern Cape which is highlighted in light pink in the inset map. Map derived from CGS data.

The mountains in the immediate hinterland to the City of Cape Town are dominated by TMG sequences and this combined with the high quality of the TMG groundwater has made the TMG

aquifer a primary target for large-scale groundwater abstraction to supplement the City of Cape Town's municipal water supply. However, before this can happen, an in-depth understanding of the recharge rate, storage capacity, and groundwater fluxes is needed to quantify the potential yield and hence long term sustainability of the groundwater resource. This is important not just for municipal groundwater usage but also to ensure that sensitive ecological systems are not impacted by over abstraction (Steube et al., 2009). Previous studies on the TMG aquifer have estimated the total potential yield to lie within the range of 5 – 50 Mm^3 (Colvin et al., 2003). However, the potential yield may have been overestimated and needs updating and revision (Jolly, 2002). For the groundwater recharge dynamics to be understood, the groundwater residence times need to be quantified as they can indicate the time taken for the aquifer to be replenished. Isotope tracers are ideally suited for this purpose. In particular, radioactive isotopes with short half-lives are excellent tracers of the interaction between surface and groundwater over short time frames and are hence ideal tracers of recharge.

Radon-222 (^{222}Rn) is an inert noble gas that is the natural intermediate daughter product of uranium 238 (^{238}U). It is a naturally radiogenic alpha- emitting noble gas with a half-life of 3.82 days (Higgins et al., 1961; Stites, 1950). Due to its gaseous state, ^{222}Rn is soluble in water and is therefore well suited as a natural tracer in hydrological and hydrogeological applications. Its occurrence in groundwater bodies is largely governed by the concentration of its radioactive parents (^{238}U and ^{226}Ra) in the rocks and soil found within the aquifer (Loomis, 1987). In contrast, in surface water and rainwater, the ^{222}Rn concentration is negligible due to the constant decay of ^{222}Rn, the outgassing of ^{222}Rn during turbulent flow and the general absence of the parent isotopes in the atmosphere (Cook et al., 2003; Hoehn and Von Gunten, 1989; Voronov, 2003). This concentration difference between surface and groundwater qualifies ^{222}Rn as tracer to delineate the interaction between surface water and groundwater and thus recharge.

In this study, the ^{222}Rn activity in groundwater in the greater Cape Town region was quantified to determine how actively the groundwater is being recharged and thus interacting with the atmosphere. As there is little data on ^{222}Rn activities in groundwater in the Western Cape, the first part of the study looked at evaluating the total range of ^{222}Rn activities in different aquifer systems. As the study utilised existing boreholes, standard hydrochemical data (electrical conductivity (EC), pH, cations and anions, including alkalinity) was first compiled and used to assign groundwater samples to an aquifer based location, geology, and comparison of the hydrochemistry to the known hydrochemical characteristics of the different aquifer systems. Thereafter, the ^{222}Rn activities were compared between different aquifers to evaluate how distinct the ^{222}Rn activity is in each. Finally, a subset of the sample locations were measured for ^{222}Rn activity over a period of several weeks before and after rainfall events to

better understand how rapidly different aquifers responded to recharge. The results will contribute to our understanding of surface and groundwater mixing relationships and aid in understanding groundwater residence times. This information is key to evaluating whether or not the TMG aquifer is in fact a sustainable source of water for municipal supplementation.

1.1.1. Problem Statement

The City of Cape Town was affected by severe drought between 2015 and 2018, and needed to find alternative sustainable water resources in order to mitigate and manage the effects of any potential future water crises. The TMG aquifer was identified as a potential alternative water supply provided the groundwater recharge dynamics are fully understood. An important component of recharge dynamics is understanding the groundwater residence time as this tells us how long the aquifer would take to be replenished. However, groundwater is usually a mix of older groundwater and modern recharge. Hence, residence times may be overestimated due to groundwater and surface water mixing relationships that develop due to heterogeneous recharge patterns. In order to understand these recharge patterns, we need to identify an effective tracer of active recharge. Short half-life radioactive isotopes are ideal tracers of rapid recharge but need to clearly differentiate surface waters and groundwaters. ^{222}Rn is a suitable isotope tracer for this purpose because the activity of ^{222}Rn in precipitation is very low but typically much higher in groundwater systems. Thus, if precipitation directly and rapidly recharges an aquifer, there should be a linked change in the ^{222}Rn activity concentration in the groundwater in the aquifer. Thus, monitoring of ^{222}Rn activities in different aquifers both before and after precipitation events should allow an evaluation of where direct and rapid recharge is occurring. This allows for a better understanding of the recharge dynamics in the TMG aquifer system and hence whether the TMG is a suitable source of water to supplement the City of Cape Town municipal network.

1.1.2. Aim and Objectives

The principal aim of this project is to develop a database of ^{222}Rn activities, including spatial and temporal variability, in groundwater of the TMG aquifer, in and around the City of Cape Town, to understand how the activity of ^{222}Rn varies as a consequence of aquifer composition and recharge dynamics. In order to achieve this, the following objectives and key questions have been developed.

Key Objective One: To identify and delineate the different aquifer types represented by the existing boreholes sampled in this study, using hydrochemistry and stable isotopes.

- Does the groundwater hydrochemistry of the existing boreholes sampled in this study allow differentiation into different aquifer types?
- What is the spatial variation in hydrochemistry of the identified aquifers and is there any correlation with elevation and groundwater depth?
- Are there any unique hydrochemical parameters that allow for the characterisation of groundwater from the different aquifers and in particular the TMG aquifer?

Key Objective Two: To quantity the ^{222}Rn activity concentration in groundwater in the greater Cape Town region.

- What is the total variation in the ^{222}Rn activity concentration in groundwater and do different aquifers have different ^{222}Rn activity concentrations?
- Do ^{222}Rn activity concentrations vary temporally and spatially in response to precipitation events?
- Does groundwater residence time play a role in the variation of ^{222}Rn activity concentrations in different aquifer systems?

Key Objective Three: To understand the relationship between groundwater ^{222}Rn activity and recharge and its bearing on sustainable groundwater management.

- Can groundwater recharge patterns be quantified with the use of ^{222}Rn activity concentrations?
- Does knowledge of the ^{222}Rn activity concentration in groundwater provide a useful indicator of sustainable groundwater?
- Can the sustainability of the TMG groundwater be evaluated using ^{222}Rn activity concentrations?

1.2. RADON IN GROUNDWATER

The chemical element radon (Rn) is an inert, colourless and odourless noble gas that is soluble in water and naturally occurs in soil, rocks, and water (Freyer et al., 1999; Fukui, 1985; Hobbs et al., 2010; Telahigue et al., 2018) (

Table 1). As a naturally occurring radionuclide, radon has three isotopes: (1) ^{219}Rn (actinon, t½ = 3.96s) the daughter product of ^{235}U; (2) ^{220}Rn (thoron, t½ =55.6s) derived from the decay of ^{232}Th; and (3) ^{222}Rn (radon, t½ =3.82 days) the progeny of ^{238}U (Akawwi, 2014; Hobbs et al., 2010; Hoehn and Von Gunten, 1989; Voronov, 2003). As both ^{219}Rn and ^{220}Rn have half-lives that are too short to record geology processes (Edsfeldt, 2001), ^{222}Rn (hereafter simply referred to as radon unless otherwise stated) is better suited as a natural tracer for hydrological and hydrogeological applications.

Table 1 - Chemical properties of ^{222}Rn (derived from Hobbs et al. (2010)).

Attribute	**Value/ description**
Atomic number (Z) = No. of protons	86
No. of neutrons (N)	136
Mass Number (A) = Z + N	222
Chemical group	Noble gas
Colour and odour	Colourless and odourless
Solubility in water at standard temperature & pressure	~0.5 µg/L
Normal boiling point	–62°C

Uranium, the radioactive parent of radon is a primordial radionuclide that was present during the formation of the Earth and has remained on Earth within the crust since its formation (Skeppström and Olofsson, 2007; Uosif et al., 2015) with an average concentration of 2.7 ppm (Siegel and Bryan, 2003). Uranium is present in relatively high concentrations in silica rich rocks due to its incompatible geochemical behaviour (Pavlidou et al., 2006). During partial melting and fractional crystallization of magma, uranium is concentrated in the liquid phase and becomes incorporated into the more silica-rich products (Uosif et al., 2015). Consequently, granitic rocks are strongly enriched in U and Th (on average 5 ppm of U and 15 ppm of Th) (Mason and Moore, 1982). However, the uranium concentration in all rocks in not constant. The way in which the rock formed, and the type of minerals concentrated within the rock affect the uranium concentration (Pavlidou et al., 2006).

Uranium exists as three naturally occurring isotopes: (1) ^{238}U (t½ = 4.5 × 10^9 years); (2) ^{235}U (t½ =7.04 × 10^8 years); and (3) ^{234}U (t½. = 246 000 years) (Jaffey et al., 1971). Both ^{238}U and ^{235}U independently decay to produce their own decay chains while ^{234}U is an intermediate daughter product of ^{238}U. Of these three, ^{238}U is the most abundant in nature and is the primary parent of radon, subsequently making radon a secondary radionuclide as it forms from the decay of the primordial nuclide ^{238}U (Skeppström and Olofsson, 2007). ^{238}U (hereafter simply referred to as uranium) undergoes a series of continuous decays, releasing alpha particles, beta particles and gamma rays until it finally reaches its stable state in the form of ^{206}Pb (Molinari and Snodgrass, 1990) (Fig. 4).

As uranium continues to decay to its stable state, intermediate daughter products such as radium (^{226}Ra) and radon (^{222}Rn) are produced (Akawwi, 2014; Coursol et al., 1990; Duggal et al., 2013). Radium (^{226}Ra) (t½ = 1600 years), is the intermediate parent radionuclide of radon. Radon's decay from radium can be described by the general equation for radioactive decay from a parent to daughter isotopes, which is described by the following formula (Eqn 1):

$$A_t = A_e(1 - e^{(-\lambda t)}) \qquad \text{Eqn 1.}$$

Where A_t is the activity of the daughter nuclide at time t, A_e is the activity of the radiogenic daughter and λ is the decay constant, which in this case is 0.18 day^{-1}

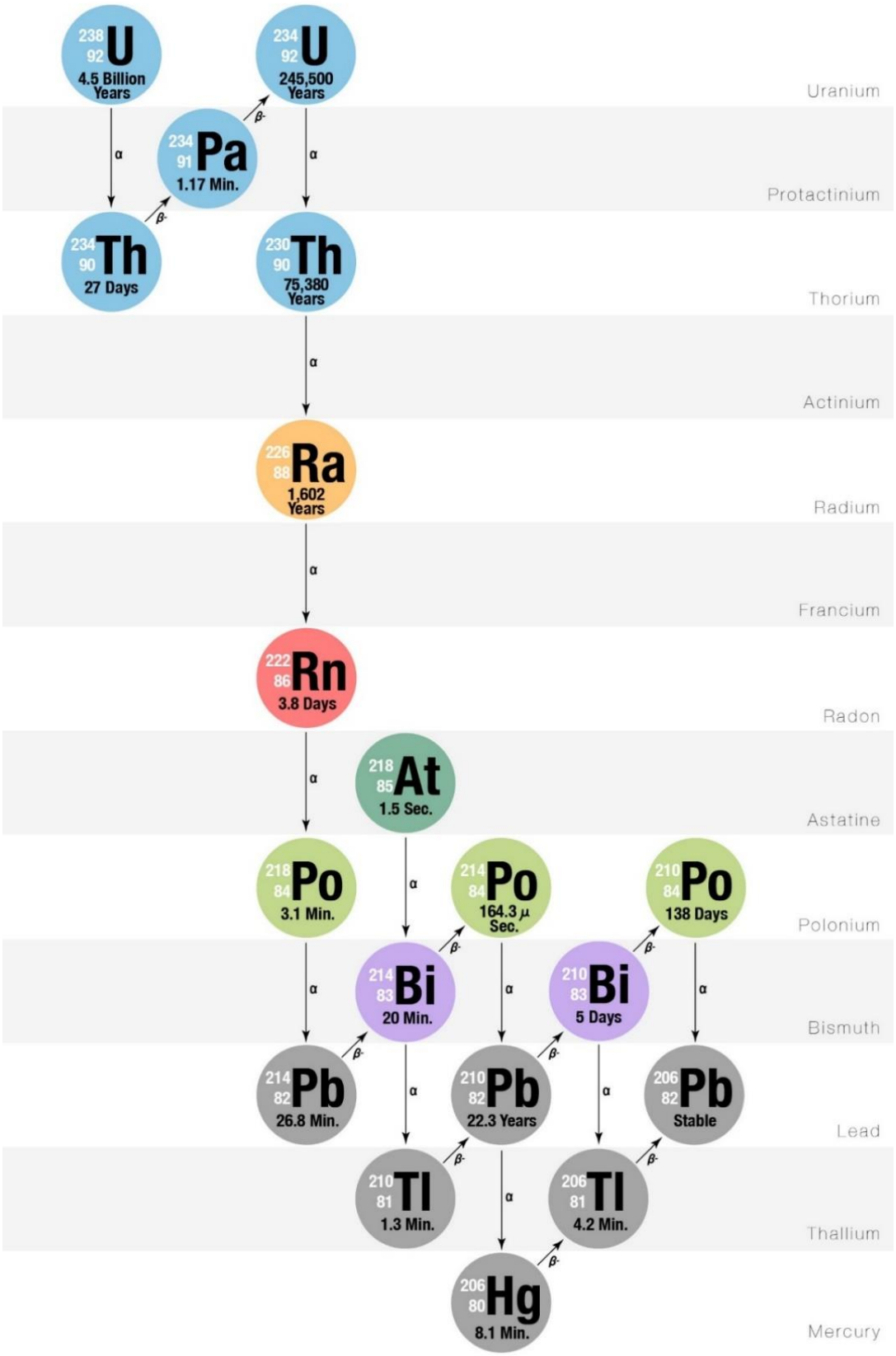

Figure 4 - ^{238}U decay series illustrating the source of decay of ^{222}Rn (in red). The half-life and the decay path of each isotope that stems from ^{238}U is depicted in the image. Radium, the intermediate parent radionuclide of radon is highlighted in yellow. Furthermore, from this decay, radon is formed from the alpha decay of radium's atoms. Image is sourced from https://www.nachi.org/gallery/radon/uranium-238-decay-chain.

1.2.1. Radon Transport Mechanisms

As radium's atoms undergo alpha decay to produce radon, radon's atoms are propelled from the site of decay and the alpha particles are recoiled in the opposite direction (Fig. 5) (Hoehn and Von Gunten, 1989; Rama and Moore, 1984; Skeppström and Olofsson, 2007). This process, known as the alpha recoil process, is considered the most effective and most important mechanism in transferring radon from within a rock to being entrained within the groundwater (Wanty and Nordstrom, 1993). However, radon's atomic location and chemical bond in the minerals and rocks influence the mobility of radon (Hobbs et al., 2010; Wanty and Nordstrom, 1993). Thus, depending on radon's position relative to the mineral grain, radon may either be buried deeper in the rock matrix or in the rock fracture where the water is carried (Fleischer, 1980).

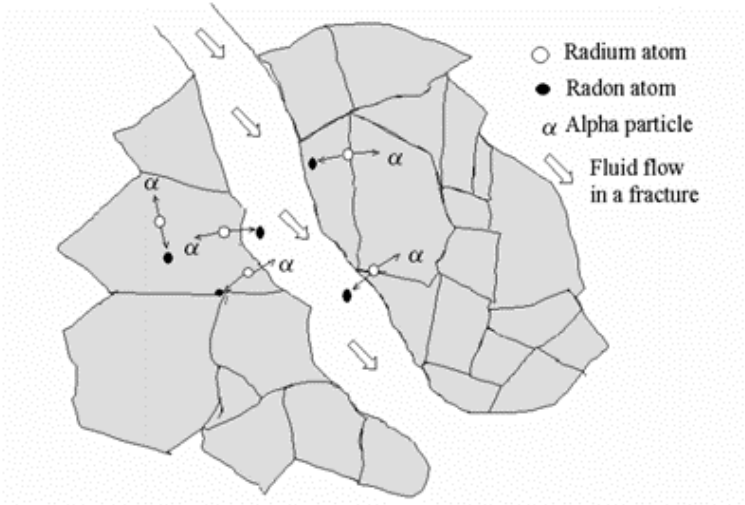

Figure 5 - The transport mechanism of radon commonly known as Alpha recoil. The above is depicting a radon atom that is emanating from mineral grains in a rock mass. The radon atom is expelled from the site of decay while the alpha particle moves in the opposite direction. From Skeppström and Olofsson, 2007.

The process by which radon atoms are expelled and escape into the water pores from the radium-bearing mineral is known as *emanation* (Akerblom and Lindgren, 1997; Edsfeldt, 2001; Hobbs et al., 2010; Voronov, 2003). The rate of emanation is dependent on the density, the temperature, the mineral composition of the rock and the environmental conditions (Voronov, 2003). Emanation is most effective when the mineral surface is wet. However, a wet mineral surface may also limit the recoil of radon atoms across pores in the adjacent mineral grains (Wanty and Nordstrom, 1993). Consequently, only 10 - 50% of radon atoms are able to escape and enter the adjacent pore space while the rest of the atoms reside within the mineral grain (Voronov, 2003). Following emanation, other processes such as permeability, diffusion and dispersion are responsible for the transport of radon.

Compared to both uranium and radium (which are both solutes), radon is highly soluble in water (e.g.; 500 ml of radon dissolves in 1 litre of water at a temperature of 0°C) due to its gaseous properties. Thus, all three isotopes (U, Ra and Rn) are transported by different mechanisms in groundwater. Radon's solubility in groundwater is dependent on the nature of the water-rock interaction, the characteristics of the aquifer, the aquifer geology, the water residence times and the material content of radium (Moore, 1999; Telahigue et al., 2018). Radon's mobility is affected by physical processes rather than chemical processes and is thus not ionized in solution nor does it precipitate in solid solutions (Hobbs et al., 2010; Wanty and Nordstrom, 1993). Uranium in rock-bearing minerals occurs as an immobile +4 oxidation state at low temperatures and pressures. However, once uranium is present within an oxidising environment, uranium is oxidised to a more mobile +6 state. Radium's occurrence and distribution in groundwater is predominantly governed by its immediate parent thorium (^{230}Th) and its removal from solution by adsorption or cation exchange processes (Herczeg et al., 1988). Consequently, radium is strongly adsorbed by minerals such as complexed sulphate ions, clay minerals, and Mn and Fe^{3+} (ferric) rich oxyhydroxides (Kraemer and Genereux, 1998).

Due to such hydrogeochemical processes, dissolved uranium and its decay products, such as radium, precipitate onto, and are enriched in, the surface of fractures and cracks (Akerblom and Lindgren, 1997). Thus, radon is able to directly emanate and enter the water from within the crack (Fig. 6). Such geochemical processes significantly increase radon's emanation efficiency within the surrounding rocks (Schumann and Gundersen, 1997). The ratio between the total amount of radon in the radium-bearing mineral compared to the amount of radon released into the pore space is known as *the radon-emanation coefficient* (Edsfeldt, 2001; Hoehn and Von Gunten, 1989; Voronov, 2003). The radon-emanation coefficient is dependent on the properties of the rock such as the type of rock, structure and porosity of the rock (Hoehn and Von Gunten, 1989; Voronov, 2003). Thus, on a microstructural view of the emanation process, the alternation of the grain surfaces, the grain size distribution and the water pore content seem to be the controlling factors for radon transport within granular aquifers (Rama and Moore, 1984).

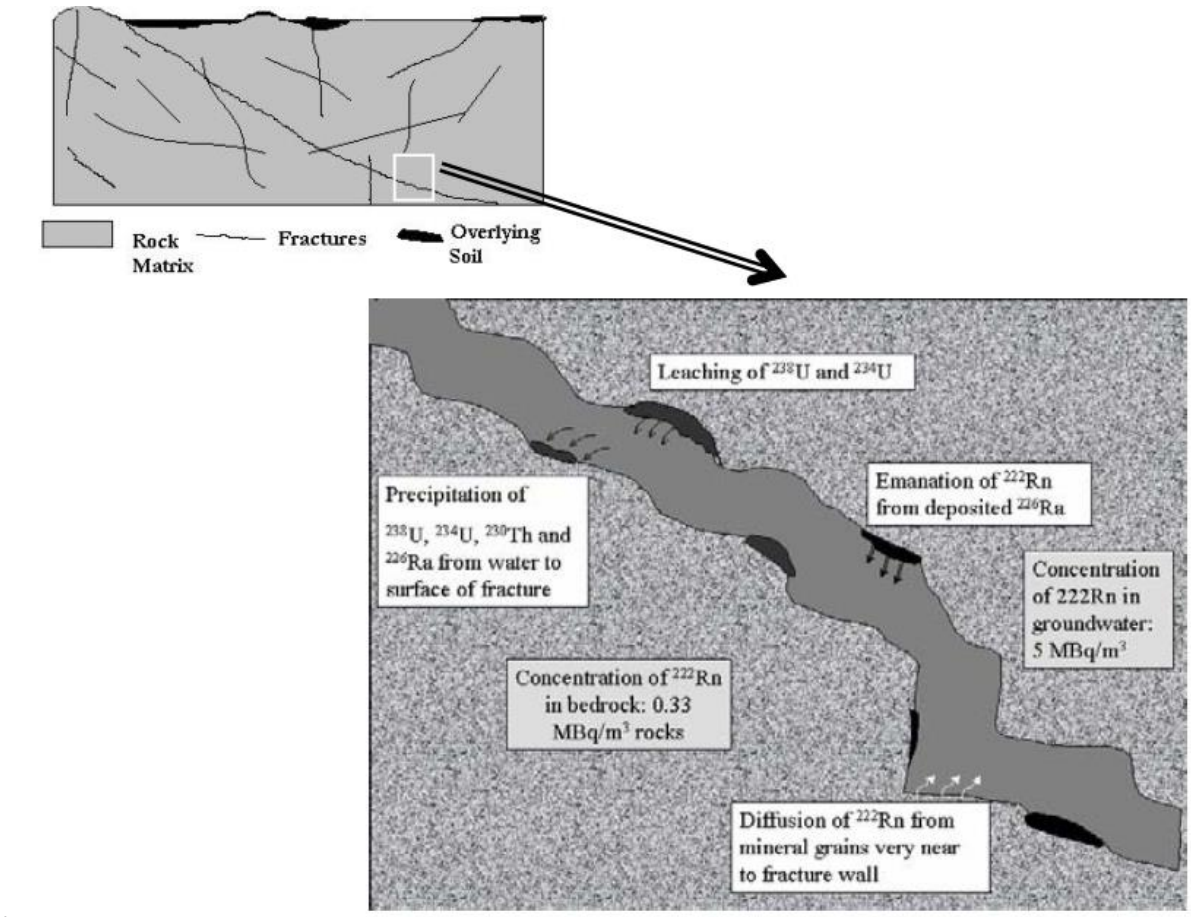

Figure 6 - Radon and uranium migration in a crystalline rock. This image illustrates the mass transfer of the radionuclides from the matrix to the groundwater. This mass transfer causes a disequilibrium of radionuclides, implying that the activity of the radionuclides in the groundwater is different to the radionuclides in the rock. Image modified from Akerblom and Lindgren, 1997 as depicted in Skeppström and Olofsson, 2007.

1.2.2. Radon Concentration Variation

The concentration of radon in water, air or gas is usually measured in the unit of Becquerels per litre (Bq/L). One Becquerel defines one nuclear disintegration/decay per second (dps), thus:

1 Bq/L = 1 dps/L = 60 dpm/L (disintegrations per minute per litre).

The disintegrations per minute per litre (dpm) is a measurement of the activity of radon within the sample (Hobbs et al., 2010). Another unit that radon concentrations are measured in are picocuries (pCi), named after the French physicist Marie Curie. One pCi is equal to the decay of about two radioactive atoms per minute (Voronov, 2003). A pCi/L is equivalent to 3.7×10^{10} Bq/L, thus 1 pCi/L is equivalent to 0.037 Bq/L (Durridge, 2018; Mook, 2000) .

Radon concentrations in geological environments are controlled by a variety of factors that could be directly linked to the concentration and mobility of uranium. Typically, intermontane groundwaters

(those groundwaters between mountains or mountain ranges) that have been enriched in uranium contain the highest radon concentrations (Voronov, 2003). Such rocks include uranium rich-granites and pegmatites and typically have radon concentrations in excess of 500 Bq/L with a maximum of 20 000 - 60 000 Bq/L (Akawwi, 2014; Akerblom and Lindgren, 1997; Dickson, 1990; Voronov, 2003). Intermontane groundwaters that are surrounded by aquifers dominated by granites, felsic gneisses, pegmatites, syenites, and felsic volcanic rocks typically have radon concentrations of 50-500Bq/L or higher (Akerblom and Lindgren, 1997; Voronov, 2003). Normal radon concentration (5 – 100 Bq/L) are found in groundwaters that are hosted by rocks that are expected to have low uranium concentrations. Sedimentary rocks such as limestones, shales and sandstones generally have radon concentrations of 5 – 70 Bq/L (Akerblom and Lindgren, 1997) (Table 2). Additionally, the presence of igneous and metamorphic bedrock aquifers as well as groundwaters that are close to fault zones result in higher radon activities (Telahigue et al., 2018; Voronov, 2003).

Table 2- Classification of radon in groundwater

Aquifer type	**Class**	**Radon activity concentration (Bq/L)**
Surface water	Low	<20
Sedimentary rocks	Normal	5-100
Igneous rocks	High	50-500
Intermontane uranium rich rocks	Exceptionally high	>500 (20 000 – 60 000)

However, exceptions do exist, and the above generalisations can only be applied to aquifers that host the radioactive parents of radon. Boreholes that have been drilled into bedrocks with low uranium concentrations but have atypical elevated radon concentrations are known. In such instances, the waters may have interacted with uranium mineralization or bedrock layers with high uranium concentrations and then travelled through the aquifer resulting in higher radon activities (Akerblom and Lindgren, 1997). Furthermore, the radon activities in groundwater where mixing has occurred would naturally be complicated as different aquifers with differing lithological properties would have different radon concentrations (Voronov, 2003). This could result in a combination of radon activities existing within a single aquifer. However, differing radon activities in groundwater is not only limited to the hydrogeological conditions of the aquifer (Telahigue et al., 2018; Virk and Singh, 1993; Voronov, 2003). The degree of metamorphism, the intensity of jointing, the presence of shear zones, the soil porosity and the uranium mineralization have all been found to influence the activity of radon in groundwater (Akawwi, 2014). The velocity at which the water circulates and the amount of water

present within rocks can also influence the radon activities in groundwater (Virk and Singh, 1993; Voronov, 2003).

1.2.3. Application of Radon in Groundwater and Springs.

Radon can be applied in numerous fields of study including seismology, atmospheric sciences, medical practices, hydrology and hydrogeology. It can be applied in hydrogeology to measure groundwater recharge and discharge from surface waters and characterise the interaction between deep and shallow groundwater systems (Cable et al., 1996). Understanding these processes are of vital importance in calculating groundwater balances, in determining the sustainable limits of groundwater extraction and for the protection of environmental surface waters (Cook et al., 2003).

Generally, radon's concentration in surface waters (≤ 2 Bq/L) is particularly low (Akawwi, 2014; Voronov, 2003) due to its high susceptibility to degassing and natural radioactive decay (Hoehn and Von Gunten, 1989). Consequently, there is a significant increase in radon concentrations upon infiltration of surface water (with negligible radon) into an aquifer system. As surface water enters an aquifer, the radon concentration begins to increase as the residence time in the aquifer increases. This increase in radon activities, as the surface or recharge water infiltrates the aquifer, is known as *radon in growth* (Hoehn and Von Gunten, 1989).

Due to this radon in growth effect, radon can be used as a tracer to identify active groundwater recharge. As surface water records negligible radon activity concentrations, the dilution of radon activity concentrations in the groundwater may be recorded during active recharge of the aquifer. However, as radon has a short half-life (3.82 days), equilibration of radon activity concentrations within groundwater (including surface water infiltration) will take place within a period of 20-25 days (five half-life's) (Cook et al., 2003; Hoehn and Von Gunten, 1989; Telahigue et al., 2018). After 20-25 days, it is difficult to distinguish between the ambient radon activity concentration in the groundwater and the newly recharged water. Therefore, only zones of active groundwater circulation are zones of interest in radon studies.

CHAPTER 2: REGIONAL GEOLOGY AND HYDROGEOLOGY

2.1. GEOLOGY

The geology of the Western Cape is dominated by four different lithological packages. These are from oldest to youngest: (1) the late-Precambrian Malmesbury Group deposited, which consists of alternating layers of dark grey, fine-grained, greywacke, sandstone and shale; (2) the Cape Granite Suite, which intruded into the Malmesbury Group at around 550 -510 Ma; (3) Palaeozoic (541 – 251 Ma) sedimentary rocks of the Cape Supergroup which were deposited on top of both the Malmesbury Group and Cape Granite Suite; and (4) Cenozoic sediments that largely represent aeolian sand deposits collectively referred to as the Sandveld Group and Quaternary alluvial deposits associated with river systems (Fig. 7).

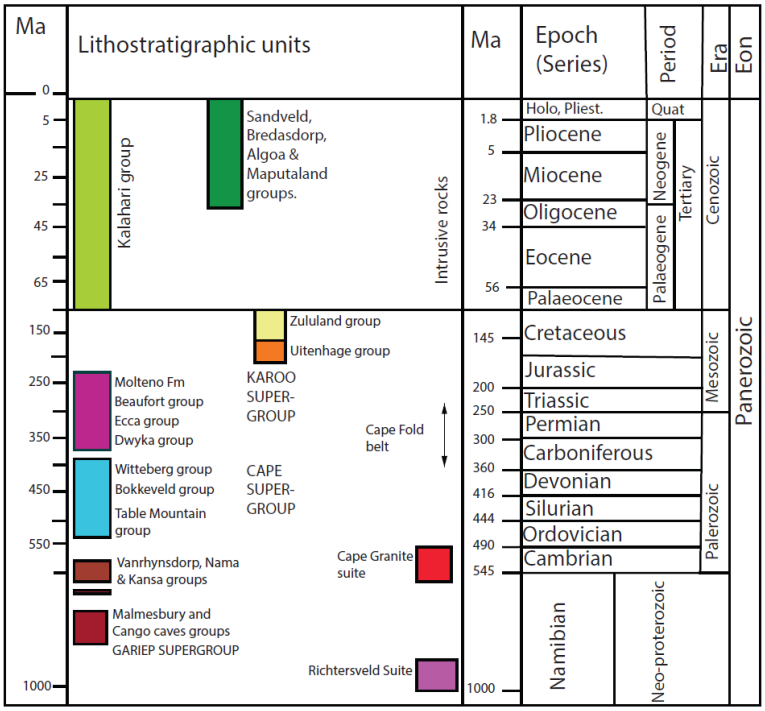

Figure 7 - Stratigraphic age of the different rock sequences in the Western Cape (after Johnson et al. (2006))

2.1.1. Malmesbury Group

As one of the oldest rock packages around the Cape Peninsula, the Malmesbury Group dates back to the late Precambrian and is 560 - 555 Ma (Frimmel et al., 2013; Kisters et al., 2015; Scheepers, 1990). These rocks are primarily low-grade metamorphic supracrustal rocks, (Belcher and Kisters, 2003) consisting of alternating layers of shale, dark grey fine-grained greywacke and sandstone. Comprising the western sections of the Pan-African Saldania Belt (Fig. 8) the Malmesbury Group is identified by pelitic sandstones and low-grade metamorphic rocks, with isolated tracts of mafic volcanic rocks (Belcher and Kisters, 2003).

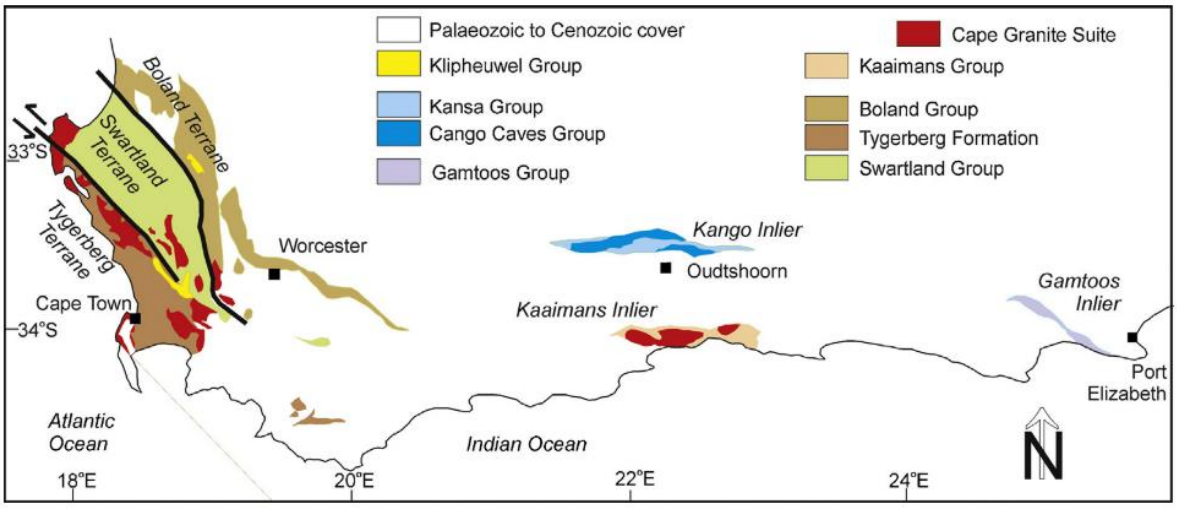

Figure 8 - General geology of the western Saldania Belt with the old tectono-stratigraphic nomenclature

The Malmesbury Group is a somewhat problematic sequence due to its poor outcrop and as a result, the origin and tectonostratigraphic evolution of the Malmesbury Group has remained enigmatic. A new lithostratigraphic subdivision of the Pan-African Saldania Belt was proposed by Belcher and Kisters (2003) and further expounded upon by Frimmel et al. (2013). Based on the lithologies and deformation characteristics, the Saldania Belt was divided into three terranes: (1) the Tygerberg Terrane; (2) the Swartland Terrane; and (3) the Boland Terrane (Frimmel et al., 2013; Scheepers and Nortjé, 2000) (Fig. 9).

The Tygerberg Terrane consists of a silty argillite, thin impure carbonate and conglomerate beds with a rhythmic turbiditic alternation of greywacke, and fine- to medium grained arenite. All these siliciclastic rocks have been overprinted by low-grade metamorphism but the sedimentary structures have been preserved (Rozendaal et al., 1999). The Swartland Terrane is separated from the Tygerberg Terrane by the Colenso Fault (Fig. 8) (Belcher and Kisters, 2003; Kisters et al., 2002). In this terrane, the dominant rock types are biotite-albite schist, phyllite, sericite-chlorite schist as well as impure cherty limestone/marble lenses (Rozendaal et al., 1999). The Boland Terrane consists of foliated and lineated feldspathic quartzites, feldspathic grits, conglomerates, greywackes, banded iron formation (BIF), some impure marly limestones and sericite schist (Rozendaal et al., 1999). These siliciclastic sedimentary rocks record evidence of a very low-grade metamorphic overprint (sub-greenschist facies) and weak deformation (Belcher and Kisters, 2003).

Gresse et al. (2006)				Belcher and Kisters (2003)		Frimmel *et al.*, 2013		
GROUP	**Subgroup**	**Formation**	**Lithology**	**GROUP**	**Formation**	**GROUP**	**Formation**	**Age (Ma)**
Boland Terrane								
KLIPHEUWEL		Populiersbos Magrug	Shale/phyllite Sandstone/conglomerate	KLIPHEUWEL	Populiersbos Magrug Franschhoek	KLIPHEUWEL	Populiersbos Magrug Franschhoek	<551 >522
MALMESBURY	Boland	Brandwacht Porterville Norree Piketberg	Greywacke/volcanic r./congl. Shale/phyllite Sandstone/volcanic r./dolomite Sandstone/conglomerate	MALMESBURY	Porterville Tygerberg Piketberg	**Boland Zone**		
Swartland Terrane						BOLAND	Brandwacht Porterville Norree/Piketberg	540 550
MALMESBURY		Franschhoek Bridgetown	Sandstone/conglomerate mafic volcanic r./dolomite				Bridgetown	<800
	Swartland	Moorreesburg Klipplaat Berg River	Greywacke Sandstone Greywacke/carbonates	SWARTLAND	Moorreesburg Bridgetown Berg River	**Malmesbury Terrane**		>552
Tygerberg Terrane						MALMESBURY	Moorreesburg/ Tygerberg Klipplaat Berg River	<554
MALMESBURY		Tygerberg	Greywacke/mafic volcanic r.					

Figure 9 - The different lithostratigraphic subdivisions of the Saldania belt according to three different authors as summarised by Belcher and Kisters (2003).

2.1.2. Cape Granite Suite

The Cape Granite Suite represented a major component of crustal growth associated with the Saldanian Orogeny during the late Precambrian (Scheepers, 1990; Scheepers and Nortjé, 2000). Large granitoid plutons intruded into all three of the Malmesburgy Groups terranes. Based on their petrological and geochemical characteristics, three different granites types were identified (S, I and A). Each type of granite is only found in a specific terranes within the Saldanian Belt (Rozendaal et al., 1999) (Table 3). The three different granites are associated with three different phases of intrusion. The first phase, occurred around 547 ± 6 Ma and is represented by S-type granites that intruded mainly into the Tygerberg Terrane and are interpreted to be collision-related syn-to post-tectonic intrusions (Da Silva et al., 2000); (Scheepers and Nortjé, 2000). The S-type granites commonly have a peraluminous chemistries and are rich in aluminium bearing minerals, such as cordierite and muscovite in addition to biotite. S-type granites contain remnants of the Malmesbury sediments (Da Silva et al., 2000; Rozendaal et al., 1999).

Phase two, or the intermediate phase, followed with post-tectonic intrusion of I-type granites with ages of 539 ± 5 Ma (Da Silva et al., 2000; Rozendaal et al., 1999; Scheepers and Nortjé, 2000) into the Swartland and Boland terranes, north of the Colenso Fault. I-type granites are metaluminous, and are related to high-potassium calc-alkaline volcanism and typically show no “interesting” minerals other than biotite (Rozendaal et al., 1999). The final phase or phase three, was associated with post-tectonic intrusion of anorogenic A-type granitoids with ages younger than 510 ± 4 Ma into the Swartland and the Tygerberg terranes (Da Silva et al., 2000; Scheepers and Nortjé, 2000). The A-type granites

represent smaller granites that represent an episode of mafic to intermediate high-K calc alkaline magmatism. A-type granites commonly are metaluminous granites, sometimes evolving towards peralkali compositions and contain amphibole in addition to biotite.

Table 3 - Granite-related plutonic events in the Saldania Belt after Rozendaal et al (1999).

Plutonism	**Association**	**Rock type**	**Examples**
Phase III (520-500 Ma)	Aa	Alkali feldspar granites, quartz syenite, syenite	**Klipberg granite and quartz syenites**
	Ab High-K calcalkaline series	Alkali feldspar granite Olivine gabbro, gabbro, monzogabbro, monzodiorite, monzonite, syenite	Cape Columbine granite, Rooiklip II granite **Yzerfontein pluton**, Mud River pluton, Botterberg pluton
Phase II (540-520 Ma)	Ib	Granite, alkali feldspar granite	Paarl fine-grained granite. Slippers Bay granite, Rooiklip I, Jongenskloof granite, Soetmelksvlei aplogranite, Slippers Bay North, Cape St. Martin dykes
	Ia	Monzogranite, granite, alkali feldspar granite	**Paarl coarse-and medium grained granite**, Vredenburg quartz monzonite, Greyton pluton, Lammershoek granite, Lemoenkloof granite, Slent granite, Riviera granite I, **Worcester granite,**
	Tholeiitic series	Olivine gabbro, gabbro, diorite, granodiorite.	Vlermuisboskloof granite porphyry, **Robertson pluton (Willem Melsrivier granite)**, Koenieboskraal granite porphyry, Modderkloof granite, Kleinfontein granite, Sardinia Bay granite, Patensie granite, Malmesbury mafic and intermediate rocks
Phase I (550-540 Ma)	Sb	Granite,	Trekoskraal granite, Karnberg granite, Rondeberg granite,
	Sa2	Granite alkali feldspar granite,	coarse porphyritic Darling granite, Trekoskraal granite, **Maalgaten granite** Stellenbosch fine-grained granite, Contreberg granite,
	Sa1	Granite	Olifantskop granite, Cuyperskraal granite, Stellenbosch granite, Schapenberg granite, Dassenheuwel aplogranite, Haelkraal granite **Peninsula granite,** Stellenbosch and Darling coarse porphyritic granites, **Darling hybrid granodiorite**, Darling biotite granite, Hoedjiespunt granite, Seeberg granite, Langebaan granite, Langesbaan biotite granite, Citruspoort granite.

2.1.3. Cape Supergroup

The Palaeozoic (500 – 340 Ma) (De Beer, 2002; Thamm et al., 2006) rocks of the Cape Supergroup are defined by continuous depositional sequences that can be divided into three groups; (1) the Table Mountain Group (TMG); (2) the Bokkeveld Group; and (3) the Witteberg Group (Booth et al., 2004; Hiller and Dunlevey, 1978). These rocks generally comprise clastic rocks derived from a northern

provenance area, deposited in a continental shelf setting (Booth et al., 2004; Tankard et al., 1982). In the Cape Supergroup, the depositional environment changed from a terrestrial and shallow marine setting with minor glacial interludes in the TMG, to a more deltaic and shallow marine setting in the Bokkeveld and Witteberg groups (Booth et al., 2004).

2.1.3.1. Table Mountain Group (TMG)

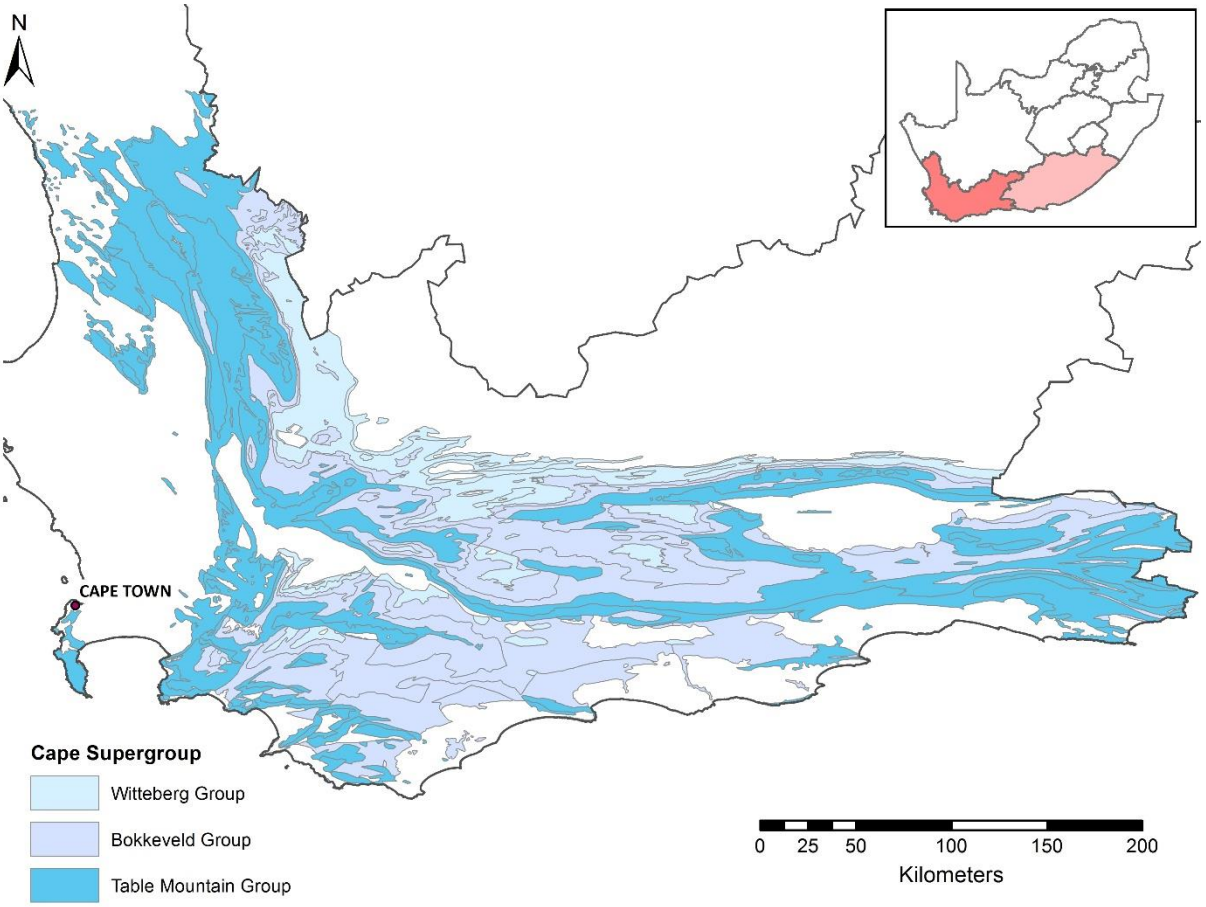

Figure 10 - Western Cape extent of the Cape Supergroup indicating the extent of the Witteberg Group, Bokkeveld Group and the Table Mountain Group. Map derived from CGS data.

The TMG forms the lower part of the Cape Supergroup (Fig. 10) and is the backbone of the Cape Fold Belt. It is composed of a thick sequence (ranging from 900 to 4,000 m in thickness) of consolidated sedimentary rocks, consisting of quartzitic sandstones that were deposited around ~500-425 Ma (De Beer, 2002; Visser, 1974) . The TMG extends over an area of ~ 248,400 km^2 (Thamm et al., 2006; Visser, 1974) along the west coast of the Western Cape and terminates in the Eastern Cape along the coast of Port Elizabeth (Jolly, 2002; Rust, 1973) (Fig. 10). Dominated by sedimentary rocks that are faulted and fractured, the TMG underwent two major tectonic events. These events included the uplift and thickening of the Cape Supergroup, known as the Cape Orogeny (280 – 220 million years ago) and the

fragmentation of the super continent Gondwana (200-123 million years ago) (Blake et al., 2010; Jolly, 2002). Fracturing and faulting generally occurred in the brittle or more competent layers such as the sandstones and quartzites.

The main sequence of the TMG is comprised of the Piekenierskloof, Graafwater, Peninsula, Pakhuis, Cederberg formations, with the Piekenierskloof Formation being the basal formation (Fig. 10). The Nardouw Subgroup, consisting of the Goudini, Skurweberg and Rietvlei (Baviaanskloof in the Eastern Cape) where the Skurweberg Formation is similar to the Peninsula Formation (Blake et al., 2010; Visser, 1974). The Piekenierskloof Formation unconformably overlies the Precambrian basement rocks of the Malmesbury Group and consists of conglomerate, quartz arenite, minor mudstones, litharenites and rudites. This formation is overlain by the semi-confining shale/siltstone Graafwater Formation (Blake et al., 2010; Rust, 1977, 1973, 1967). Both these formations are predominantly found within the western branch of the Cape Fold Belt.

The Peninsula Formation, consisting of thickly bedded quartzitic arenites occurs throughout the TMG and ranges in thickness from 1000 to 2000 m (Rust, 1967). The Peninsula Formation is the thickest formation in the TMG, accounting for two-thirds of the total TMG thickness. It is also a significant water resource due to the prominent fracture-hosted secondary porosity (Kotze, 2002; Xu et al., 2009). The Pakhuis Formation comprises about 40-80 m of glacially derived sediments but is restricted to the south-western Cape (Du Toit, 1954; Rust, 1977, 1973, 1967). A thin shale/ siltstone layer with an average thickness of 70 meters makes up the Cederberg Formation, which acts as a confining layer (aquitard) that separates the Peninsula Formation from the Nardouw Subgroup above.

2.1.3.2. Bokkeveld Group

About 400 Ma ago, subsidence in the rift valley floor brought about the deposition of deep water, fine grained sediments of the Bokkeveld Group (Theron, J, 1972; Weaver et al., 1999). The sedimentary rocks are divided into an upper mainly argillaceous sequence and a lower argillaceous and arenaceous sequence (Booth et al., 2004) (Table 4). The Bokkeveld Group reflects a history of tectonically controlled deposition of sediments during transgression and regression episodes, conformably onto those of the TMG (Booth et al., 2004; Weaver et al., 1999). These rocks are distinguishable from the TMG as they are dark grey to black in colour and are predominantly argillaceous as opposed to the dominant sandstone character of the TMG formations.

2.1.3.3. Witteberg Group

The upper layers of the Bokkeveld Group become increasingly sandy, grading into a sandstone succession known as the Witteberg Group. The Witteberg Group is the northernmost outcrop of the Cape Supergroup. These rocks were deposited in a shallow marine environment, considered to be the remnant of the Agulhas Sea (about 370 – 330 Ma) (Cotter, 2000). The rocks in the Witteberg Group are mostly arenaceous and are composed of predominantly light grey to brownish-coloured quartzites, sandstone, siltstones and shales (Table 4) (Booth et al., 2004; Brunsdon and Booth, 2009; Whittingham, 1987).

Table 4 - Stratigraphy of the Bokkeveld and Witteberg groups derived from Booth et al (2004).

Group	**Sub-Group**	**Formation**	**Main Lithologies**	**Age (Ma)**
Witteberg	Lake Mentz	Kweekvlei	Dark grey to black shale, meta-siltstone and quartzites	-375
		Witpoort	White quartzite, lesser shales, intercalated brown-weathering quartzites and shales	
		Weltevrede	Khaki to purple weathering shales and meta-siltstones, lesser grey quartzites	
Bokkeveld	Traka	Sandpoort	Green and maroon to grey silty shales, black shales, lesser quartzites	-400
		Adolphspoort	Green, grey and black shale, lesser meta-siltstones and pale grey quartzites Shales, meta-siltstones, discontinuous quartzite beds	
		Karies	Shales, meta-siltstones, discontinuous quartzite beds	
	Ceres	Boplaas	Reddish quartzites, green and purple meta-siltstones, buff-weathering shales	
		Tra-Tra Hex River Voorstehoek	Shales, lesser fine-grained quartzites Dark grey quartzites Green and purple shales, meta-siltstones, lesser quartzites	
		Gamka	Green shales, siltstones, lesser quartzites	

2.1.4. Cenozoic (Quaternary) Sediments

Throughout the study area, there are a variety of different types of recent sedimentary deposits. Some of these have been formalised with the best known being the Sandveld Group, which is dominated by aeolian sediments that unconformably overlie the Malmesbury Group, Cape Granite Suite and TMG (Adelana and Xu, 2006; Roberts et al., 2006; Schalke, 1973). The Sandveld Group also is host to the

Cape Flats Aquifer close to Cape Town. These sediments were deposited from Cape Hangklip to Elandsbaai and are believed to have been derived from two sources: (1) aeolian sand from beaches; and (2) the weathering and deposition of quartzite and sandstones of the Malmesbury Group and the TMG. The resultant deposits are dominantly aeolian and are composed of clay, clayey sand, interbedded sands, sandstone, limestone, coarse gravels and peats (Table 5) (Roberts et al., 2006). However, there are also very recent alluvium deposits associated with the Berg and Breede rivers as well as their minor tributaries. These sediments are often unconsolidated and contain numerous river cobbles in a clayey/sandy matrix and it is unclear how these recent alluvium deposits relate to the Sandveld Group. For this reason, in this study, these recent unconsolidated sediments will be referred to as Quaternary sediments even though they likely have similar characteristics to some of the recognised Sandveld Group formations.

Table 5 - Cenozoic formations in the Western Cape, sourced from Adelana, Xu and Vrbka (2010*).*

Group	Formation	Description	Age	
Sandveld	Witzand	Aeolian, calcareous, quartzose sand	Holocene	
	Langebaan (Wolfgat)	Aeolian, calcrete-capped, calcareous sandstone Velddrif	Pleistocene	
	Velddrif	Littoral, calcrete-capped coquina		
	Milnerton	Fluvial gravel, marine clay and littoral sand		
	Springfontyn (Philippi)	Aeolian, quartzose sand with intermittent peaty clays		
	Varswater	Quartzose and muddy sand, and shelly gravel, phosphate-rich	Pliocene	
	Saldanha	Conglomeratic sandy phosphorite	Late	Miocene
	Elandsfontyn	Angular quartzose gravely sand and peaty clays	Middle	

2.2. HYDROGEOLOGY

Although this study is primarily focussed on the hydrogeology of the TMG aquifer system, the study also examined the radon in groundwater derived from other aquifers in the same area. This is partly because the study used pre-existing boreholes and the host aquifer was not always correctly identified by the owners of the boreholes. For this reason, a review of the hydrogeological characteristics of the above four geological units is provided. Generally, the hard rock units of the Malmesbury Group, the Cape Granite Suite and the TMG are fractured rock aquifers and hence groundwater is hosted by secondary porosity structures. The Quaternary sediments are largely unconsolidated though and are dominated by groundwater hosted in primary porosity structures. As of the significance of the TMG to this study, an overview of the hydrogeology of the TMG is provided in this section, but more detail

is provided in Section 2.3. Note that since each rock unit (ie Malmesbury Group, Cape Granite Suite) is not divided into specific aquifer units (ie. shales as opposed to sandstones, or Peninsula Formation as opposed to Skurweberg Formation) they will be referred to as aquifer systems.

2.2.1. Malmesbury Group

The hydrogeology of the Malmesbury Group has not been studied extensively as it was thought to be largely an aquiclude on a regional scale due to the presence of weak phyllites and slates that are incapable of supporting open fractures below the near-surface weathered zone (Conrad et al., 2019). It was also not regarded as an important aquifer due to its relatively low yields (0.1 to 0.5 l/s) and high groundwater salinities. However, it is now recognised that groundwater in the Malmesbury Group is often hosted both within large fractures with high yields and in pore spaces within the shales, with low yields. Groundwater associated with the Malmesbury Group is noted to have variable water quality with electrical conductivity (EC) values spanning the range <1000 µS/cm to >10000 µS/cm (Conrad et al., 2019). Typically, the large fractures with high yields are associated with better quality groundwater.

2.2.2. Cape Granite Suite

Typically, granitic rocks have limited groundwater potential as their crystalline structure contains no primary porosity and permeability. However, fracturing and faulting of the granites can increase both the porosity and permeability. In the case of the Cape Granite Suite, groundwater is predominantly contained within intergranular interstices in the jointed and faulted bedrock (DWAF, 2003). Thus, the hydraulic conductivity in the Cape Granite Suite, is likely to be highly variable and could be within the range of 7 x 10^{-4} m/d to 30 m/d, while in solid granite the hydraulic conductivity is likely to be around 3 x 10^{-9}m/d to 2 x 10^{-5} m/d (SRK, 2009). In the study area, the EC of groundwater in granitic hosted aquifers was within the range 1500 to 3000 µS/cm (SRK, 2009).

2.2.3. Cape Supergroup

The Cape Supergroup hosts some of the most important aquifers in the Western Cape. The hydrogeology of the Cape Supergroup is divided into the three groups within the Cape Supergroup being considered in this study, i.e. the TMG, the Bokkeveld Group and the Witteberg Group. A brief explanation of the hydrogeology of the TMG is given here but more detail is provided in Section 2.3

2.2.3.1. TMG

In the TMG, the Peninsula and the Skurweberg formations are the two main aquifer units and are separated by the Cederberg Aquitard (Table 6) (Kotze, 2002). Both these aquifers are fractured rock aquifers, with low primary porosity. Consequently, the flow of water throughout this aquifer is along heterogeneous fracture networks that are controlled by folding and faulting of the TMG. These fracture networks are variably interconnected, and this facilitates groundwater flow. The density and distribution of the fracture networks is thought to vary with depth in the aquifers and facilitates movement of groundwater along long flow paths from considerable depths (Diamond, 2014; Lin et al., 2014). Large parts of this aquifer are under artesian flow, and hence springs are common, particularly along the mountains between Franschhoek and Paarl where they are used for bottled water production (Miller et al., 2017), as well as on Table Mountain itself (Diamond and Harris, 2000). The TMG aquifer generally yields high quality water with TDS typically lower than 50 mg/L (Smart and Tredoux, 2002) and characterised by an absence of calcium and magnesium that is a function of the inert quartzitic nature of the host rock. The aquifer is generally assigned a storativity of <0.001 (Hartnady and Hay, 2002).

2.2.3.2. Bokkeveld Group

Groundwater associated with the Bokkeveld Group is distinct to groundwater associated with the TMG due its increased salinity (TDS within the ranges of 150 - 2000 mg/L) (Boyer, 2018; Hartnady and Hay, 2002b). In some areas the yield from the aquifer may be high, provided there is sufficient recharge however this aquifer generally renders yields of less than 1 L/s (Boyer, 2018; Weaver et al., 1999).

2.2.3.3. Witteberg Group

The groundwater associated with the Witteberg Group is generally brackish with ECs ranging 2000 and 7000 µS/cm. This, combined with the low potential yield, on the order of 0.5 L/s – 5 L/s, means that the Witteberg Group is not regarded as a viable groundwater source (Netili, 2007).

2.2.4. Quaternary Sediments

The hydrogeology presented here will be on the sedimentary deposits surrounding the study area, and this includes the Sandveld Group which are more generally recognised closer to the coast (e.g the Cape Flats Aquifer and around Atlantis). The Sandveld Group are dominated by sands that are well rounded and well sorted resulting in hydraulic conductivities within the ranges of 15 – 30 m/d (Gerber,

1981) and transmissivities within the range of 50–650 m^2/d. The effective total porosity is considered to be within a range of 0.10 – 0.12 Φ and the potential yield within the ranges of 0.5 L/s - 2 L/s (Adelana et al., 2010; Meyer and Jonck, 2001). These values are assumed to be applicable to the alluvial deposits lining the Berg River where many of the groundwater samples are taken.

2.3. HYDROSTRATIGRAPHY OF THE TMG AQUIFER

A lithological and hydrostratigraphic unit are two completely different terms. A lithological unit refers to the character and physical properties of a rock or outcrop. However a hydrostratigraphic unit is a formation, a part of a formation or a group of formations that contain similar hydrogeological properties allowing for it to be grouped into aquifers and associated confined layers (Xu et al., 2009). With respect to a secondary porosity aquifer, a hydrostratigraphic unit may consist of one or more lithological units, with specific fracture networks and structural orientations that promotes a well-established groundwater circulation system for recharge, through flow and discharge (Xu et al., 2009).

As previously mentioned, the Cape Orogeny caused folding and faulting of stratigraphic units in the TMG that led to low grade metamorphism of the rock units in the TMG. This resulted in phyllites and quartzites rather than shales and sandstones (Hälbich et al., 1983). With this low-grade metamorphism, the mineral grains were recrystallized leading to the reduction, and in many places, disappearance of primary porosity. Thus the TMG is principally known as a secondary porosity aquifer, with groundwater flowing through fractures and joints (Brown et al., 2003; Xu et al., 2009). Accordingly, the TMG aquifer is generally strongly compartmented by faults or fault zones formed in Palaeozoic and reconstructed during Mesozoic tectonics (Jia, 2007). However, despite this recrystallisation, the TMG rocks still maintain their original sedimentary features/structures and are thus referred to as sedimentary rocks rather than metamorphic rocks (Newton et al., 2006).

The depth of the TMG is evidenced by thermal springs that are found throughout the aquifer (Brown et al., 2003; Kingsley, 1969; Xu et al., 2009) (Table 6). These hot springs can reach temperatures of 64°C indicating they are circulated at depths of at least 2000 m below ground level (Brown et al., 2003; Xu et al., 2009). The TMG aquifer system is comprised of three units: (1) The Peninsula Aquifer (Peninsula Formation); (2) Nardouw Aquifer (Nardouw Subgroup); and (3) the Cederberg Aquitard (Cederberg Formation) which separates the two main aquifer units (Kotze, 2002) (Table 6). The demarcation of these aquifers/aquitards were purely based on their hydrogeological characteristics linked to their lithologies, fracturing styles etc. Accordingly, such characteristics influence each aquifer system's water bearing capacity, groundwater quality and groundwater yield (Jia, 2007; Xu et al., 2009).

The Peninsula Formation consists of pure quartz arenites with a very low primary porosity due to the cementation of individual sand grains. Porosity has been further reduced by low-grade metamorphism associated with the Cape Orogeny. However, increased rock induration led to a higher potential for brittle fracturing during deformation resulting in a well-developed secondary porosity allowing for effective groundwater storage and groundwater flow paths. The Peninsula Formation usually crops out at elevated altitudes and thus receives more recharge. Hot springs are typically situated within the Peninsula Aquifer and are linked to either the contact between the over or underlying aquitard or the impermeable fault zone, or where the Peninsula Aquifer is hydraulically connected with the Nardouw Aquifer due to faulting (Brown et al., 2003).

The Nardouw Subgroup contains silty or shale interbeds and is associated with a higher feldspar content compared to the Peninsula Formation. This increase in feldspar has led to chemical weathering that resulted in the formation of clays that essentially clog up the secondary flow paths and thus reduce permeability of the aquifer (Jolly and Kotze, 2002). However, the presence of these shale layers had a significant impact on the fracturing and folding of the TMG aquifers, giving rise to large variations in hydraulic conductivity. These two aquifers are separated by the Cederberg Formation. The Cederberg Formation is an aquitard, which indicates that it may contain water, however it may not transmit large amounts of water, unless intercepted by a fault. The barrier nature of the Cederberg Formation also can be seen in the numerous spring occurrences at the Cederberg/Nardouw and Cederberg/Peninsula boundary in the Western Cape. The Piekenierskloof Aquifer and the overlying Graafwater Aquitard, which underlie the Peninsula Aquifer, are found predominantly in the western branch of the Cape Fold Belt. The Piekenierskloof Aquifer forms the base of the TMG aquifer and is restricted to the western coastal area (Jia, 2007).

Table 6 - Summary of the stratigraphy and hydrostratigraphy of the domains within the TMG. Table 6 is derived from Blake et al (2010).

Stratigraphy and hydrostratigraphy of the TMG storage model domains									
Stratigraphy					Hydrostratigraphy			Max. Thickness (m)	
Age Range (Ma)	Supergroup	Group	Formation	Description	Super-unit	Unit	Subunit		
0-2		Sandveld/Bredasdorp	Various	Alluvium		Quaternary Aquifer			
136		False Bay Suite		Dolerite dykes					
~~*Major unconformity*~~~~~									
354-417	Cape	Table Mountain	Bokkeveld	Various	Shales and minor sandstone	Table Mountain Superaquifer	Gydo Mega-aquitard		
			Rietvlei	Skurweberg	Feldspathic sandstone;minor shale		Nardouw Aquifer	Rietvlei *Subaquifer*	280
								Verlorenvalley *Mini-aquitard*	
					Thickly bedded quartzite			Skurweberg *Subaquifer*	290
417-443				Goudini	Reddish brown quartzitic sandstone		Cedarberg/Winterhoek Mega-aquitard	Goudini *Meso-aquitard*	230
				Cedarberg	Dark grey shale and siltstone			Cedarberg *Meso-aquitard*	120
				Pakhuis	Diamictite and quartz sandstone			Pakhuis *Mini-aquitard*	40
				Peninsula	Thickly bedded quartzite		Peninsula Aquifer	Platteklip *Subaquifer*	1800
								Leeukop *Subaquifer*	
				Graafwater	Impure sandstone,shale		Graafwater	Graafwater *Meso-aquitard*	420
				Piekenierskloof	Quartz sandstone,conglomerate, shale		Piekenierskloof	Piekenierskloof *Aquifer (Limited)*	900
~~*Major unconformity*~~~~~									
495-545	Saldanian	Cape Granite Suite		Granite		Basement aquicludes			
545->750		Malmesbury		Metasediments					

CHAPTER 3: THE HYDROCHEMICAL CHARACTERISATION OF GROUNDWATER

3.1. INTRODUCTION

In this study, existing boreholes (usually production boreholes with pumps installed) were targeted for radon sampling. Before the radon data can be properly analysed though, it was necessary to properly characterise each sampling location to determine which aquifer was being sampled. The study was specifically targeting the TMG aquifer because this aquifer system is being targeted as a source of water to supplement the City of Cape Town's municipal water supply. As the TMG aquifer is made up of quartz-dominated lithologies, groundwater associated with the TMG aquifer typically has a low EC (≤ 50 µS/cm) and specifically low alkalinity as well as having acidic pH values (Smart and Tredoux, 2002; Weaver, 2002). These features are reasonably distinctive in the Western Cape where the other main aquifer systems typically have higher EC, pH or alkalinity linked to the difference in their host rock compositions. Thus, hydrochemistry should be able to provide a reasonably good indication of which aquifer system each borehole is accessing. The main aquifer systems (refer to Chapter 2) being considered are: (1) the Malmesbury Group; (2) the Cape Granite Suite; (3) the TMG, (4) the Bokkeveld Group; (5) the Witteberg Group; and (6) Quaternary sediments.

In some instances, geologically defined boreholes with hydrochemical data allowed for the establishment of the hydrochemical character of each aquifer. These samples served as model hydrochemistries for the respective aquifer. The boreholes with undefined geology allow for hydrochemical characterisation of the groundwater. These samples could then be compared to those established hydrochemical characters for the allocation of each sample to an aquifer system. In

addition to the normal hydrochemical parameters of EC, pH, alkalinity, cations and anions, the stable isotopes of O and H were also examined to see how well they differentiated different aquifer systems.

3.2. METHODOLOGY

The sample sites were selected based on their proximity to their inferred host aquifers and their proximity to the City of Cape Town. 48 samples were obtained from the six different aquifer systems. Sites considered suitable for radon sampling were visited in August 2018 and March 2019 to assess the hydrochemistry and identify the geology that that the borehole was drilled into.

3.2.1. Sampling Locations

Data collection and sampling for this study was done during two separate sampling seasons. Initially the sampling approach was divided into three categories: (1) – sample locations in and around the City of Cape Town, (2) locations within a 100 km radius from Stellenbosch; and (3) locations within a 200 km radius from Stellenbosch. Distance to sampling location was an important consideration due to the analysis limitations associated with radon (see Chapter 4). The first sampling season included sample sites that extended from Porterville to Robertson and Barrydale (thus within a 50 – 200km radius from Stellenbosch). In the second sampling season increased attention was placed on locations in and around the City of Cape Town. The final sampling locations are shown on a simplified geological map of the aquifers that surround the City of Cape Town (Figure 11).

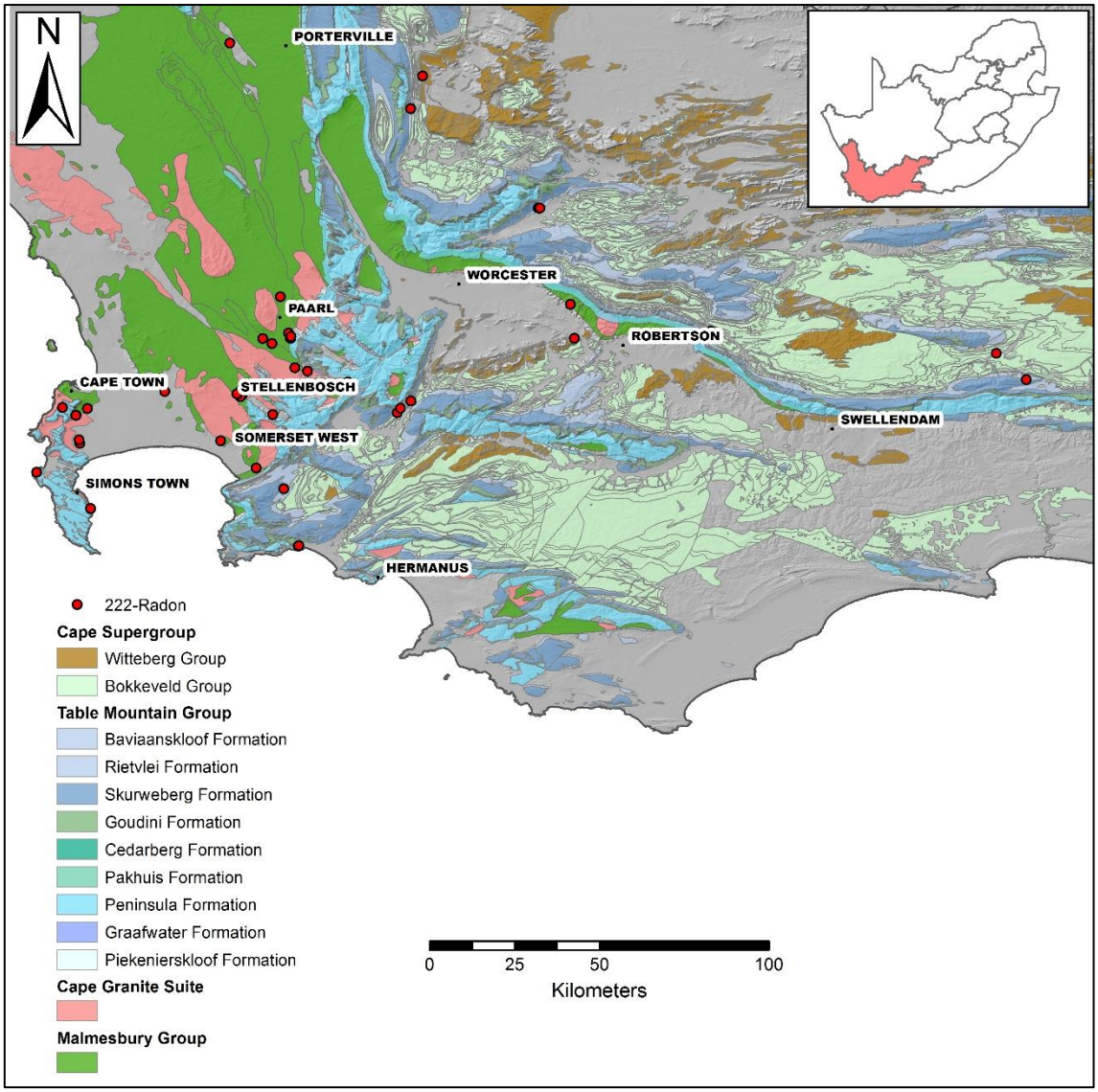

Figure 11- Distribution of sampling locations superimposed on the regional geology.

3.2.2. Sampling Protocol

All groundwater samples were collected using the following protocol. Samples were filtered through 0.45 μm cellulose acetate filters into either 15- or 50-ml sterilized polypropylene tubes. These samples were kept cool while in the field and later refrigerated during storage prior to analysis. All groundwater samples were analysed for electrical conductivity (EC), pH, cations, anions and $\delta^{18}O$ and $\delta^{2}H$ values. Separate sample bottles were taken for each sample type. Cation samples were acidified with 0.5 ug 65% ultrapure HNO_3 prior to analysis.

3.2.3. Analytical Techniques

3.2.3.1. EC, pH and alkalinity

EC and pH were determined in a laboratory immediately after returning from the field sampling (i.e. daily) on an Eutech CON700 and Eutech pH700 respectively. The alkalinity of each sample was measured on a Metrohm 702 SM also on a daily basis after return from the field. During the analysis for alkalinity, each sample was titrated with 0.01 M of HCl acid until buffering capacity was reached. Once buffering capacity was reached, the initial pH and the final pH were recorded. The final pH was associated with the volume change from the addition of the titrant. This volume of titrant was substituted into Eqn 2 in order to calculate the alkalinity:

$$(Vol\ of\ titrant\ (ml) * 0.01) * \frac{50000}{10} \qquad \text{Eqn 2.}$$

3.2.3.2. Cations and anions

Major ion concentrations for F^-, Cl^-, Br^-, NO_3^-, SO_4^{2-}, PO_4^{3-}, Na^+, K^+, Mg^{2+} and Ca^{2+} in the groundwater samples were analysed on a Dionex 1100/1200 Ion Chromatograph (IC) in the Environmental Geochemistry Laboratory, Institute of Earth System Dynamics at the University of Lausanne. A minimum of 10 ml of sample was required for the analysis of both the cation and anion concentrations. The data quality was monitored by the inclusion of standards and blank samples in each sequence.

Due to the EC sensitivity of the IC autosampler, the dilution factor for samples with EC values between 500 and 1000 µS/cm was 2x, while samples that had EC values >1000 µS/cm was 5x. In both cases they were diluted with Milli-Q water. As analysis commenced, the samples were injected into an ion-exchange column that separated the ions according to their retention times. A conductivity meter detected the concentrations of ions eluted from the column and recorded the ion concentration. The lower detection limit was approximately 0.1 mg/L. Total analysis time for all ions was between 30 and 35 minutes.

Once the data was obtained, the quality of the data was evaluated by calculating the charge balance for each sample. This was done by converting the ion concentrations in mg/L to meq and then calculating the percentage difference between the cations and anions as per Eqn 3. Charge balance was calculated using the cations Na^+, K^+, Mg^{2+} and Ca^{2+} and anions. Cl^-, NO_3^-, SO_4^{2-}, and HCO_3^-.

$$\left(\frac{\sum Cation - Anion}{\sum Cation + Anion}\right) * 100 \qquad \text{Eqn 3.}$$

Samples with low ECs generally did not balance due to the low concentration of the ions which were close to the detection limit of the IC. As a result, their measurement error was larger, resulting in larger charge balance errors. The charge balance limit was set at 5%, thus the lower the EC the more likely the charge balance would be greater than 5%. As the TMG aquifer typically recorded low ECs, the TMG also recorded poorer charge balance results than samples from other aquifer systems. Samples with higher EC values typically recorded a better charge balance lower than 5% (Fig. 12).

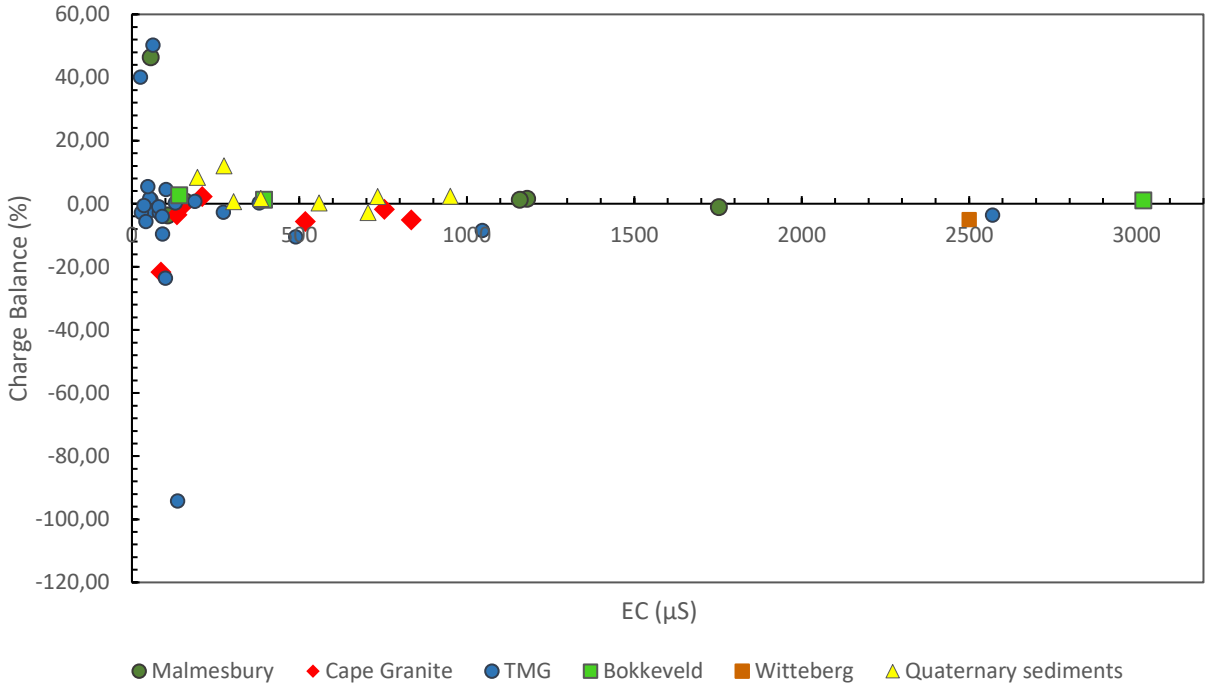

Figure 12 – EC vs charge balance for the different groundwater samples indicating that low EC samples had more difficulty in making the 5% charge balance limit.

3.2.3.3. Stable isotopes of hydrogen and oxygen

Stable isotopes of oxygen and hydrogen were determined by cavity ring down spectroscopy (CRDS) using a Picarro L1102i in the Stable Isotope Laboratory, Institute of Earth System Dynamics at the University of Lausanne in Switzerland. The Picarro uses time-based, optical absorption spectroscopy of target gases to determine the isotopic composition of hydrogen and oxygen. Laser light is injected into a cavity containing reflective mirrors and then shut off initiating the "ring-down" event. The intensity of the light decays exponentially during this time. When gas is introduced into the cavity, it absorbs the light, altering the laser decay time. All gas molecules have a specific near-infrared absorption spectrum and therefore individual isotope concentrations are determined by examining the height of their specific absorption peaks. The analytical precision of the Picarro was between ±0.4 ‰ and ± 0.07‰.

Due to the sensitivity of the Picarro instrument, samples with ECs greater than 1500 µS/cm were distilled a day prior to analysis. The distillation process involved the evaporation of the groundwater sample for 24 hours. Once the sample was distilled, each groundwater sample was placed into a small glass vial that accommodated approximately 0.780 µL. During analysis the vial was injected with a needle, allowing for a pressure gradient to be created by the release of helium allowing the sample to move up into the CRDS. The water sample was vaporized before entering the CRDS cavity where the wavelengths of the gases were used to determine the isotopic composition of the water sample. Each vial was injected 12 times to ensure accurate measurements as there was often a "memory effect" from the previous samples which was usually evident in the first four readings. Distilled water and V-SMOW (Vienna Mean Standard Ocean Water) standards were analysed in conjunction with the groundwater samples to evaluate data quality. The data was reported in the usual δ notation where R represents the $^{18}O/^{16}O$ isotope ratio (Eqn 4).

$$\delta\ (‰) = \left(\frac{Rsample - Rstandard}{Rstandard}\right) * 1000 \qquad \text{Eqn 4.}$$

3.3. RESULTS

The inferred aquifer host was determined by using the borehole location, elevations and depth relative to the surrounding geology. These inferred aquifer hosts were then further evaluated using EC values, pH and total ion concentrations. 48 groundwater samples were taken. The results are here separated into four categories. These are: (1) pH; (2) EC; (3) cation and anion concentrations; and (4) stable isotopes (δD and $\delta^{18}O$ values).

Table 7 - Field parameters results. The colours in this plot are kept consistent in all other plots in this study. Accordingly, dark green illustrates groundwater samples associated with the Malmesbury Group, red the Cape Granite Suite, light blue the TMG, lighter green the Bokkeveld Group brown the Witteberg Group and yellow Quaternary sediments.

Sample number	Lithology	Location	Borehole Depth (m)	pH	EC (µS)	TDS Cal (mg/L)	Alkalinity (mg/L)	d18O VSMOW	dD VSMOW	Cl- (mg/L)	NO-3 (mg/L)	SO2-4 (mg/L)	HCO- (mg/L)	Na+ (mg/L)	Mg 2+ (mg/L)	K + (mg/L)	Ca 2+ (mg/L)	Na/Cl (mg/L)
YAD18SVL001	Malmesbury	Paarl		6.61	158.7	90.02	23.6	-3.6	-14.8	30.35	0.01	6.32	24.21	18.12	2.31	0.25	8.45	0.60
YAD18PV001	Malmesbury	Porterville	55	6.88	1753	817.61	90.2	-3.4	-17.5	382.64	5.12	27.41	126.50	218.03	33.83	8.88	14.87	0.57
YAD18ROB002	Malmesbury	Robertson		6.97	1180	602.44	213.1	-6.2	-34.1	142.42	1.11	17.02	264.20	103.52	25.51	1.04	47.62	0.73
YAD18DB001 (a)	Malmesbury	Paarl	120	5.99	106.8	67.47	18.4	-3.9	-15.0	21.07	0.18	1.91	24.66	13.28	2.43	0.28	3.67	0.63
YAD18DB005	Malmesbury	Paarl	160	6.63	56.3	53.14	50.4	-3.7	-13.9	18.10	0.10	1.50	2.00	18.01	4.79	1.32	7.33	0.99
YAD19PAA001	Malmesbury	Paarl		7.63	1158	699.60	92.7	-4.3	-19.4	294.09	0.04	2.36	155.37	222.03	8.68	1.31	15.56	0.75
YAD18RivFarm001	Cape Granite	Paarl	70	4.45	834	101.85	2.6	-3.1	-12.1	44.25	5.15	0.68	19.99	27.89	3.33	0.15	0.41	0.63
YADKB001 (The School)	Cape Granite	Cape Town	70	5.83	134.4	80.85	16.3	-3.3	-12.3	27.74	0.74	4.10	22.50	17.96	2.19	2.73	2.70	0.65
YADKB002 (The AppleBoom)	Cape Granite	Cape Town	70	5.97	86.5	127.25	3.75	-3.3	-12.5	25.19	0.43	3.00	71.33	18.54	2.29	2.05	4.15	0.74
YAD18SW001	Cape Granite	Somerset West	50	5.26	518	164.29	14.4	-4.1	-18.1	71.64	5.72	3.29	32.01	42.25	5.40	2.47	1.52	0.59
YAD18SW002	Cape Granite	Somerset West		5.67	754	426.26	35	-3.8	-17.0	168.08	19.65	40.85	61.36	99.20	20.54	6.19	10.40	0.59
YAD19Frans003	Cape Granite	Franschhoek	100	6.37	150.1	95.76	27.9	-4.0	-16.4	26.55	2.71	0.97	35.20	19.34	1.72	2.83	6.24	0.73
YAD18Frans002	Cape Granite	Franschhoek		6.81	210	159.11	76.5	-4.1	-17.5	19.46	0.08	1.94	90.45	23.74	1.74	3.40	18.24	1.22
YAD18DB002	TMG	Paarl		5.32	56.6	116.38	3.5	-4.1	-15.7	63.02	3.19	5.37	1.25	35.32	4.76	1.00	1.54	0.56
YAD18DB003	TMG	Paarl		4.9	53	24.74	3.2	-4.1	-17.1	12.83	0.62	1.06	1.63	7.16	0.89	0.08	0.33	0.56
YAD18DB004	TMG	Paarl		4.89	54.5	25.38	3.6	-4.1	-16.0	12.64	0.69	1.03	2.37	7.17	0.92	0.09	0.30	0.57
YAD19Cer002	TMG	Ceres	36	5.06	28.5	16.30	4.9	-5.8	-30.7	6.47	0.79	1.11	2.78	3.77	0.48	0.54	0.37	0.58
YAD18DD001	TMG	De doorns	258	5.37	25.3	23.83	5.4	-5.9	-32.0	8.47	0.71	0.63	4.84	5.05	0.62	2.62	0.91	0.60
YAD18DD002	TMG	De doorns	180	5.78	47.1	25.37	10.8	-5.8	-33.5	6.44	0.56	1.48	6.42	3.80	0.27	6.12	0.28	0.59
YAD18BD002	TMG	Barydale		5.11	101.4	57.89	4	-6.7	-37.2	27.71	0.47	1.41	10.97	14.46	1.88	0.39	0.62	0.52
YAD18VilI001	TMG	Villiersdorp		5.05	91.3	52.63	3.7	-5.2	-27.8	17.75	12.38	1.63	4.56	11.68	2.06	1.73	0.85	0.66
YAD18Frans001	TMG	Franschhoek		6.04	81.4	43.50	24.9	-4.4	-20.1	20.55	0.01	1.33	8.73	11.14	1.30	0.18	0.25	0.54
YAD19MP001	TMG	Millers point	N/A	5.18	489	234.82	2.1	-4.0	-16.6	131.88	0.20	12.15	4.70	73.70	9.12	1.22	1.86	0.56
YAD19NW001	TMG	Cape Town		5.49	129.6	2251.30	4.6	-3.0	-11.4	30.35	2.14	3.57	2191.94	16.99	2.81	1.02	2.47	0.56
YAD19TM001	TMG	Cape Town		4.33	136	87.74	0	-3.6	-12.8	25.91	0.48	3.83	3.60	14.96	2.15	0.58	36.24	0.58
YAD19SprFrans001	TMG	Franschhoek	N/A	4.3	62.4	23.95	1	-5.0	-23.4	7.85	0.26	0.47	10.10	4.61	0.49	0.06	0.11	0.59
YAD19Vills002	TMG	Villiersdorp	100	5.1	99.5	275.65	4.4	-5.3	-29.8	154.78	4.07	9.74	6.75	82.43	9.83	5.84	2.21	0.53
YAD19Vills003	TMG	Villiersdorp	120	5.21	79.5	43.46	6	-5.3	-29.0	16.71	4.94	0.97	7.51	8.62	1.88	0.99	1.73	0.52
YAD19GB001	TMG	Grabouw	unsure	4.63	90.1	47.82	3.2	-4.0	-15.8	18.66	0.24	5.55	9.19	10.26	1.42	0.63	1.87	0.55
YAD19KM001	TMG	Kleinmond	1.8288	5.57	1046	285.58	7.8	-3.1	-13.2	124.88	0.35	32.30	34.54	71.50	9.46	2.79	9.59	0.57
YAD19KM002	TMG	Kleinmond		3.78	2570	286.01	0	-2.8	-12.8	159.00	0.90	19.13	2.60	83.82	11.96	1.59	7.02	0.53
YAD19Kmond001	TMG	Kommetjie	15.5	5.04	187.5	96.74	1.8	-3.7	-16.2	46.79	1.01	6.35	9.76	27.53	3.18	0.80	1.31	0.59
YAD19Kmond002	TMG	Kommetjie	14	5.18	273	147.26	2	-3.9	-17.5	70.52	0.22	16.09	8.23	42.29	5.52	1.41	2.99	0.60
YAD19Kmond003	TMG	Kommetjie	10	5.73	380	208.71	6.4	-3.4	-15.1	56.15	31.34	26.88	30.62	47.73	3.10	6.48	6.42	0.85
YAD18Cer001	Bokkeveld	Ceres	120	6.49	394	470.78	65.3	-5.8	-32.8	52.75	0.05	231.36	43.60	53.99	19.59	9.23	60.22	1.02
YAD18BD001	Bokkeveld	Barydale	100	6.52	3020	1848.30	132.7	-5.3	-28.9	756.77	0.12	284.44	185.48	420.39	85.40	5.21	110.51	0.56
YAD18MON001	Bokkeveld	Montaqu		6.53	141.2	90.05	41.7	-6.4	-33.1	16.51	0.34	2.55	43.18	9.12	2.68	4.03	11.65	0.55
YAD18ROB001	Witteberg	Robertson		6.79	2500	1826.37	426.3	-6.3	-35.0	643.29	0.06	105.44	543.61	333.99	64.72	4.66	130.62	0.52
YAD018Ra222-01	Quaternary	Stellenbosch	55.6	6.02	559	276.27	30.8	-3.5	-14.7	123.31	3.56	11.60	44.40	69.98	12.19	3.31	7.92	0.57
YAD018Ra222-02 (a)	Quaternary	Stellenbosch	47.3	5.71	195.5	104.76	30.9	-3.0	-14.5	35.79	0.03	4.64	25.00	25.11	3.00	4.12	7.03	0.70
YAD018Ra222-04	Quaternary	Stellenbosch	51.6	5.92	385	169.62	38.9	-1.8	-7.8	78.56	2.62	18.13		38.94	9.98	2.48	18.90	
YAD018Ra222-05	Quaternary	Stellenbosch	50.8	6.13	275	139.73	54.8	-3.3	-14.3	30.10	0.00	30.47	29.30	25.62	8.19	3.47	12.55	0.85
YAD018Ra222-06	Quaternary	Stellenbosch	59.9	6.8	304	130.48	50.3	-3.7	-16.4	54.52	0.01	15.76		38.09	7.48	4.36	10.27	
YAD19TK001	Quaternary	Cape Town		4.97	734	286.99	4.6	-2.7	-12.0	105.80	24.81	36.87	24.90	55.77	15.34	3.46	20.05	0.53
YAD19TK002	Quaternary	Cape Town		5.49	705	296.44	8.6	-2.8	-12.2	123.04	11.49	30.59	36.08	62.74	11.25	3.66	17.60	0.51
YADKR001	Quaternary	Kuilsriver	30	7.06	951	1137.19	28.5	-2.9	-12.4	351.93	0.32	211.15	185.52	227.79	25.26	20.58	114.64	0.65

3.3.1. pH

Overall, the pH values ranged between from 3.8 - 7.6 with significant overlap between the different groups. The groundwater associated with the Malmesbury Group had a pH of 6.0 – 7.6. The Groundwater associated with the Cape Granite Suite had a pH of 4.5 - 6.8 and this overlapped considerably with the pH of groundwater associated with the TMG (3.8 – 6.0). The groundwater associated with the Bokkeveld Group and Witteberg Group had a pH of 6.5 and 6.8 respectively. Groundwater associated with the Quaternary sediments had a pH of 4.5 – 7.0 which is very similar to groundwater derived from the Cape Granite Suite (Fig. 13). The pH of the groundwater samples was grouped and plotted according to their inferred aquifer hosts as presented in the

Table 7. Comparison of pH to EC shows distinct differences in the TMG and the 5 additional aquifer systems (Fig. 14).

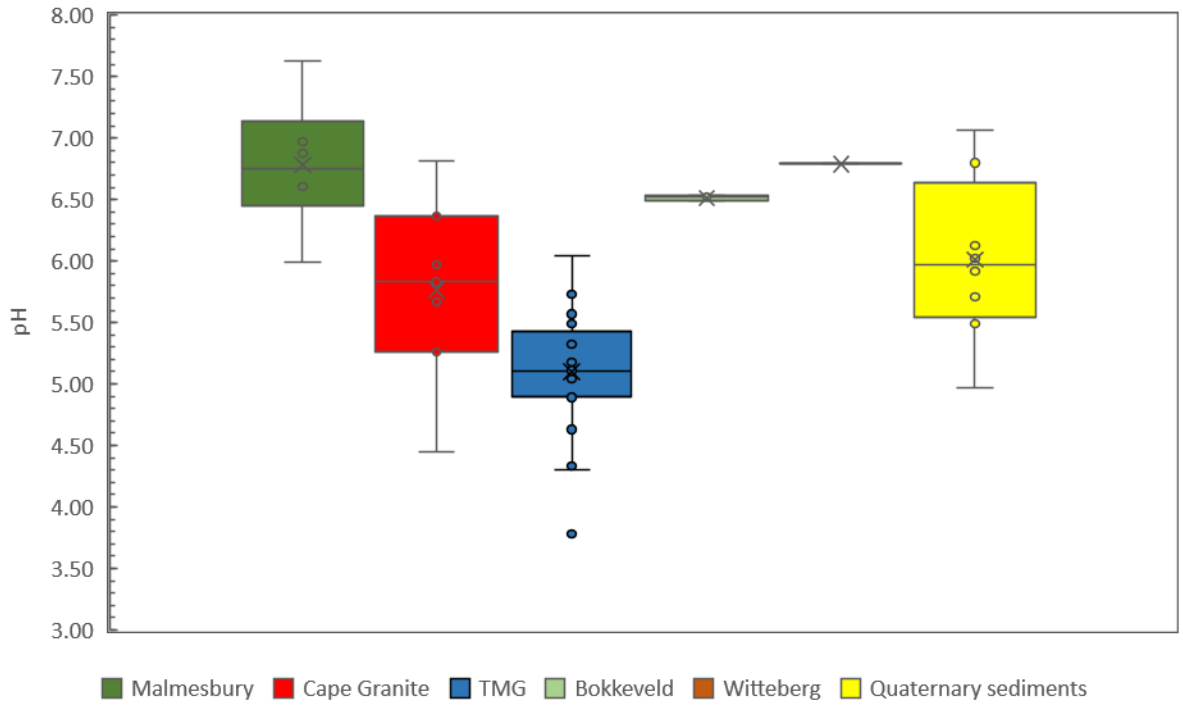

Figure 13 - pH vs proposed aquifer host. These pH values were characterised based on their inferred aquifer's as Table 7 illustrated.

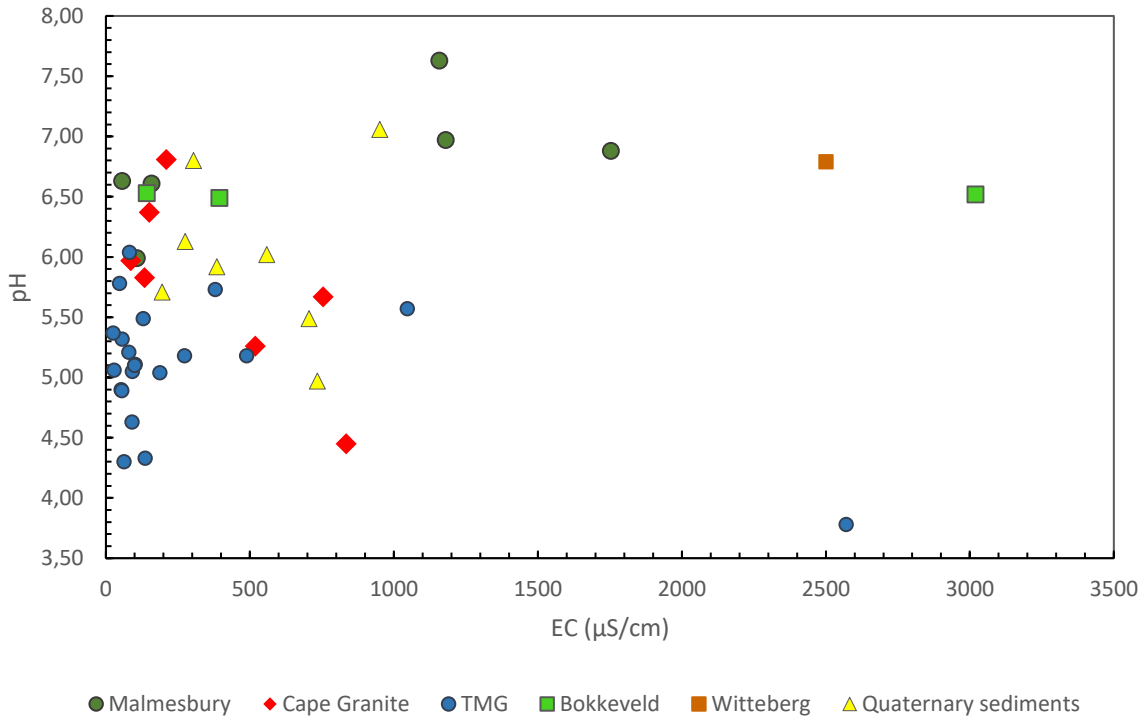

Figure 14 - Comparison of pH and EC in groundwater samples.

Groundwater samples in this study had pH values that were more alkaline, with samples typically in the TMG and Cape Granite Suite being more acidic. The groundwater associated with the TMG typically recorded a low pH (ranging from 4 to 6) (Fig. 15) with low alkalinity (≤ 20 mg/L). In groundwaters where the pH is low (acidic and high concentration of free H^+ ions) the alkalinity (typically carbonate and bicarbonate) would be low. Accordingly, the pH of a groundwater sample is proportional with the alkalinity (Fig. 15). Thus, as the pH increased in groundwaters the alkalinity would be expected to increase.

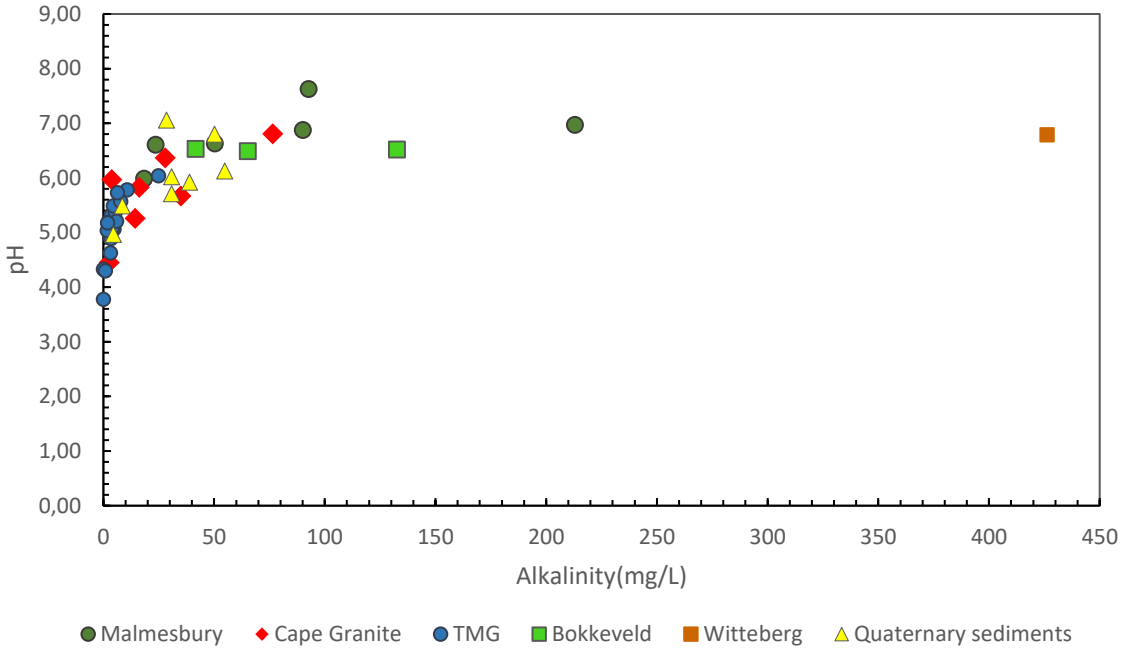

Figure 15 - pH vs Alkalinity diagram in order to illustrate the relationship between the pH and the alkalinity in the groundwater samples

3.3.2. Electrical Conductivity (EC)

The groundwater has an electrical conductivity ranging between 25.3 and 3020 µS/cm (Fig. 16) with significant overlap between the different groups. Groundwater associated with the Malmesbury Group had EC values of 1158 – 1753 µS/cm with the exception of three samples collected in Paarl with lower EC values of 56.6 – 158 µS/cm, which overlapped with some groundwater associated with the TMG. The groundwater associated with the aquifer had EC values within the range of 86.5 – 834 µS/cm. Groundwater assumed to be associated with the TMG had low EC values (25.3 – 489 µS/cm), however, two coastal TMG samples had elevated EC values of 1046 and 2570 µS/cm respectively which overlapped with the Malmesbury Group and Witteberg Group (2500 µS/cm). Groundwater associated with the Bokkeveld Group had EC values of 141 – 394 µS/cm, with the exception of one

sample collected further inland in Barrydale that exceeded 3000 µS/cm. Groundwater associated with the Quaternary sediments recorded EC values of 196 - 951 µS/cm, samples collected in Stellenbosch had lower ECs compared to samples collected in Kuilsriver and Cape Town (Fig. 16).

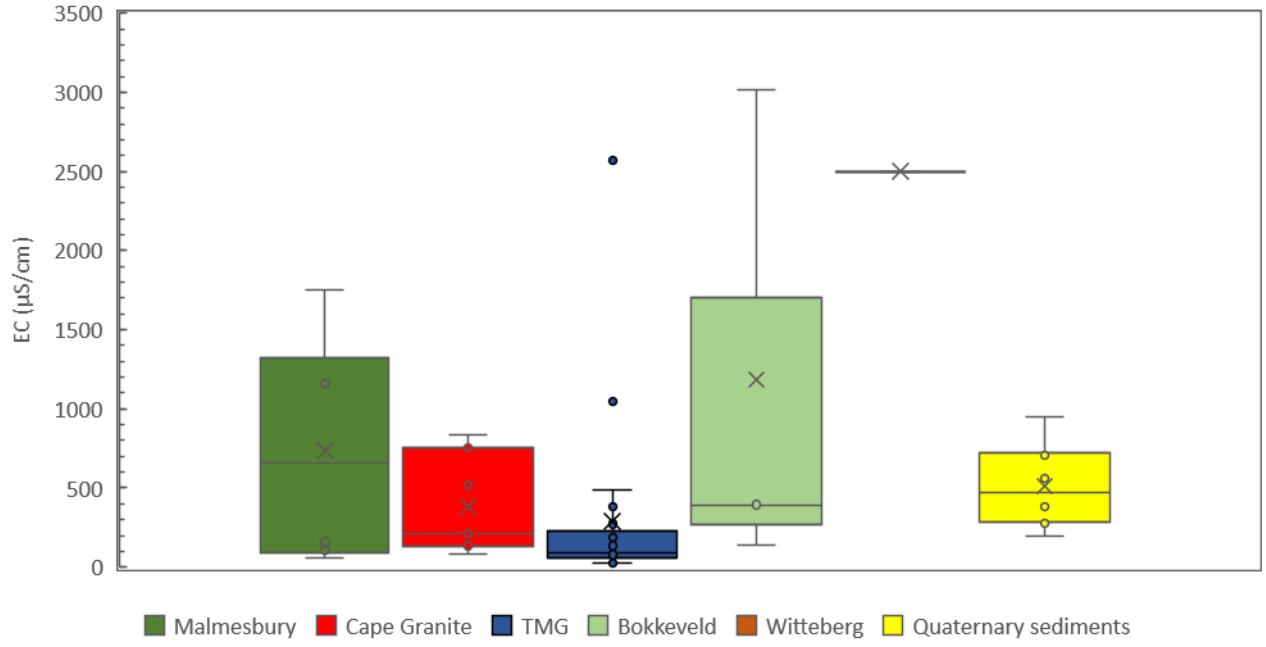

Figure 16 - Electrical Conductivities (EC) of the groundwater samples within their inferred host aquifers.

3.3.3. Cations and Anions.

Groundwater alkalinity ranged between 0 and 426 mg/L. Groundwater associated with the Malmesbury Group recorded variable alkalinities between 18.4 – 213 mg/L. Groundwaters associated with the Cape Granite Suite recorded moderate alkalinities ranging between 2.60 to76.5 mg/L. Groundwater associated with the TMG aquifer recorded the lowest range in alkalinity from 0 to 24.9 mg/L. Groundwater samples associated with the Bokkeveld Group recorded alkalinities from 41.8 to 133 mg/L. A single groundwater sample associated with the Witteberg Group recorded the highest alkalinity in dataset of 426 mg/L. Groundwater associated with the Quaternary sediments recorded moderate alkalinities ranging from 4.60 to 54.8 mg/L and similar to the pH showed a significant overlap with the alkalinity range recorded by the Cape Granite Suite. The alkalinity of the groundwater associated with the Quaternary sediments resembled that of the groundwater associated in the TMG aquifer as being low in some cases (4-8 mg/L) but generally within the ranges of 30 - 55 mg/L.

Groundwater associated with the Malmesbury Group had low Mg^{2+} and Ca^{2+} concentrations with slightly elevated Na^{+} and Cl^{-} concentrations. The groundwater associated with the Cape Granite Suite had higher concentrations of Na^{+}, Cl^{-}, Mg^{2+} and SO_4^{2} with lower HCO_3^{-} concentrations and once again,

similar to the Quaternary sediments, did not show a distinct groundwater type. Groundwater associated with the TMG has a distinct hydrochemical composition with higher concentrations of Cl^- and Na^+, and very low concentrations of Ca^{2+} and Mg^{2+}, resulting in the groundwater being classified as a saline water type despite the very low EC values. Groundwater associated with the Bokkeveld Group had varied ion concentrations. A sample from Ceres (Cer001) had elevated concentrations of SO_4^{2-} and Ca^{2+} with lower Na^+ and Cl^- concentrations, while a sample from Barrydale (BD001) had moderate Ca^{2+} and Mg^{2+} concentrations with lower concentrations of SO_4^{2-}. A sample obtained from Montagu recorded moderate Ca^{2+} and Mg^{2+} concentrations. The single groundwater sample from the Witteberg Group had elevated Ca^{2+} and Mg^{2+} concentrations. Groundwater associated with the Quaternary sediments was challenging to characterise. Ca^{2+} concentrations were low, Na^+ and Cl^- concentrations were moderate and SO_4^2 concentrations were elevated and this combination of concentrations did not result in a distinct groundwater type. (Fig. 17).

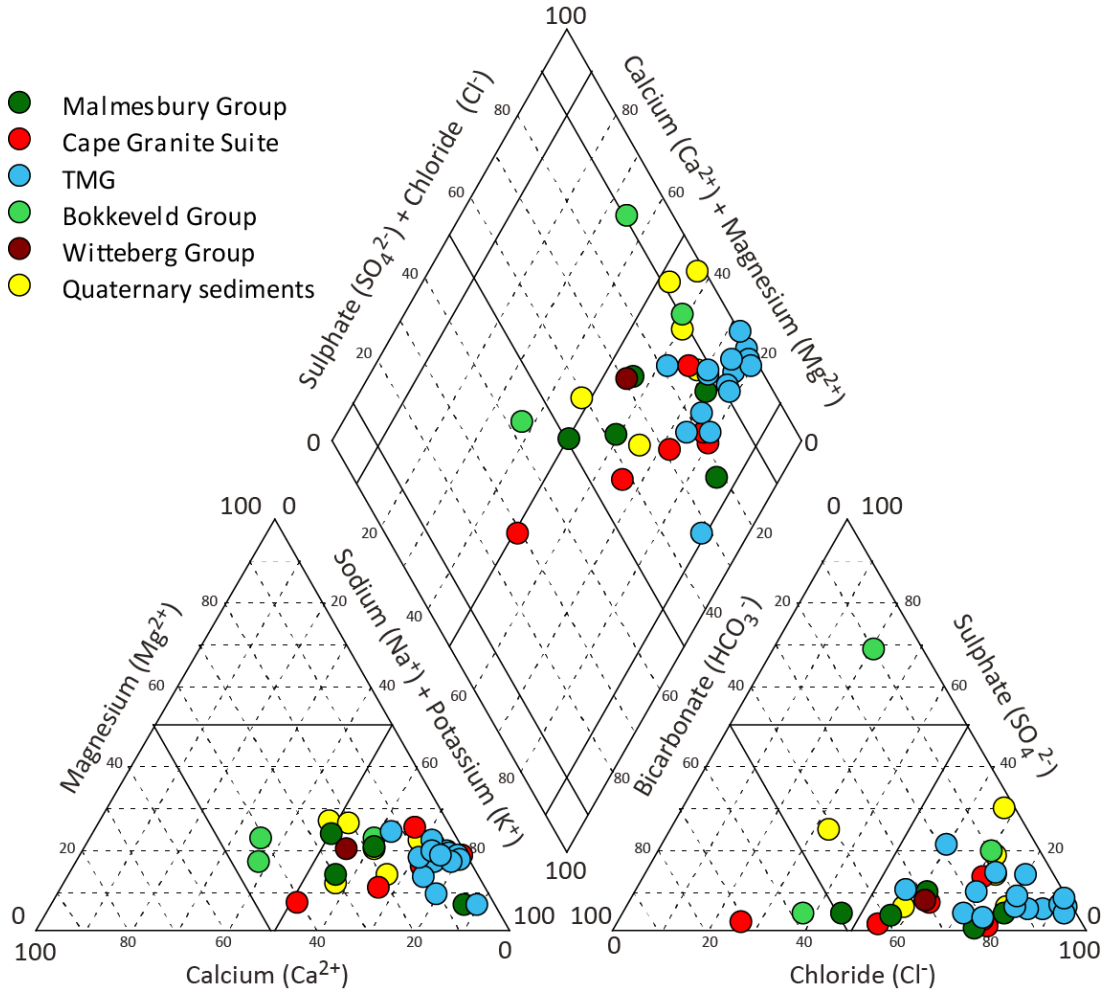

Figure 17 - Piper Diagram of all groundwater samples collected during this study. The samples were assigned different colours according to their aquifer type. Accordingly, Light Green represented samples associated with the Malmesbury Group, red the Cape Granite Suite, blue the TMG, dark green the Bokkeveld Group aquifer, brown the Witteberg and yellow indicated samples collected in Quaternary sediments.

The borehole depth (as provided by the borehole owner) was plotted against major ions such as Na^+ and HCO_3^-. The borehole depths ranged between 1.83 m and 258 m. Groundwater associated with the Malmesbury Group and the Cape Granite Suite showed little change in their ionic concentrations as a consequence of change in depth. Groundwater samples associated with the TMG aquifer plotted at low ionic concentrations and these samples recorded little change with depth (Fig. 18). The groundwater associated with the Quaternary sediments generally plotted closely together at shallow depths with low ionic concentrations and little change in the ionic concentration as a consequence of depth was noted. Borehole depths were not provided for the Witteberg Group sample (Fig. 18).

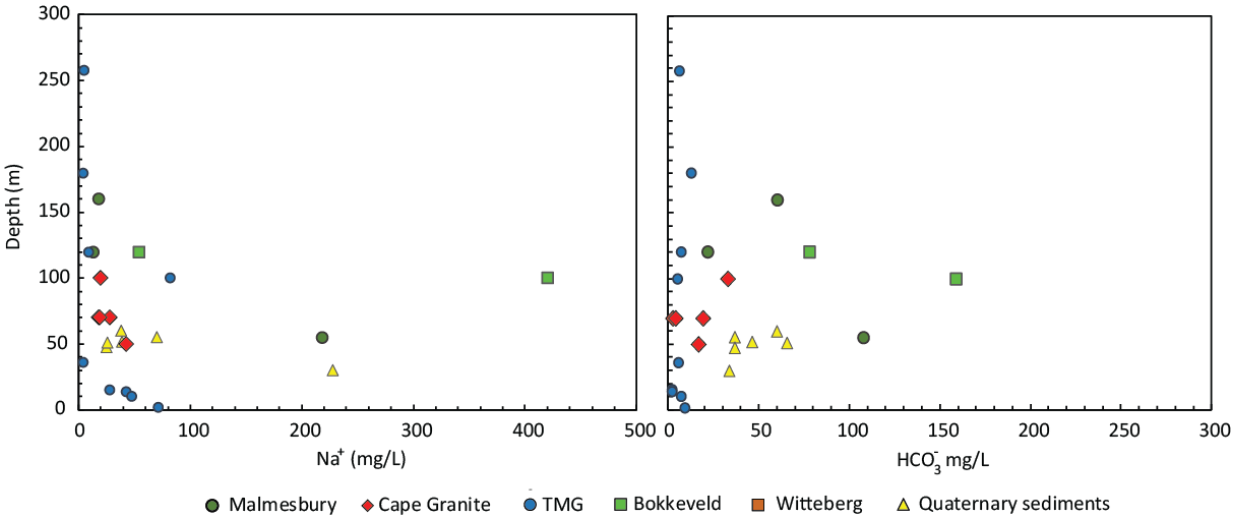

Figure 18 - Ion concentration as a function of borehole depth. The borehole depths were plotted as a function of the assumed aquifer. Borehole depths were provided verbally by the farmers or borehole owners.

3.3.4. Stable Isotopes (δD and $\delta^{18}O$)

The groundwater samples had mean δD and $\delta^{18}O$ values of -26 ‰ and -4.3 ‰ respectively. δD and $\delta^{18}O$ values show a strong correlation (r^2 =0.94) with a straight - line relationship of $\delta D = 6.7\ \delta^{18}O + 8.7$ The results correlate with the LMWL derived by Harris et al. (2010) and a slight evaporation and concentration trend is observed in the samples in comparison to the Global Meteoric Water line (GMWL) (Craig, 1961) (Fig. 19).

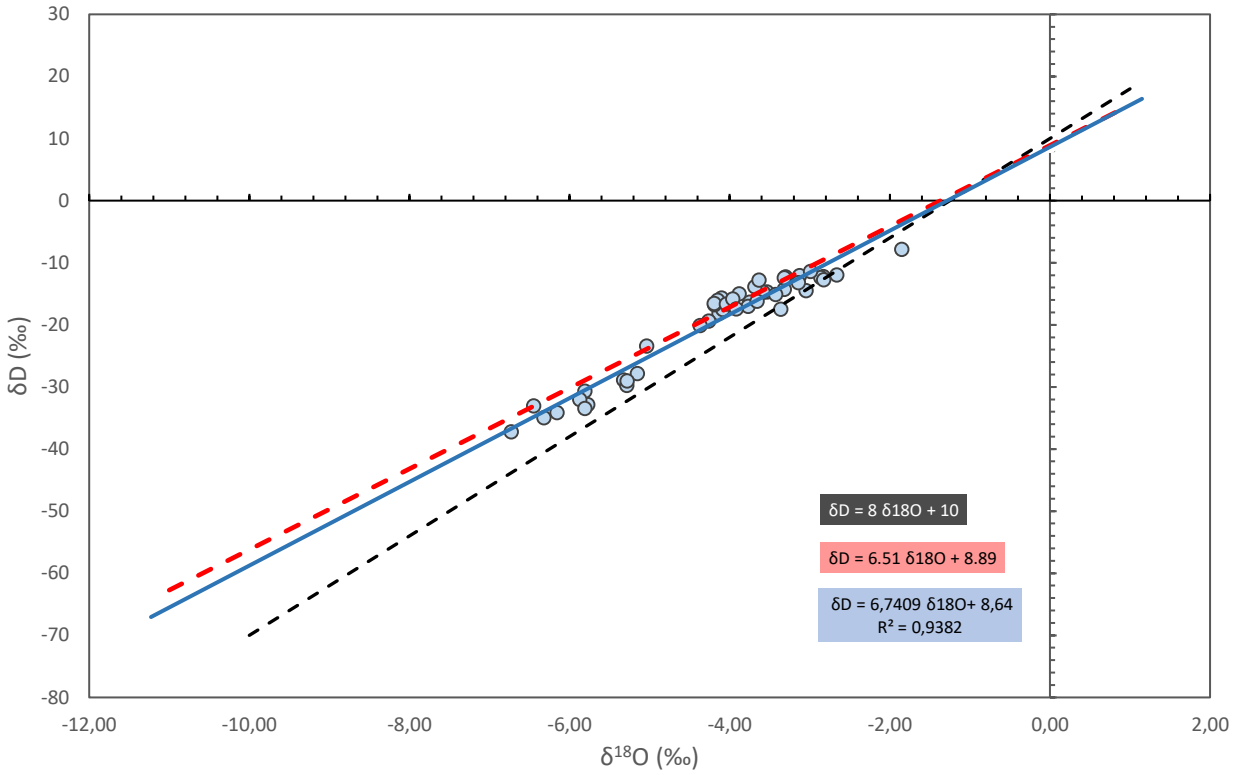

Figure 19 - Local Groundwater line plotted against Cape Town's LMWL and the GMWL. The groundwater samples were highlighted in Blue while the LMWL was in red with the GMWL indicated by the Black line.

The groundwater samples further illustrated a strong correlation with change in altitude (Fig. 20). Groundwater samples collected closer to the coast, at a lower elevation (obtained from 70-125 m above sea level (asl)) recorded more positive δD and $\delta^{18}O$ values, ranging between -20.1 and -7.8 ‰ and -4.4 and -1.9 ‰ respectively. Areas of higher elevations, further inland and along the Cape Fold Belt (obtained at higher elevations than 500-700 m asl) recorded more negative mean δD and $\delta^{18}O$ values of -30.3 ‰ and -5.9 ‰ respectively.

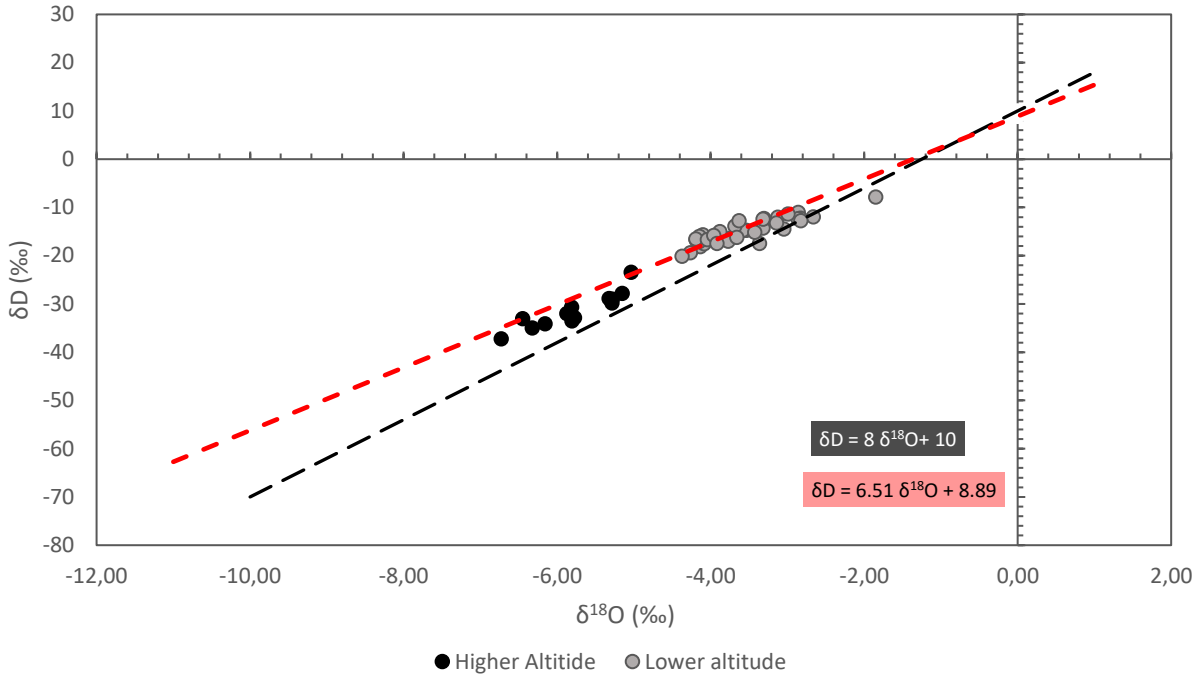

Figure 20 - Groundwater samples plotted as a function of altitude with the samples divided into two groups. Groundwaters obtained at lower elevations were obtained from 70-125 m above sea level(asl) while samples obtained at higher elevations were obtained at 500-700 m asl. Local Groundwater line plotted along Cape Town's LMWL (red line) derived by Harris et al. (2010) and the GMWL (black line) derived by Craig, 1961.

3.4. DISCUSSION

Hydrochemical parameters were applied to the groundwater samples collected in this study to determine their respective host aquifers. In addition to the hydrochemistry presented, the characterisation of the groundwater samples was done by utilizing literature and previous hydrochemistry and sample location relative to surrounding geology. Seven groundwater samples with known hydrochemical properties were obtained from geologically defined boreholes, five from the TMG, one from the Bokkeveld Group and one from the Malmesbury Group. These seven groundwater samples were included in the data and were used to establish the hydrochemical character within these respective aquifers. Figure 21 illustrates a distribution of the hydrochemical results as a function of the inferred host aquifer. The pH throughout the aquifers was within the range of 5 to 7. The majority of the groundwater samples had alkalinities that were typically ≤ 100 mg/L while the EC values were divided into three groups. Group (1): groundwater samples with EC values of ≤ 500 µS/cm, group (2) groundwater samples with EC values between 550 and 1800 µS/cm and group (3) groundwater samples with EC values that exceed 2000 µS/cm. Furthermore, two groups are identified in the δD and $\delta^{18}O$ values, samples tending to be more positive in their $\delta^{18}O$ values (-4.5 – (-1.0) ‰) and samples tending to be more negative in their $\delta^{18}O$ values (≤ -5.0‰). A general overview

of the main characteristics associated with the aquifer types is given below in addition to the applicability of the hydrochemistry in order to delineate and identify these host aquifers.

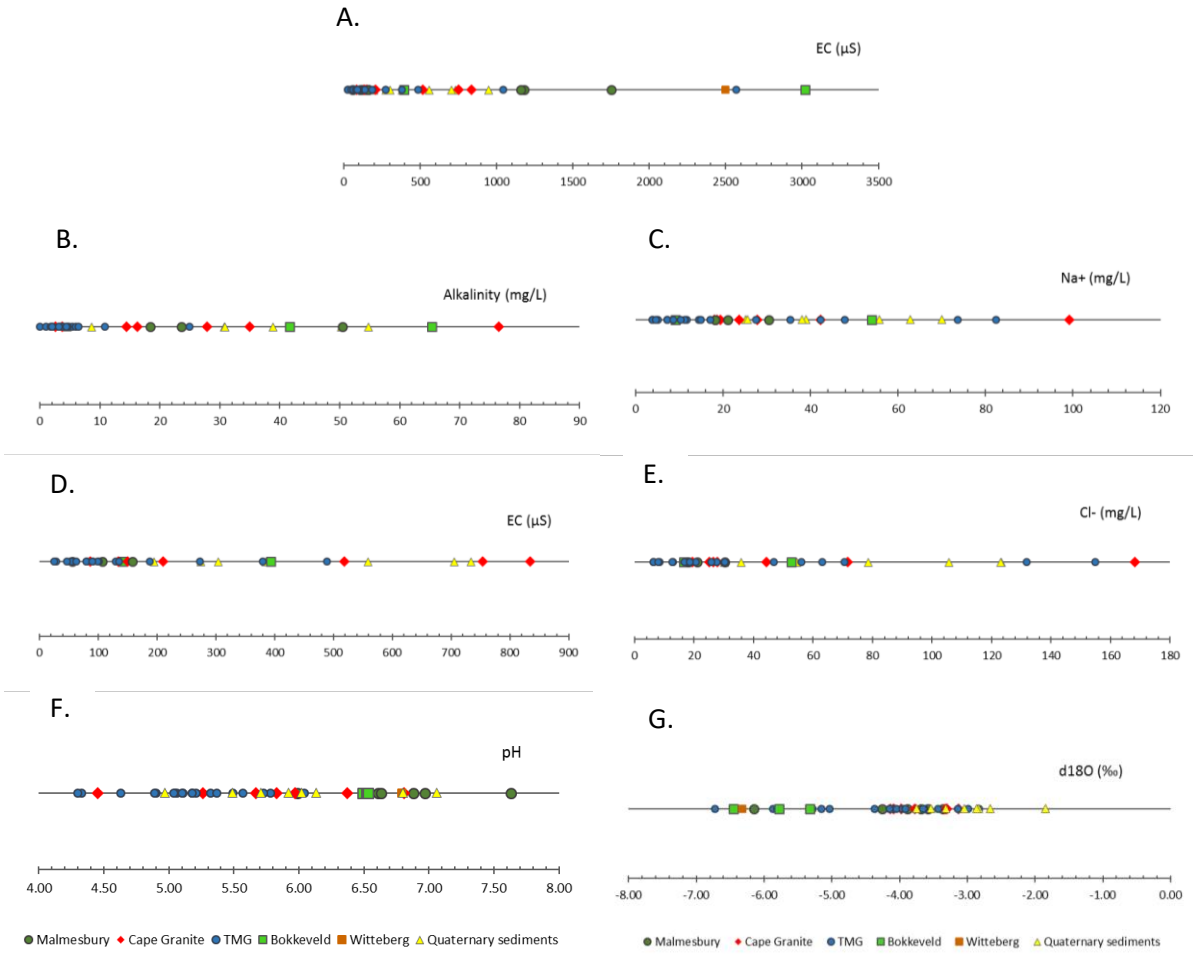

Figure 21 - Distribution of hydrochemical parameters in inferred aquifer. The major outliers were removed out as they skewed the data, consequently the Witteberg sample was removed. (A) Shows all the samples on an EC plot, with the same plot with the outliers removed given as (D). Only Na^+ and Cl^- were illustrated for the ion concentrations within each aquifer. (B) to (G) illiterates the alkalinity, Na^+, EC, Cl^-, pH and $\delta^{18}O$ respectively.

3.4.1. Geological Characterisation of Groundwater

Prior to utilising the hydrochemical properties of the groundwater, the borehole surroundings and its geological location were taken into account. By identifying the geological location of the borehole based on the owner's knowledge of the borehole casing and depth and intercepted geology, the groundwater was characterised accordingly. Five groundwater samples were associated with the TMG and two groundwater sample were associated with the Malmesbury Group. In both cases adequate knowledge about the borehole casing, depth and aquifer intercepted was known. These samples were then characterised as being associated with those respective groups and thus served as ideal model samples for that respective group. It should be noted that although limited information was known about the borehole, it was believed that the dominant aquifer intercepted would dominate in the

groundwater obtained. Therefore, its hydrochemical properties would dominate, thus enabling the groundwater to be characterised based on the hydrochemistry.

3.4.2. Hydrochemical Characterisation of Groundwater in TMG

The TMG was the initial targeted aquifer but due to different contributing factors, additional aquifers were included in the study. A distinctive trait of groundwater associated with the TMG aquifer is its low ionic concentrations which is linked to its low EC levels. The five groundwater samples characterised as being associated with the TMG based on their geological location possessed these hydrochemical attributes. Groundwater associated with the TMG is dominant in sodium (as its major cation) and chloride (as its major anion) and is hence classified as being Na-Cl dominant (Smart and Tredoux, 2002). Accordingly, these groundwater samples clustered to the bottom right of the Piper diagram indicating elevated Na^+ and Cl^- concentrations with very low Ca^{2+} and Mg^{2+} concentrations. Due to its low Ca^{2+} and Mg^{2+} concentrations and alkalinity, buffering capacity of the carbonate system particularly low. This in conjunction with high acidity have led to the groundwater associated with the TMG being corrosive (Smart and Tredoux, 2002).

One groundwater sample associated with the TMG aquifer deviated from the general hydrochemical characteristics of this aquifer, as it had elevated HCO_3^- concentrations. The increased concentrations of HCO_3^- made this sample an outlier (Fig. 17). However, this sample had a low alkalinity (≤ 5 mg/L) but with a slightly higher EC (≈ 100 µS/cm). This sample was similar to the TMG in its alkalinity and ionic concentration of Na^+ and Cl^-. However, its elevated EC and elevated HCO_3^- concentrations are suggested to result from groundwater mixing. Two coastal groundwater samples associated with the TMG were identified as being influenced by sea water intrusion. This was based on either elevated EC values that exceeded 1000 µS/cm or anomalously high concentrations of Na^+ and Cl^-. In order to determine if the groundwater samples were influenced by sea water intrusion, the following formulae were applied:

$$(Cl^-/(\sum \text{anions}) \qquad \text{Eqn 5.}$$

$$Na^+/(Na^+ + Cl^-) \qquad \text{Eqn 6.}$$

Groundwaters with chloride/total anion ratios greater than 0.8 typically indicate an origin from either the dissolution of halite or seawater intrusion. Groundwaters with Na^+/ (Na^++Cl^-) ratios equal to 0.5 indicate derivation from the dissolution of halite. Based on Eqn 6 groundwaters with Na^+/ (Na^++Cl^-) ratios that are less than 0.5 indicate sea water intrusion. When applying these formulae to the two coastal samples, it would seem that there was some seawater influence in the aquifer (Hounslow,

1995; Kortatsi, 2006). Based on these equations, it is not clear whether this is direct sea water ingress or wind-blown marine aerosols washed into the aquifer. Although the EC is elevated, it is still a long way from sea water (55 000 µS/cm) and hence the Na/Cl ratios are most likely controlled by wind-blown marine aerosols(Saidian et al., 2016; Stuyfzand, 2014). The atmospheric Na/Cl ratio, related to sea salt, increases in continental rain due to the separation of Na and Cl during transportation from sea to continent (Mæller, 1990; Saidian et al., 2016; Stuyfzand, 2014). Therefore, during precipitation or dry deposition, Na^+ and Cl^-concentrations are elevated and therefore contribute to an increased Na^+/Cl^- concentration in groundwater.

3.4.2.1. Hydrochemical characterisation of groundwater into additional aquifers.

EC and alkalinity were the primary parameters used to identify groundwater that was not associated with the TMG aquifer. Groundwaters associated with the other five aquifers generally had elevated EC values (Fig. 21). Groundwater associated with the TMG has low ionic concentrations while the rest of aquifers have higher concentrations (Fig. 22A, B). Based on these factors, groundwaters associated with elevated EC, alkalinity, pH and/or ionic concentrations were deemed to be not associated with the TMG aquifer. These groundwaters were then further characterised into one of the other aquifers.

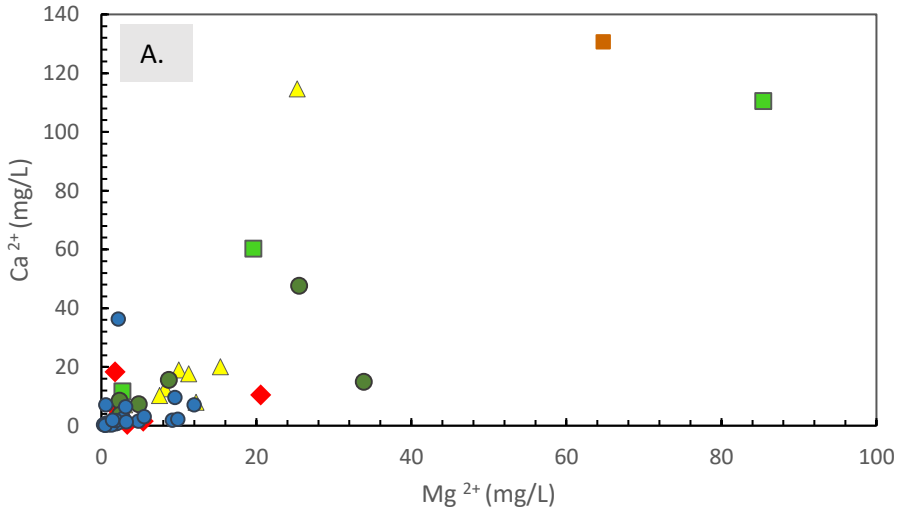

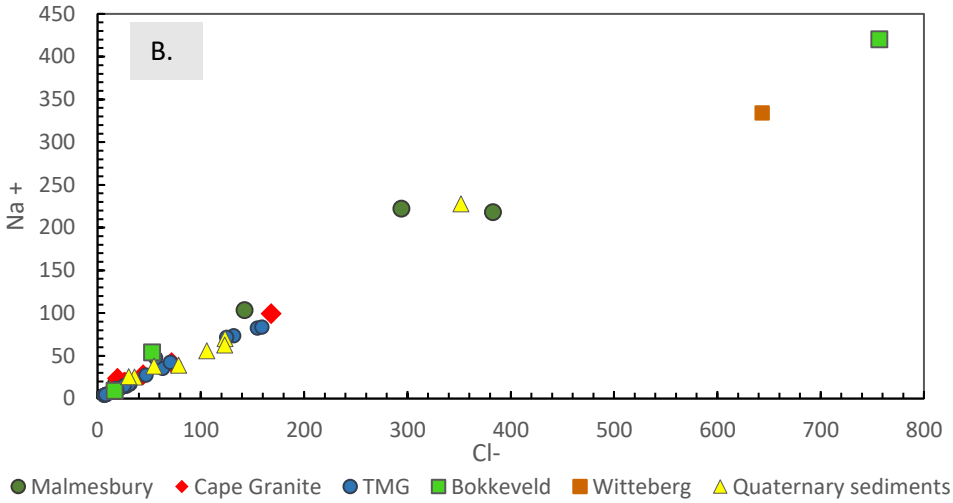

Figure 22 - (A) Ca^{2+} vs Mg^{2+} concentration distribution of all groundwater samples. (B) Na^{+} vs Cl^{-} plot of all groundwater samples indicting one to one relationship

Groundwater associated with the Malmesbury Group was expected to have high ECs and alkalinities due to the host rock composition, which is dominated by shales). Shales are enriched with clay minerals that have a high cation-exchange capacity (CEC) (Saidian et al., 2016; USDA, 2011). During infiltration and percolation, these ions are leached from soils and are transferred into the groundwater contributing to elevated ion concentrations. Therefore, groundwaters associated with the Malmesbury Group were characterised as having ECs in excess of 1000 µS/cm (with the exception of three samples with ECs in the range of 50-100 µS/cm), with alkalinities ≥ 90 mg/L (with the exception of three samples with alkalinities in the range of 18-50 mg/L and a pH of ≈ 6.5). These hydrochemical properties were consistent previous work on the Malmesbury Group aquifer in Paarl (Conrad et al., 2019).

Groundwater associated with the Cape Granite Suite was more acidic with varied alkalinity. This varied alkalinity was further associated with variable EC values in this aquifer. These variations were further pronounced in the ionic concentrations of these groundwater samples and thus indicated three end members. The first end-member group was defined by groundwater samples obtained at lower elevation, along coastal regions such as Somerset West, with EC values within the range of 500 - 700 µS/cm, elevated Ca^{2+}, Mg^{2+} and SO_4^{2-} and Na^{+} concentrations (generally exceeding 42 mg/L of Na^{+}). The second end member was defined by samples obtained at higher elevations (such as Paarl) with elevated EC values (≥ 800 µS/cm) and moderate Na^{+} and Cl^{-} concentrations (within the range of 20 - 40 mg/L respectively). In both groups, elevated Ca^{2+}, Mg^{2+} and Na^{+} concentrations suggest fluid-rock interaction with alumino-silicates such as weathered albitic plagioclase, hornblende and pyroxenes (Kortatsi, 2006). The third end member within the Cape Granite Suite was defined by groundwater

samples with elevated HCO_3^- and [Mg^{2+}+Ca^{2+}] concentrations, EC values between 80 – 200 µS/cm and higher pH values above 6.

A sample obtained from Montagu springs was characterised as being associated with the Bokkeveld Group due to its geological location and literature. This sample recorded high HCO_3^- concentrations and was identified to be situated along an E-striking fault, along the TMG-Bokkeveld Group contact (Diamond, 1997; Netili, 2007). As the thermal spring is situated on the contact, it could be a product of groundwater mixing between the Bokkeveld Group and TMG groundwater. Two more samples were characterised as being associated with the Bokkeveld Group due to its distinct ion concentrations and EC values that exceeded 1000 µS/cm. These samples were obtained in Barrydale and Ceres. These samples had moderate Mg^{2+}, Ca^{2+} and SO_4^{2-} concentrations and low Na^+ and Cl^- concentrations. The observed increase in certain ions such as Ca^{2+} can be attributed to the dissolution of calcic minerals within the rock such as plagioclase feldspar. The Ceres sample had increased HCO_3^- concentrations possibly indicating fluid-rock interaction associated with silicate rock weathering as well as incorporation of atmospheric CO_2 into soil horizons through which percolation occurs.

A single groundwater sample associated with the Witteberg Group plotted independently due to its hydrochemical parameters (Figure 17) of elevated ionic concentrations of Na^+ and Ca^{2+} (≥ 300 and 100 mg/L respectively) and elevated HCO_3^- concentrations (≥ 500 mg/L). The elevated concentrations of Na^+ and Ca^{2+} suggest the weathering of plagioclase feldspar, while the presence of HCO_3^- may have been derived from CO_2 in the atmosphere similar to the Bokkeveld Group.

The groundwater associated with Quaternary sediments had low concentrations of Ca^{2+} and Mg^{2+} with slightly elevated concentrations of Na^+ and Cl^- (within the ranges of ± 100 mg/L). This hydrochemistry were consistent with work on the Cape Flats alluvial aquifer (Adelana et al., 2010). The general dominance of the anions and cations in the Quaternary sediments was Cl^- > HCO_3^- > SO_4^{2-} and Na^+> Ca^{2+}> Mg^{2+}> K^+ respectively. These groundwaters recorded elevated EC values that varied as a consequence of distance to coast. Groundwater samples obtained further inland (in Stellenbosch) recorded EC values between 190 - 300 µS/cm while samples obtained closer to the coast recorded EC values that were significantly higher (≥700 µS/cm). The samples obtained closer to the coast were noted to have been obtained from within the Cape Flats aquifer. The Cape Flats aquifer is characterised by dense human settlements along with numerous industrial and agricultural activities. Due to the aquifer's shallow depth, this aquifer is prone to pollution and thus contributing to its elevated EC value (Hay et al., 2015).

In characterising the groundwaters into their respective host aquifers, some data uncertainties were identified. The assignment of groundwaters to different aquifer systems was based predominantly on the hydrochemistry of the groundwater samples. However, in order to make conclusive findings, additional knowledge about the borehole depth, borehole casing and which aquifer was being pumped from was required. Insufficient knowledge about these field observations introduced additional uncertainties surrounding the data interpretations. In knowing the exact borehole depth and type of borehole casing, the groundwater characterisation would have been better substantiated. Unfortunately, for most of the borehole sample sites used here, knowledge about the borehole casing construction and borehole depths were obtained from the owners. However, in many cases the boreholes were old and the farms had changed hands at least once and as a result, information about the borehole construction had been lost. In future, it should be mandatory for all boreholes that are installed to log the borehole geology and construction and lodge this information in a central in perpetuity repository such as the National Groundwater Archive. Although legislation exists already requiring this, it is not always acted on and certainly for older boreholes much of this information appears to be lost.

3.4.3. δD and $\delta^{18}O$ Spatial Variation in Groundwater.

Analysis of the stable isotope data provided additional insights to the hydrochemical variability of the groundwater. Enrichment in the heavier isotopes closer to the coast and a depletion in the lighter isotope further inland was expected due to the influence of coastal and orographic precipitation. During precipitation the heavier isotope will condense faster than the lighter isotope because of the energy involved during the partitioning of the different isotopic water molecules (Gat, 1996). Rayleigh fractionation describes a model that accounts for the preferential movement of the lighter or heavier isotope based on kinetics and temperature (Celle-Jeanton et al., 2004). As precipitation continues, the rain progressively becomes isotopically lighter (depleted in the heavier isotope). Thus, rain originating over the ocean and traversing inland, becomes isotopically lighter as a consequence of Rayleigh fractionation (Craig, 1961). This trend in the rainwater is what accounts for the δD and $\delta^{18}O$ signature observed in the groundwater. As numerous factors affect the δD and $\delta^{18}O$ values in rainwater such as the type of rainfall, the origin of the precipitation, the above conclusions were based on the assumption that the region receives precipitation that originates from the ocean and proceeds further inland.

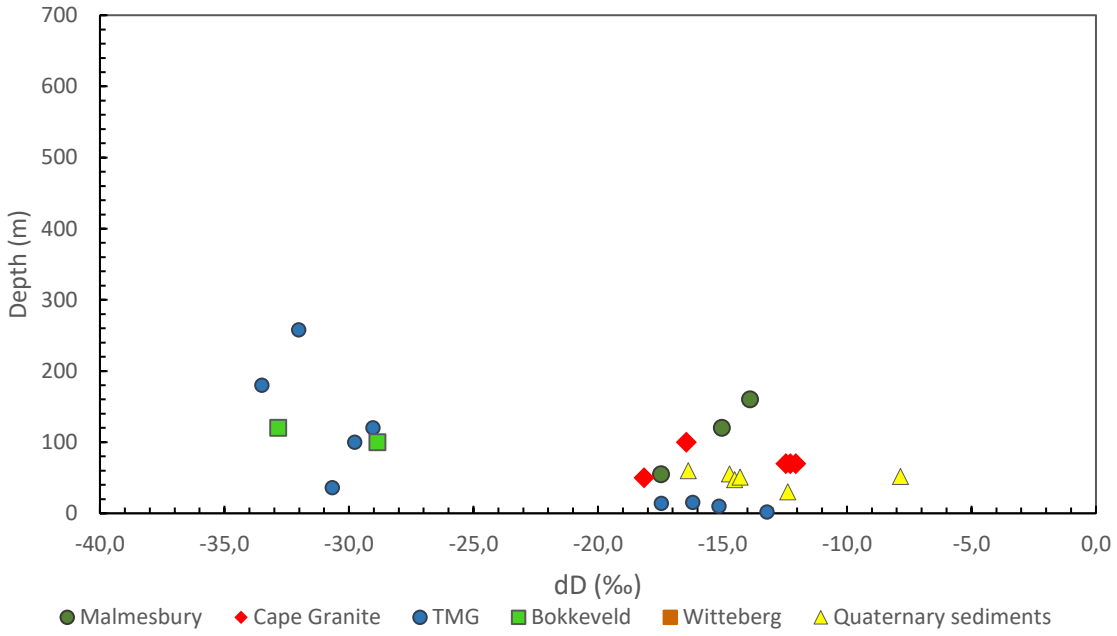

Figure 23 - Changes in δD and δ18O values as a consequence of borehole depth

In plotting the δD and $\delta^{18}O$ values against borehole depth (Fig. 20), it was noted that deeper groundwater samples recorded a more pronounced depletion in the heavier isotopes. Two of these samples were associated with being older in age (pMC ≤ 65 %) (Harilall, 2020). Older groundwaters at increased depths were associated with increasingly depleted values in the heavier isotope due to limited modern groundwater recharge (Kulongoski et al., 2004; Swana, 2016). The rest of the samples however, at increased depths that are depleted in their δD and $\delta^{18}O$ values could be a result of changes in altitude as these were obtained further inland (Fig. 23).

3.5. CONCLUSIONS

Opportunistic sampling of pre-existing boreholes is usually associated with a lack of information about the borehole construction as well as aquifer host material. In some situations, owners of the boreholes had some knowledge about the surrounding geology, borehole casing and borehole depth which aided in establishment of the hydrochemical character of each groundwater sample and allowed each sample to be assigned to a specific aquifer. These well constrained boreholes and associated borehole chemistries served as “type localities” for that specific aquifer. For many of the groundwater samples though, this information was not available, and each groundwater sample had to be assigned to an aquifer based on hydrochemistry alone through comparison to these “type localities”. On this basis 23 samples were assigned to the TMG aquifer, six to the Malmesbury Group, seven to the Cape Granite

Suite, three to the Bokkeveld Group, one to the Witteberg Group and nine samples were assigned to Quaternary sediments. Groundwater associated with the TMG was distinguishable from the other aquifer systems by being characterised by distinctly lower EC and alkalinity. In future hydrochemical studies, additional knowledge about the borehole depth, borehole casing and surrounding geology would greatly enhance the characterisation of groundwater into their respective aquifers. This would require though an obligation for people installing boreholes to keep records of this information and to store this information in a public access datastore. In the following chapter, the aquifer characterisations made here are used to understand the variation in radon activity concentration in groundwater and hence how each aquifer responds to groundwater recharge.

CHAPTER 4: RADON IN GROUNDWATER

4.1. INTRODUCTION

In this chapter, the boreholes sampled in Chapter 3 are used to examine the activity of radon in groundwater. The aquifer characterisations delineated in Chapter 3 will be applied here to compare and contrast the radon activity in each aquifer. As previously indicated, serious consideration is being given to utilising the TMG aquifer to supplement municipal supply. If the potential yield of the aquifer has been overestimated, an in depth understanding of the aquifer system in terms of recharge rates will be an essential part of understanding the sustainability of the aquifer system. Radon-222 (hereby referred to as radon) is an ideal tracer in evaluating recharge dynamics due to the concentration differences observed in precipitation and groundwater. Rainwater has negligible radon activities while the radon activity concentration within an aquifer is generated from the decay of the uranium parent isotope which is found in the host rock matrix. Hence, the radon activity concentration should increase whilst the groundwater is in contact with the aquifer matrix and decrease when active recharge occurs due to the diluting effect of the precipitation. The rate of increase is related to the amount of parent isotope present in the aquifer matrix and is hence a function of aquifer rock composition and the rate of decrease is a balance between radioactive decay of radon and dilution from active recharge.

On the basis of the above, radon can be used to evaluate to different processes in the aquifer system. The first is to differentiate the different aquifer systems with regards to radon activities and the second is to demonstrate how these activities change as a consequence of groundwater recharge. By delineating the radon activity concentration within each aquifer, activity changes as a consequence of recharge may be identified. As the TMG is considered to contain groundwater with low residence times (Miller et al., 2017) and hence is actively recharged, recharge should dilute the radon activities in this aquifer making the radon in the TMG particularly low. If the dilution effect of precipitation can

be measured and the recovery time monitored this may also provide a means for estimating the timescales over which recharge occurs.

In understanding the groundwater recharge patterns, the sustainability of the groundwaters in this region may be defined. The application of radon in groundwater has not been applied in this way in South Africa and thus the data presented here is of vital importance as it introduces a new perspective for groundwater recharge studies in South Africa.

4.2. METHODOLOGY

The same sample locations used in Chapter 3 (Fig. 11) are used here for radon sampling. These locations were targeted based on their proximity to the City of Cape Town, as well as their accessibility and distance from Stellenbosch University where analysis took place. This was a key consideration as radon must be analysed within nine hours of collection owing to the short half-life of radon. Analysis after more than nine hours from collection means that a correction factor needs to be applied to account for radioactive decay and this reduces the accuracy of the results.

4.2.1. Sampling Protocol

As mentioned in Chapter 1, radon in its natural form is a gas and is therefore prone to degassing during turbulent flow. Consequently, groundwater samples collected for radon analysis must be collected in such a way to promote laminar flow to ensure that no radon diffused out of the water sample (Fig. 24). Prior to sampling, the groundwater was purged for at least 10-15 min (depending on borehole diameter and the depth to water) to ensure that standing water in the borehole pipe was not sampled and that “fresh” groundwater was sampled.

In a situation where a spring or an artesian aquifer was sampled, particularly where fresh water was pooling at the surface, radon was sampled by placing a 250 ml glass vial horizontally in the water (as close as possible to the eye) allowing for water to enter the vial under laminar flow conditions. Once the sample vial was filled, it was sealed under the water, ensuring that no air bubbles were present.

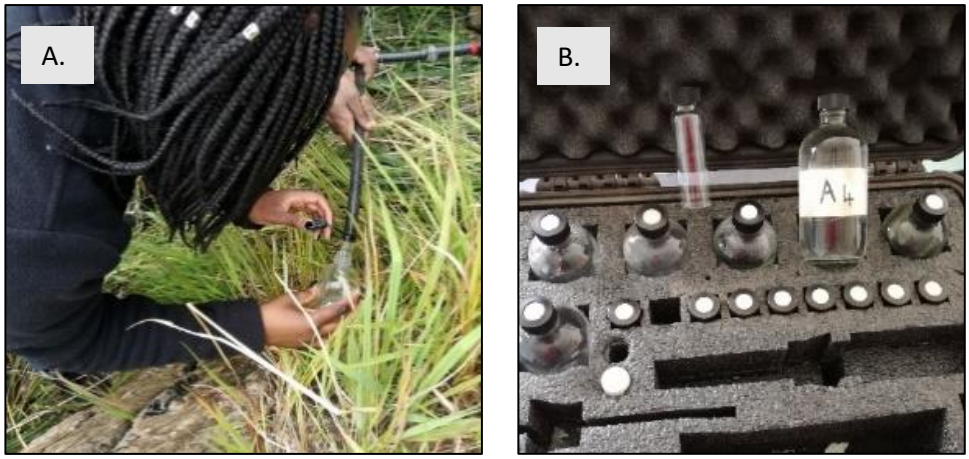

Figure 24 - Radon groundwater collection. (A): Each sample was collected in such a way that promoted laminar flow to limit radon degassing. (B): Each sample was collected in the 250 ml glass vials. The 50 ml glass was not used in this study as this wouldn't be enough of a water to indicate the radon concentration within the aquifer

4.2.2. Radon Analysis

Radon was analysed using a Durridge RAD7 detector within the Health Physics Lab (HPL) in the Merensky Building at Stellenbosch University. Due to the RAD7's sensitivity to changes in humidity, the radiation lab was constantly well-ventilated. Prior to analysis, the detector was purged to ensure that any background radon was lowered to 0.0 count per minute (CPM), and that the relative humidity was below 10%. A blank test was done to ensure that no background radon was being analysed and that the relative humidity was below 10%. Once no radon was detected during the blank tests, the instrument was ready to begin measuring the samples.

In order to acquire accurate results, each sample was analysed for 50 minutes (10-minute intervals repeating each cycle five times) (Fig. 25). These parameters were to represent the time required for precise and accurate data. It was possible to increase or decrease the amount of cycles and repetitions taken depending on the availability of time and the output data quality. Due to the time constraint of analysing each sample within nine hours of collection, increasing the cycles and repetitions would not have increased the data quality as increasing the time and thus the precision would be counteracted by having to correct for radioactive decay.

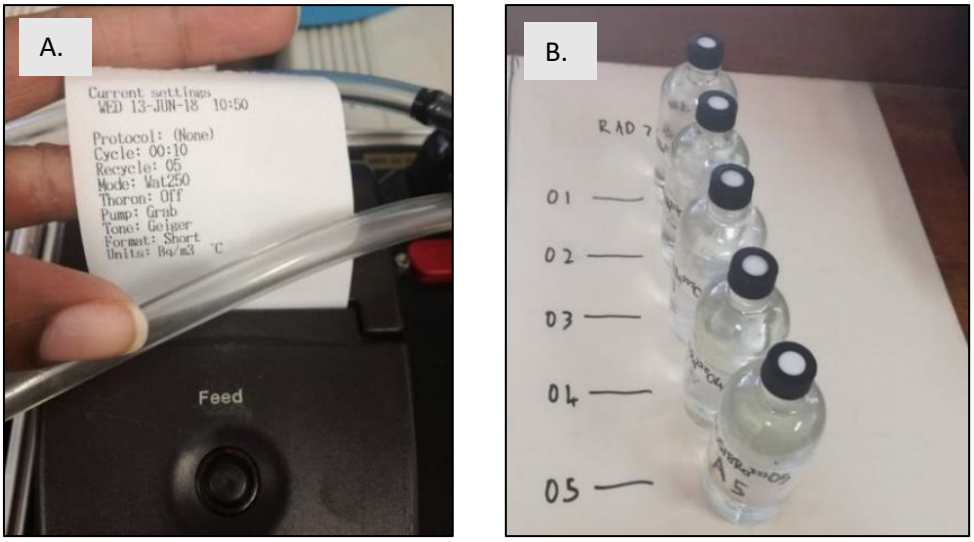

Figure 25 - RAD7 set parameters prior to radon detection. (A): These parameters are kept the same for each groundwater sample. The unit is set to measure radon in Bq/m³ (1000 Bq/m³ = 1 Bq/L³). Image (B) depicts how the samples are prepared prior to radon testing.

After all the above parameters were set and the relative humidity was below 10%, analysis was initiated. The humidity needed to be low as the radon gas would attach itself to the water molecule in the air and therefore contaminate the radon in that sample. Due to the nine-hour window period, the first sample collected was the first sample to be analysed. A glass probe (known as the frit) was inserted into the 250 ml glass vial (Fig. 26B). Once the analysis routine commenced, the frit began aerating the sample, a process that lasts approximately five minutes. This aeration process creates bubbles and allows dissolved radon to escape from the water and go into the air where the RAD7 was able to detect its activity within the headspace of the 250 ml glass vial (Fig. 26).

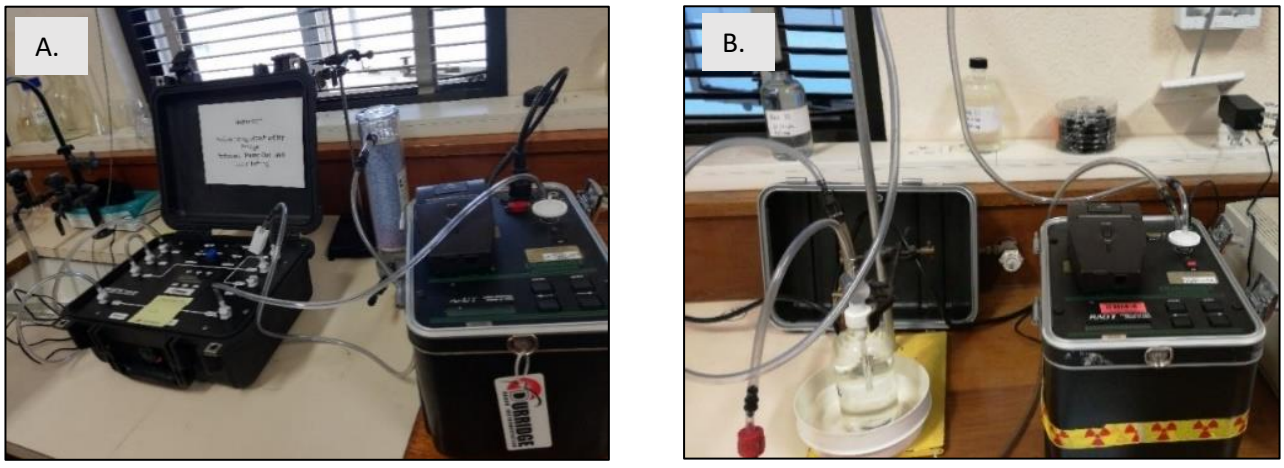

Figure 26 – (A) RAD7 detector set up with the DRYSTIK attached to it on the left. The DRYSTIK is the dehumidifier; (B) connecting the sample to the RAD7 detector with the glass vial with the frit insertedinto the water sample.

After each analysis, the detector was purged once again with a dehumidifier to reduce the relative humidity and remove any background radon in the detector, as both increase during sample analysis. The purge in-between the samples does not have a set time and is dependent on the relative humidity and the amount of radon detected in the previous sample. Consequently, the purging after each sample lasted between 20 to 60 minutes. Once the analysis was complete, the detector printed out a receipt indicating the radon activity concentration for each sample (Fig. 27). These results were saved on a hard drive within the RAD7 that was later transferred to a computer with the use of CAPTURE, software that enables the RAD7 to be linked a computer.

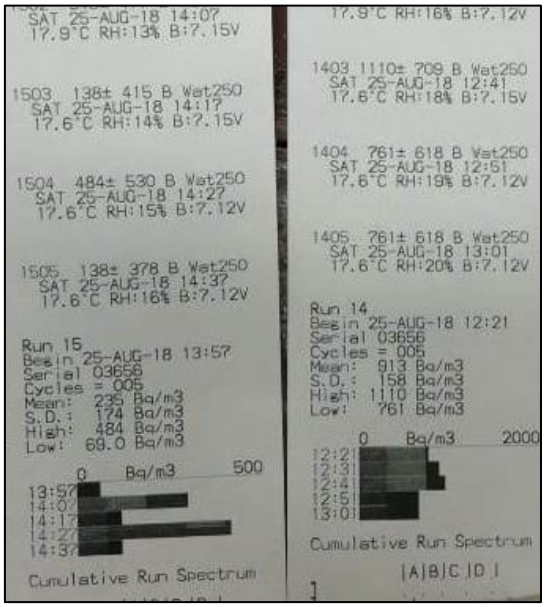

Figure 27 - Print out receipt of radon measurements for two samples tested by using the rad-7 detector. As seen in the image the measurements are presented in Bq/m³, when one uploads the data on to the computer, you can change the unit to Bq/L.

4.2.3. RAD7 Maintenance and Data Corrections

The RAD7 detector relies on α-spectroscopy as the main radiation detection method and has a radon detection range of 4.0 - 750 000 Bq/m^3 (1000 Bq/m^3 = 1 Bq/L^3) (Durridge, 2018). The RAD7's detection chamber consists of a 0.7 L internal chamber coated with an electrical conductor that utilises a solid-state ion-implantation, planar and silicon alpha detector. The detector is required to be calibrated by DURRIDGE every 12-15 months. In the event that the detector was utilised outside its 12-month calibration window, a drift could begin to occur in the radon results obtained. During this study most of the measurements were done within the detectors 12-month calibration window except for a few samples analysed on a detector that was recently outside of its calibration window (about 3 weeks out). Consequently, these samples required data corrections.

The data corrections began with split measurements. Split measurements were done in order to assess the validity of the results and to identify the magnitude of the drift in the radon results. These split measurements were done by comparing the results obtained from the out-of-its-calibration-window detector with a recently calibrated detector. These split measurements were done by obtaining 10 samples from a known high radon activity borehole (in excess of 200 Bq/L). These 10 samples were halved between the newly calibrated and the older out-of-its-calibration-window detector and were analysed individually every 4 days. During this time these 5 samples are analysed simultaneously by both detectors to record the rate of decay in radon and to highlight the difference in the radon activities recorded between the two detectors. A significant difference was noted between the two detectors, hence the data obtained from both detectors was processed independently.

For the data presented here, the data processing was done with Mr Ryno Botha and an r^2 value of 0.9831 was determined. Based on this value, Eqn 7 was applied to the uncorrected data, where $p1$ = 2.011, $p2$ = 1.899 and $x1$= uncorrected radon activity concentration (Bq/L, "Old Detector") and $f(x)$ = Y1: corrected radon activity concentration.

$$f(x) = (p1 * x1) + p2 \qquad \text{Eqn 7.}$$

Eqn 8 (which is identical in form to Eqn 7) was used to determine the measurement uncertainty, where $p1$ = 1.675, $p2$ = -0.6325 and $x1$= uncorrected radon activity concentration, (Bq/L, "Old Detector") and $f(x)$ = Y1: corrected radon error activity concentration with an r^2 of 0.968.

$$f(x) = (p1 * x1) + p2 \qquad \text{Eqn 8.}$$

These calculations were applied to all the samples that were analysed on the older out-of-its-calibration-window detector (27 out of 156 measurements). In some cases, there seemed to be either an overestimation or underestimation of the results. However, the error was within one sigma and thus the corrected data was accepted. Further data corrections were applied to the data if the overall relativity humidity for a sample was higher than 20%. This correction was done by the CAPTURE software which is linked to the raw data obtained from the RAD7.

In addition to the above, decay corrections were applied to results from samples that were analysed outside of the 8-10-hour analysis window. The average duration between sampling and a radon measurement in this study was approximately six hours. However, in order to calculate if the sample required any decay corrections, Eqn 9 was applied, where $A(0)$ was the original activity count at time zero, $A(t)$ was the activity at time t, λ is the decay constant, and t is the elapsed time.

$$A(t) = A(0) * e^{-\lambda t} \qquad \text{Eqn 9.}$$

The decay constant in Eqn 9 is calculated according to Eqn 10, where $t_{(1/2)}$ is the half-life of the radioactive element.

$$\lambda = \frac{\ln(2)}{t(1/2)} \qquad \text{Eqn 10}$$

By making use of Eqn 9 and Eqn 10 to perform a decay correction, a sample with a radon activity concentration of 121 ± 6.6 Bq/L $A(t)$ would have been analysed within the average six-hour duration (t). During these six hours of sampling and measurements, this sample would have decayed 5.6 Bq/L. Taking into account that the measurement uncertainty was 6.6 Bq/L, and the sample decayed, 5.6 Bq/L, which is within the measurement error of that sample (6.62 Bq/L), decay corrections for this sample were not applicable. Consequently, the general rule that was followed was that if the decay was greater than the measurement uncertainty, a decay correction was applied. On this basis, for the data presented in this study, no decay corrections were applied.

4.3. RESULTS

For the radon analysis, 49 groundwater sample locations were analysed, and these locations are derived from the same locations described in Chapter 3. Table 8 summarises the results of the radon analysis for each of these locations during the initial sampling in August 2018 and March 2019. From these 48 locations, nine locations were chosen to do twice weekly radon analysis between August and November 2019. In total, 156 radon analyses were completed, and full results are compiled in Appendix 1).

Table 8 - Radon in groundwater according to its respective aquifer.

Sample number	Lithology	Elevation (m)	222Rn (Bq/L)	Radon Uncert (Bq/L)
YAD18SVL001	Malmesbury	152	54.6	4.5
YAD18PV001	Malmesbury	175	63.1	4.6
YAD18ROB002	Malmesbury	224	118	6.5
YAD18DB001 (a)	Malmesbury	130	112	6.2
YAD18DB005	Malmesbury	130	166	8.1
YAD19PAA001	Malmesbury	167	22.0	3.0
YAD18RivFarm001	Granite	185	152	6.8
YADKB001	Granite	241	140	7.1
YADKB002	Granite	241	298	12
YAD18SW001	Granite	142	304	11
YAD18SW002	Granite	20	360	13
YAD19Frans003	Granite	261	370	13
YAD18Frans002	Granite	340	112	6.2
YAD18DB002	TMG	628	60.7	4.6
YAD18DB003	TMG	628	70.0	4.6
YAD18DB004	TMG	628	170	8.1
YAD19Cer002	TMG	1037	9.66	2.0
YAD18DD001	TMG	492	13.5	2.1
YAD18DD002	TMG	490	102	5.9
YAD18BD002	TMG	383	53.7	4.2
YAD18Vill001	TMG	361	28.3	3.0
YAD18Frans001	TMG	273	6.58	2.0
YAD19MP001	TMG	202	14.3	2.2
YAD19NW001	TMG	28	33.7	3.3
YAD19TM001	TMG	900	1.04	0.7
YAD19SprFrans001	TMG	486	28.4	3.1
YAD19Vills002	TMG	361	50.2	4.1
YAD19Vills003	TMG	361	33.4	3.3
YAD19GB001	TMG	279	14.0	2.4
YAD19KM001	TMG	11.0	19.6	2.2
YAD19KM002	TMG	11.0	3.80	1.3
YAD19Kmond001	TMG	27.0	12.0	2.0
YAD19Kmond002	TMG	27.0	4.32	1.2
YAD19Kmond003	TMG	27.0	3.36	1.1
YAD18Cer001	Bokkeveld	519	7.36	1.7
YAD18BD001	Bokkeveld	383	15.1	2.2
YAD18MON001	Bokkeveld	224	121	6.6
YAD18ROB001	Witteberg	192	12.0	2.1
YAD018Ra222-01	Quarternary	136	35.5	3.4
YAD018Ra222-02	Quarternary	136	653	20
YAD018Ra222-04	Quarternary	136	76.8	5.4
YAD018Ra222-05	Quarternary	136	98.4	6.2
YAD018Ra222-06	Quarternary	136	127	7.6
YAD19TK001	Quarternary	26.0	13.7	2.1
YAD19TK002	Quarternary	26.0	8.74	1.7
YADKR001	Quarternary	55.0	2.94	1.2

4.3.1. Aquifer Radon Activity

The results presented here are all the radon activity concentrations recorded during August 2018 and March 2019 (Fig. 28). Radon activities in groundwater are quite varied. The lowest radon activity concentration was recorded in a spring on Table Mountain with an activity concentration of 1.04 ± 0.7 Bq/L, while a sample collected in Stellenbosch recorded the highest radon concentration of 653 ± 20 Bq/L. The radon activity concentration in groundwater associated with the Malmesbury Group was between 22.1 ± 3.0 and 166 ± 81 Bq/L. The radon activity concentrations in groundwater associated with the Cape Granite Suite are distinctly higher than the other aquifer systems and were between 112 ± 6.2 and 370 ± 14 Bq/L. The radon activity concentration in groundwater associated with the TMG aquifer was between 1.04 ± 0.7 and 61 ± 4.8 Bq/L albeit with outliers of 102 ± 5.9 Bq/L and 170 ± 8.1 Bq/L. The radon activity concentrations in the TMG are similar to those of the Quaternary sediments where radon activity concentrations were between 2.9 ± 1.2 Bq/L and 98 ± 6.2 Bq/L with an outlier of 653 ± 20 Bq/L. The three samples from the Bokkeveld Group had variable radon activity concentrations between 7.4 ± 1.7 and 121 ± 7.0 Bq/L, whilst the Witteberg Group sample had a relatively low radon activity concentration of 12.0 ± 2.12 Bq/L respectively.

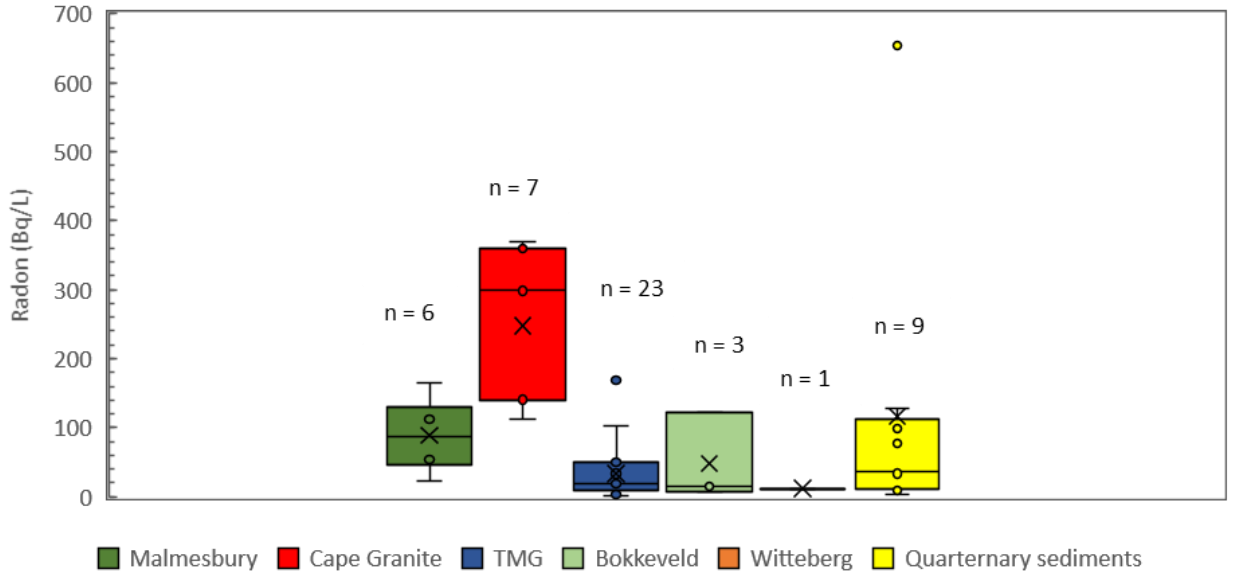

Figure 28 - Radon results according to inferred aquifer host.

A single hot spring analysed in this study (the Montagu Hot Spring) recorded a radon activity concentration of 121 ± 6.6 Bq/L, which was higher than several cold springs that were analysed from the TMG aquifer. The cold springs generally recorded radon activity concentrations of ≤ 60 Bq/L (with the exception of one spring that recorded 170 ± 8.1 Bq/L) (Fig. 29).

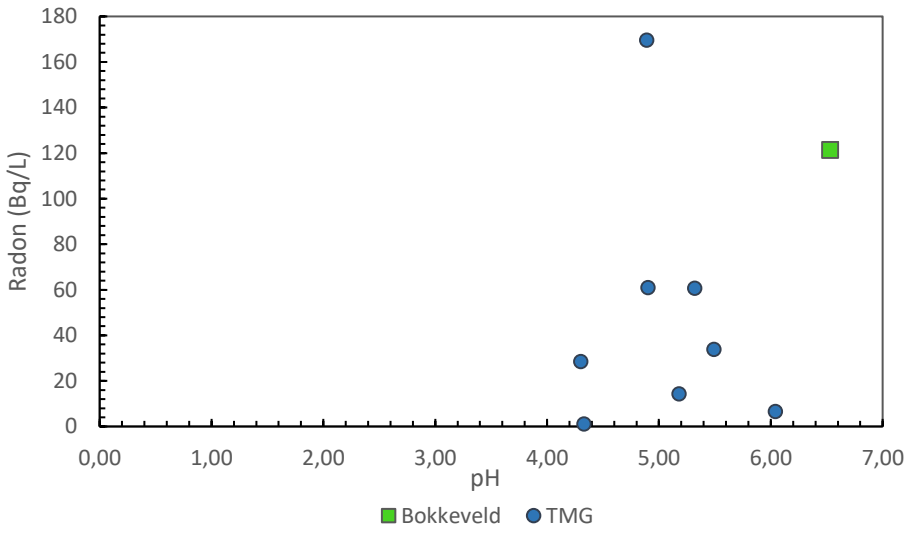

Figure 29 - Hot and cold spring radon activity. The cold springs were samples predominantly collected in the TMG and are therefore identified as the dark blue circles. The hot spring was collected along a fault boundary between the TMG and Bokkeveld aquifers, in Montagu and is identified as the green square.

4.3.2. Temporal and Spatial Variation in Radon

Once the range of radon activity concentrations had been determined for the different aquifer systems, nine sites were selected for repeated analysis before and after rainfall events. The locations for this repeat sampling were in Stellenbosch, Somerset West, Franschhoek and Paarl (Fig. 30). In the figures below, an initial radon activity is recorded before a rainfall event. After the rainfall event, radon activity concentrations were measured to assess the change in the radon activity concentration in response to percolation and recharge to the aquifer systems. These 12-weeks were spread out over a 3-month period and typically began a few days after a large rainfall event (sufficient to recharge the aquifer). The first sampling period in this round began on the 13th of August and terminated on the 29th of August 2019, with samples taken every Tuesday and Thursday, thus amounting to six samples for each location. The samples were obtained from Somerset West, Paarl and Stellenbosch (Fig. 30). These samples were obtained after an extended period of rain between the 30th of July and the 7th of August 2019 and hence for this block of sampling, a sample prior to the rain (recharge) event was not collected. Each colour on the graph represents a different date on which the sample was collected at that specific area. Three of the sample locations (Somerset West, Ou Hoof Gebou and Stias) show low

radon activity concentrations for the first sample date (13th of August 2018), with the radon activity concentration increasing for the remaining five sampling dates. Two other locations (Riverby Farm and Durr Bottling) showed inconsistent results whilst the remaining location, Simonsvlei, recorded quite variable and low radon concentrations (Fig. 31).

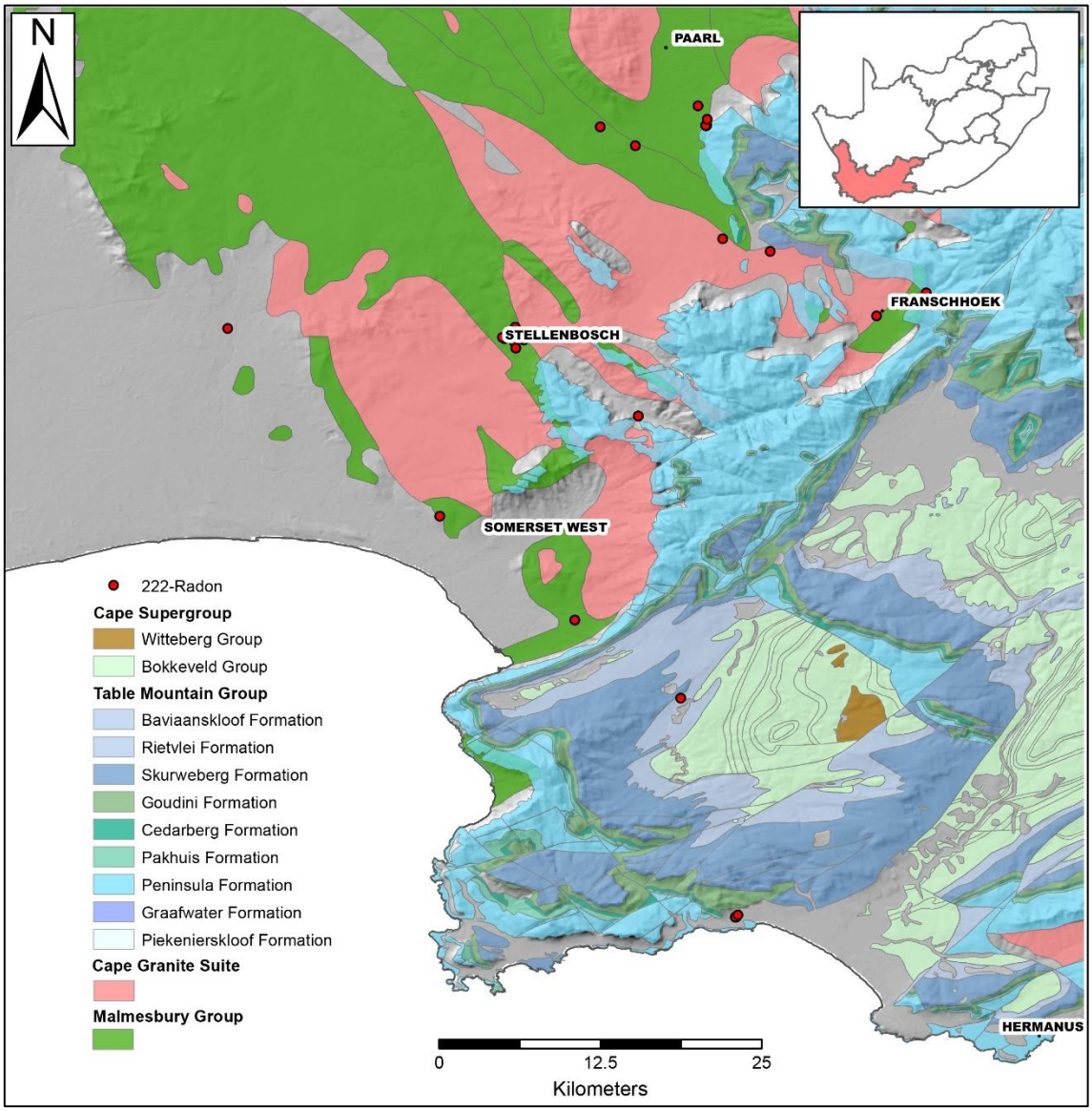

Figure 30 - Sample distribution map of samples collected in Stellenbosch, Somerset West, Franschhoek, Paarl and Hermanus.

The Simonsvlei radon activity concentrations were described as "odd" as the radon activity fluctuated abnormally. In some instances, the radon activity was below 10 Bq/L while in other cases it was above 70 Bq/L. These trends did not coincide with potential recharge events. It was subsequently realised that the sample taken from Simonsvlei was actually groundwater within the pipe and not groundwater directly obtained from the borehole (a misunderstanding from the borehole owner), and this was

interpreted to account for the odd and variable radon concentrations. The data obtained from Simonsvlei indicated how sensitive the radon activity concentration was to sampling protocols, and how significant data errors could be introduced into the study. In utilising the radon activity concentration for groundwater recharge evaluation, the groundwater analysed needs to be groundwater from the borehole. With regards to the Simonsvlei sample, using this data would have resulted in an incorrect interpretation of the data. This is a problem for boreholes that are not purged long enough and where the purging times are inconsistent as this can introduce data uncertainties.

In the first sampling season a reference sample prior to the rainfall event was not taken. However, the radon activity concentration varied as a consequence of recharge. As evidenced by the sample taken from Stellenbosch (Stias), the radon activity concentration was 147 ± 7.4 Bq/L after the rainfall event and increased to 542 ± 17 Bq/L and eventually peaking at 776 ± 21 Bq/L. A similar trend was seen the groundwater sample obtained from Somerset West as the radon activity concentrations gradually increased after the rainfall event

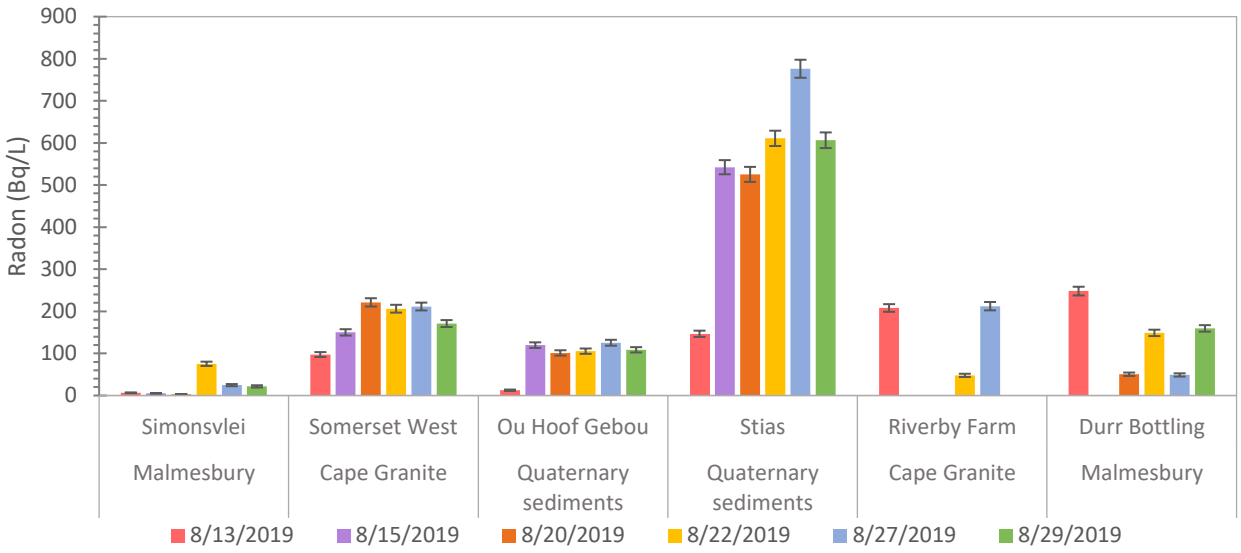

Figure 31 - First temporal and spatial variation sampling season indicating the radon variation over different locations after a large rainfall event. Note that for this sampling period, the rainfall event was an extended rainfall event between the 30th of July and the 7th of August and a reference sample was not taken prior to this.

The second data collection occurred after a large rainfall event came through on the 12th and 13th of September 2019. For this resampling campaign a pre-rainfall sample was taken on the 11th of September with subsequent samples taken twice weekly until the 9th of October 2019 (Fig. 32). The second data collection occurred after a large rainfall event came through on the 12th and 13th of September 2019. For this resampling campaign a pre-rainfall sample was taken on the 11th of September with subsequent samples taken twice weekly until the 9th of October 2019 (Fig. 32). Radon

activity concentrations in this sampling round dropped substantially after the rainfall event compared to before the rainfall event. For the Somerset West sample, the radon activity concentration peak at 314 ± 10 Bq/L after the rainfall event and subsequently dropped to 161 ± 7.9 Bq/L as a consequence of rapid recharge. After this drop, the radon activity concentrations gradually increased to 369 ± 11 Bq/L. For the Paarl (Durr Bottling) sample, the radon activity concentration peaked at 158 ± 7.1 Bq/L after the rainfall event and gradually decreased from 141 ± 7.4 Bq/L to 118± 6.1 Bq/L.

During this campaign, the number of sample sites and duplication of samples previously analysed increased compared to that of the first resampling session. These samples were collected from Franschhoek, Somerset West, Paarl and Stellenbosch (Fig. 32). Three sample locations that were collected and analysed during the first resampling session, were re-analysed during the second resampling session to determine continuous changes in the radon activity concentration.

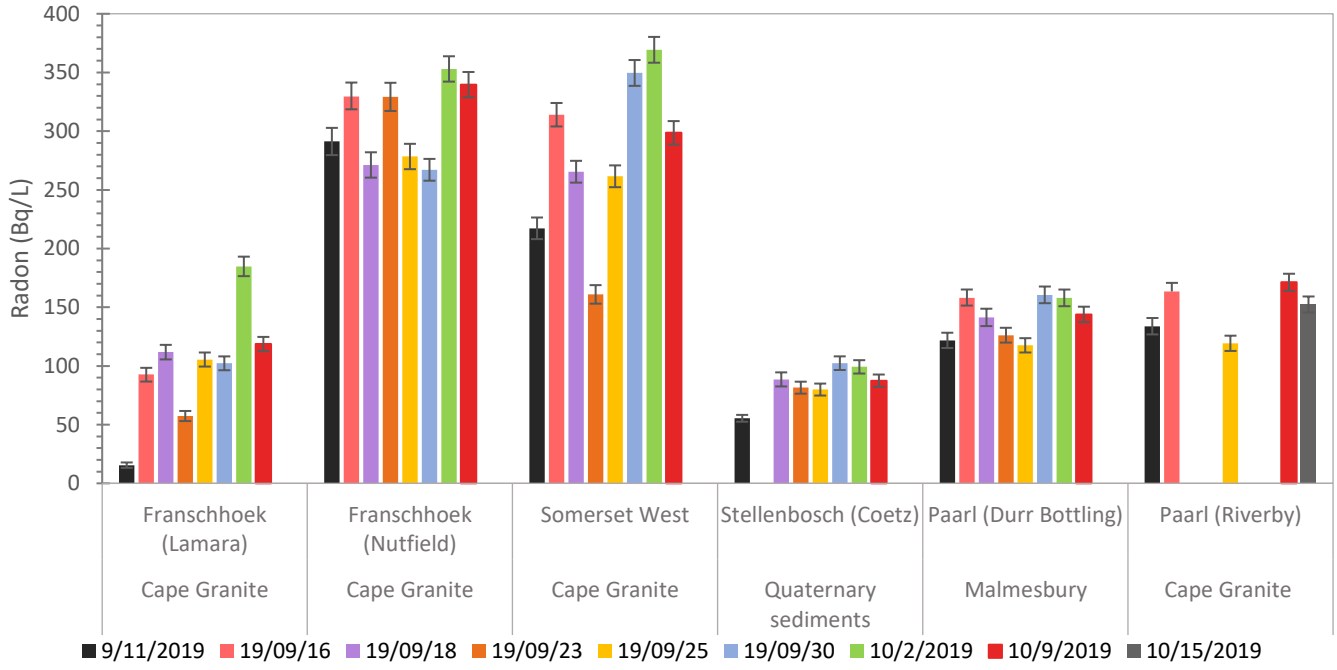

Figure 32 - Temporal and spatial variation of Radon during the second sampling session. Black bars indicate the sample taken prior to the rainfall event.

A third resampling campaign was done after a rainfall occurred from the 25th- 28th of October 2019. This third session began on the 29th of October and terminated on the 12th of November 2019. During this time fewer sample locations were resampled and only two sample sites were replicated from the second resampling session. In this third resampling session a TMG groundwater sample was incorporated into the study and thus illustrated the TMG aquifers response to recharge (Fig. 33). The drop-in radon activities after a rainfall event was illustrated in areas such as Franschhoek and Stellenbosch (groundwaters associated with the TMG and Quaternary sediments aquifers.) These

radon activities dropped from 58.2 ± 4.4 Bq/L to 27.0 ± 3 Bq/L in Franschhoek and 561 ± 14 Bq/L to 389 ± 11.2 Bq/L in Stellenbosch (Fig.32). The groundwater associated with the Quaternary sediments recorded an immediate drop in the radon activity concentration in response to rapid groundwater recharge (See Appendix 1).

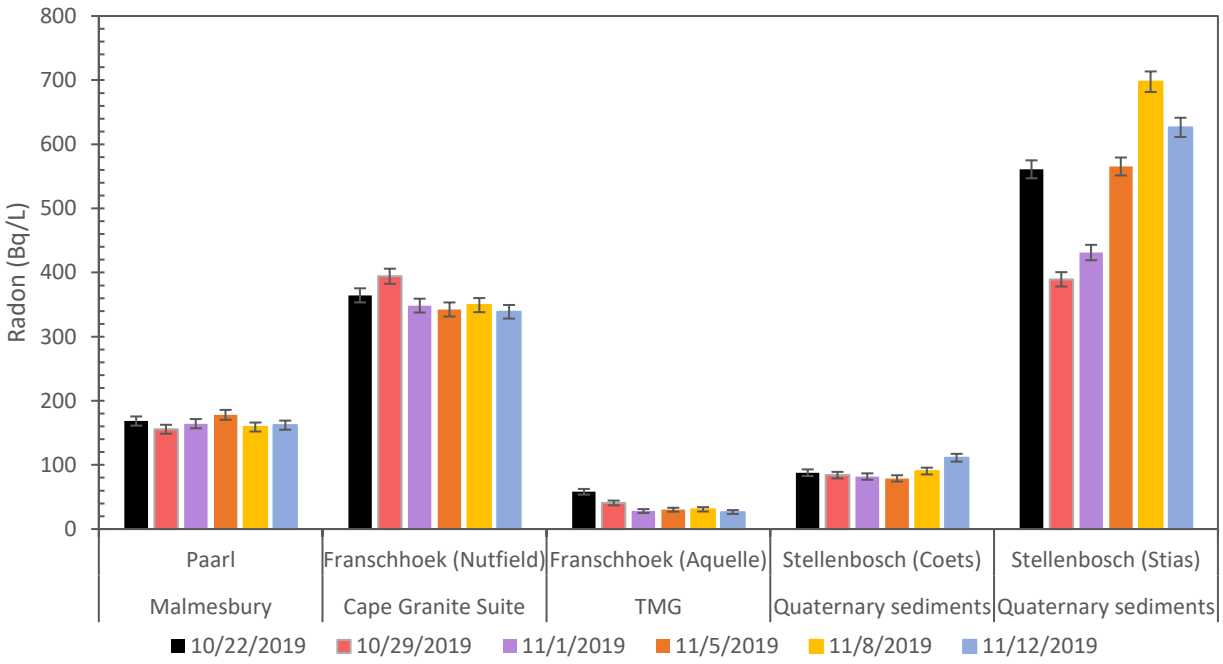

Figure 33- Third resampling session. Black bars indicate the sample taken prior to the rainfall event.

Throughout these three resampling campaigns, three sample locations were continuously analysed for their radon activity concentration in response to recharge. The radon activity concentrations from these three locations were plotted alongside the amount of rainfall recorded during those 12 weeks. This was done to better illustrate the effect that rainwater had on the radon activity concentration in groundwater (Fig. 34, 35 and 36). In Somerset West, the first recharge event caused the radon activity concentration to drop below 100 Bq/L and gradually increase 230 Bq/L. The second recharge event (12 Sept 2019) caused for the radon activity concentration to drop to 160 Bq/L on 23 Sept 19 and then sharply increase to 360 Bq/L on the 10 Oct 2019 (Fig. 34).

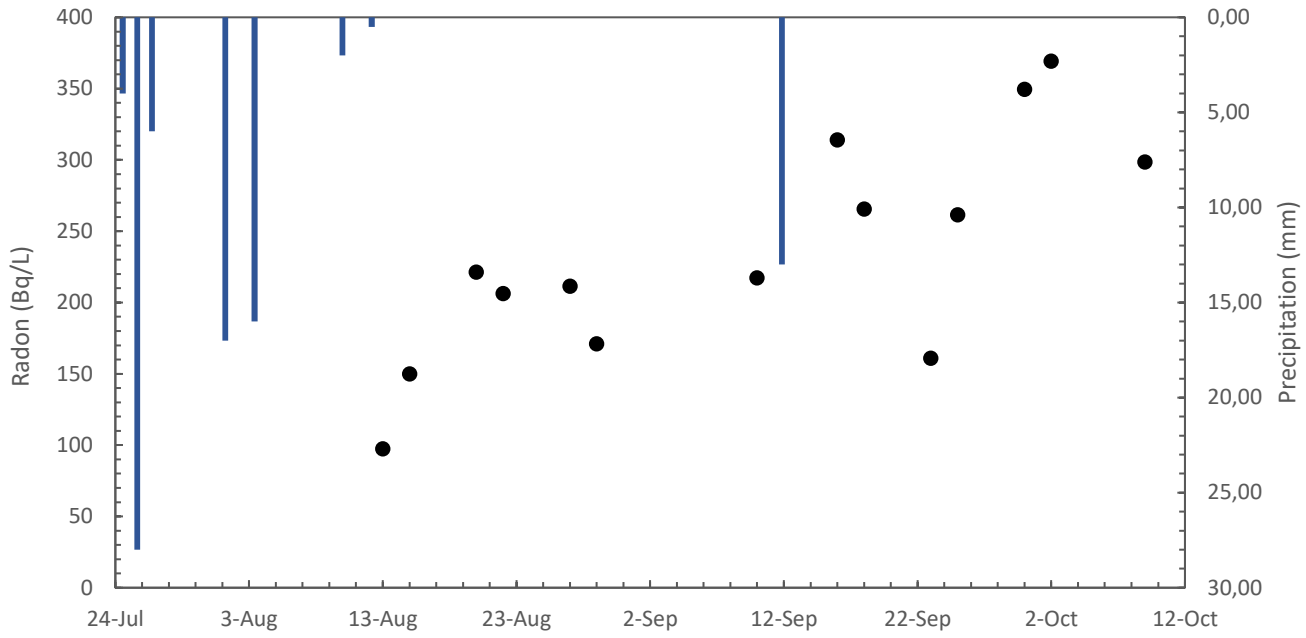

Figure 34 - Somerset West samples (Cape Granite Suite): blue bars indicate the rainfall events alongside the radon concentrations collected from a borehole in Somerset West. These samples were collected from August to October of 2019. The graph begins in July to indicate the pre-rainfall events.

In Paarl (Durr Bottling plant) (Fig.35), the effect that recharge had on the radon activity concentration was marked by a delayed response as radon activity concentration dropped a few days after the recharge. After a rainfall event the radon activity concentration would remain at about 250 Bq/L and then drop to 50 Bq/L (Fig. 35). However, a few days later the radon activity dropped again from 150 Bq/L to 48 Bq/L indicting a second injection of recharge into the aquifer. This was further confirmed after a second rainfall event, where the radon activity concentrations remained at 140 – 160 Bq/L and then drop to less than 120 Bq/L a few days later.

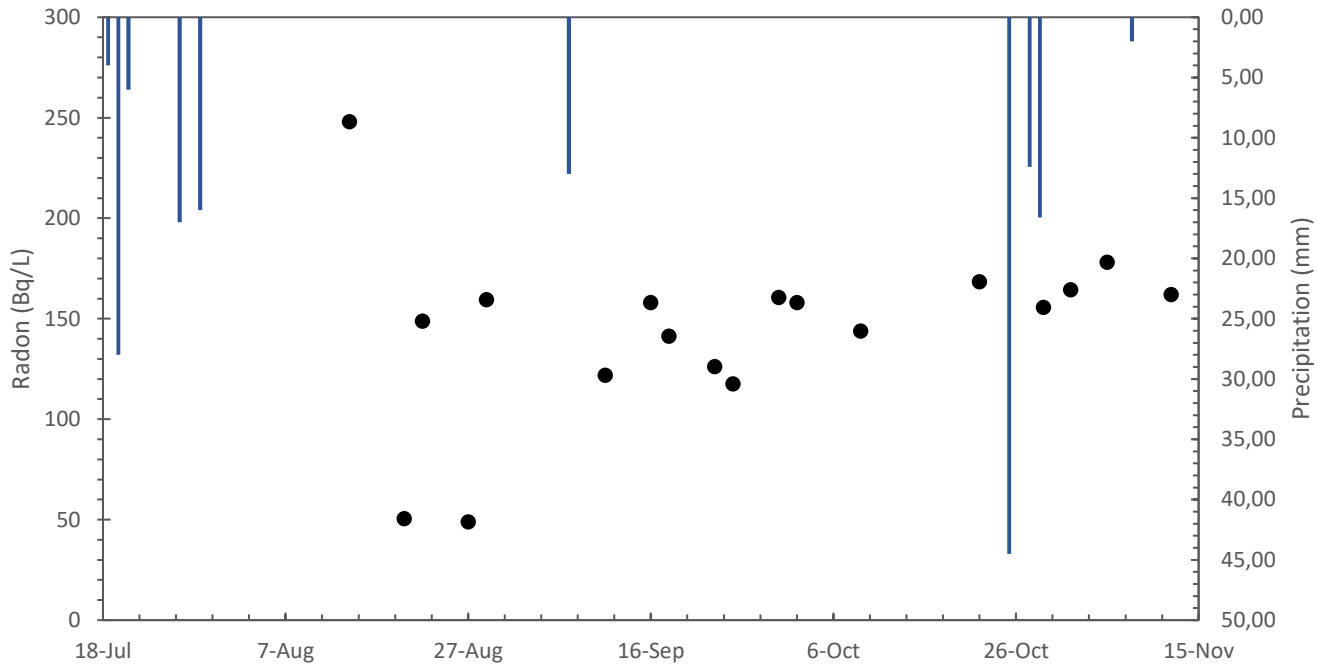

Figure 35 - Durr Bottling plant (Malmesbury Group aquifer): blue bars indicate the rainfall events alongside the radon concentrations collected from a borehole just outside Paarl. These samples were collected from August to November 2019. The graph begins in July to indicate the pre-rainfall events.

A sample obtained in northern Paarl (Riverby farm) (Fig. 36) from a granitic hosted aquifer, recorded slight changes in its radon activity concentration as sampling commenced but gradually maintained elevated radon activities within the range of 170 Bq/L and 117 Bq/L.

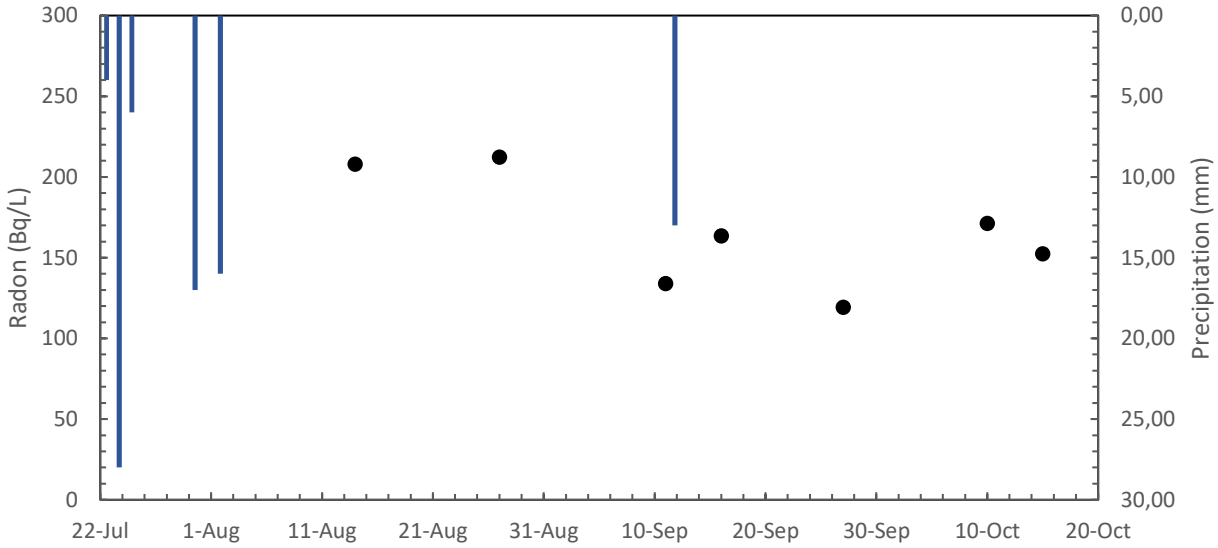

Figure 36 - *Riverby sample (Cape Granite Suite): blue bars indicate the rainfall events alongside the radon concentrations collected from a borehole just outside Paarl. These samples were collected from July to October 2019. The gap at the 10th of October indicates missing data. The graph begins in July to indicate the pre-rainfall events.*

4.4. DISCUSSION

Chapter 3 categorised the groundwater samples into their respective host aquifers using standard hydrochemistry. This characterisation was based on groundwater EC values and ion concentrations and the same characterisation was brought through to the radon analysis. Differences observed in radon activity concentrations between the different aquifers are considered to be controlled by aquifer host composition and length of contact time (flow path) within the host lithologies. Furthermore, activity concentration differences between radon in surface and groundwater can be utilised in order to delineate groundwater recharge. A general overview of the main factors that control the radon activity in groundwater and how radon is utilised as a tracer in identifying groundwater recharge are discussed in the sections below.

4.4.1. Groundwater Radon Activities

The radon activity concentrations presented in this study were quite variable in some locations but were a direct reflection of the host rock lithology within the aquifer. Radon's presence within an aquifer is governed by the concentration of its radioactive parents (U and Th) within the soil layers but more so in the aquifer host rocks (Loomis, 1987). As U is a primordial element, its composition within a rock is governed by its geochemical partitioning during partial melting and fractional crystallization of magma. U is a highly incompatible element and thus during partial melting and fractional crystallization, it is concentrated into a liquid phase that is incorporated into more silica-rich products such as zircon ($ZrSiO_4$) (Hazen et al., 2009; Uosif et al., 2015). Consequently, U and Th concentrations are elevated in the continental crust.

Silica rich rocks such as granites typically have elevated U and Th concentrations within the range of 5 ppm and 15 ppm respectively as a result of the fractionation processes described above (Pavlidou et al., 2006). However, as U and Th continuously decay to produce radon, the radon activities should also increase. This association was recognized in the groundwater samples associated with the Cape Granite Suite where the average radon activity concentration was 248 ± 9.9 Bq/L (Fig. 28). Sedimentary rocks record variable U concentrations, linked to the mineralogy of the detrital source rocks and the redox-chemistry of U (which is strongly influenced by the geochemical processes operating during the weathering of the source rock and the sediment transport) (Tye et al., 2017). As most of the aquifers encountered in this study are sedimentary hosted aquifers, the variation in U concentrations was reflected in the variable radon activity concentrations in the different groundwaters. For example, groundwater from the Malmesbury Group aquifer, which is dominated by shales, recorded radon activity concentrations that were significantly higher than that of groundwater from the TMG aquifer,

which is dominated by sandstones. Shale is a sedimentary rock that stems from muds and clays, and typically concentrates clay minerals which allows for the absorption of U and the retention of Th in heavy resistant minerals such as zircon and monazite. Consequently, shales have U and Th concentrations within the range 1 - 5ppm and 10 - 13 ppm respectively (Cumberland et al., 2016; Tye et al., 2017). The average radon activity concentration in groundwater associated with the Malmesbury Group was 89.3 ± 5.5 Bq/L (n=6).

Sandstones however, typically have low U and Th concentrations within the range of 1-5 ppm and 1-7 ppm respectively, while limestones have even lower U and Th concentrations within the range ≤ 0.1–9 ppm and ≤ 0.05 - 3 ppm respectively (Tye et al., 2017). The low U and Th concentrations typically found within sandstones and limestones would account for the low radon activity concentrations in groundwater derived from the TMG, Bokkeveld and Witteberg aquifers (Table 9). Groundwater associated with the Quaternary sediments recorded variable radon activity concentrations. In the areas of where groundwater was sampled from Quaternary sediments, the alluvium in the riverbed courses, is derived from various lithologies, which have different U and Th concentrations. Therefore, the radon activity concentrations measured within the Quaternary sediments should vary depending on the dominant sediment origin at the different sample locations.

Taking the above into account, it was expected that each aquifer system would be associated with different radon activity concentrations and that this could be utilised to generate a baseline radon activity concentration for each aquifer. However, each aquifer system had significant variability and as a result there is overlap between the radon activity concentration ranges for several of the aquifer systems (Fig. 28; Table 9). Furthermore, a number of the aquifers had samples with anomalous (outlier) radon activity concentrations that skewed the average and mean values. Moreover, there are not enough samples from each aquifer system to be truly representative of the total range of values. The only aquifer system that has a reasonable number of samples is the TMG aquifer, with 23 samples, and this aquifer had consistently had low radon activities irrespective of where the aquifer was sampled.

Table 9 – Average radon activity in the aquifers in Cape Town and its surrounds. As the radon activity concentrations within each aquifer were quite variable (as indictaed by the standard deviation), a geomean was also calculated. These calculations were done by excluding the major outlier (653 Bq/L) from the Quaternary sediments.

Aquifer	**Dominant lithology**	**Average (Bq/L)**	**Strd Dev**	**Mean (Bq/L)**	**Standard error on Mean**
Malmesbury Group	Shale	89.4	52.1	74.2	21.3
Cape Granite Suite	Granite	248	110	224	42.0
TMG aquifer	Sandstone	34.4	40.1	18.3	9.1
Bokkeveld Group	Shale and minor sandstone	48.0	64.0	24.0	37.0
Witteberg Group	Sandstone and limestone	12.0	0.00	12.0	0.00
Quaternary sediments	Aeolian sand	52.0	49.1	28	19.0

The variability in radon activity concentrations in the groundwater associated with the Quaternary sediments is well illustrated by the samples obtained in Stellenbosch. Samples taken 500 – 1000 m apart had quite different of radon activity concentrations between 36 ± 3.4 Bq/L and 127 ± 7.6 Bq/L with an anomalously high radon activity of 653 ± 20 Bq/L (Fig. 37). These variable radon activity concentrations are thought to be related to the different sediment sources within the aquifer, the hydraulic conductivity and hydraulic gradient. As the hydraulic conductivity within the Quaternary sediments is within the range of 10 – 50 m/per day (Adelana and Xu, 2006), water transmissivity though the aquifer would affect the acquired radon activity. As the radon activity stems from increased groundwater and wall rock interaction, high conductivities would result in lower radon activities. The sample with an anomalously high radon activity in groundwater (653 ± 20 Bq/L) could signify granitic detrital material in the aquifer at this location.

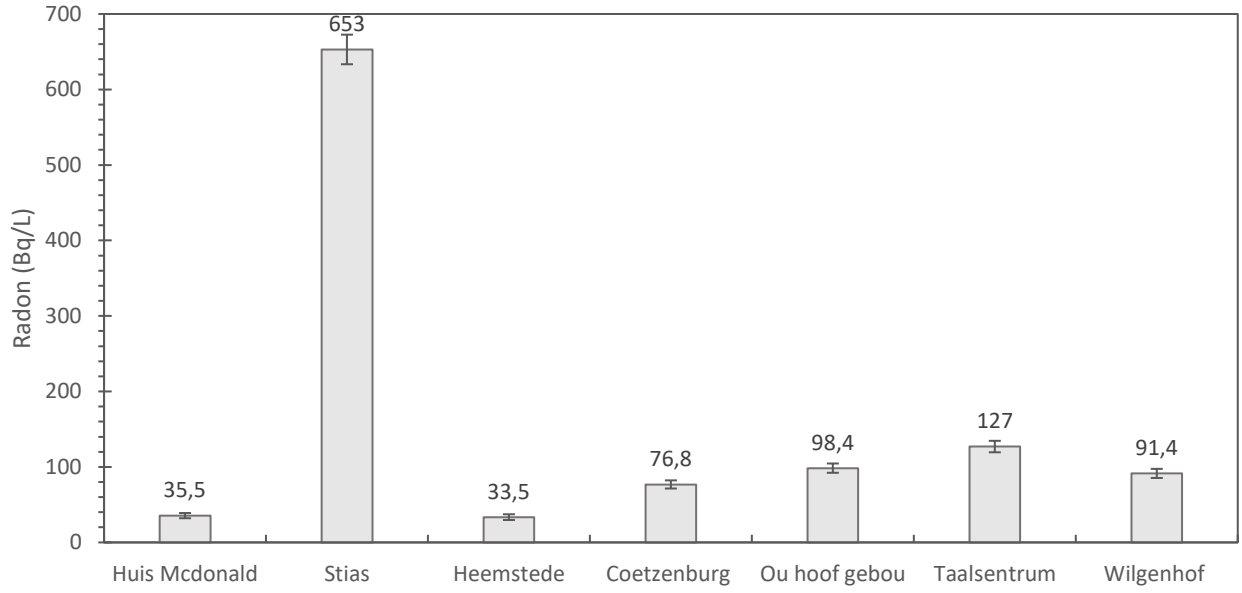

Figure 37 - Variation in ^{222}Rn within Stellenbosch. The names of the boreholes were linked to the sample sites location.

The radon activity in the hot spring and the five cold springs was not linked to the U and Th concentration within the surrounding host rock (as both types of springs originated from sandstone hosted aquifers) but rather from fault zones and atmospheric interaction. A spring is essentially a contact at which an aquifer intercepts the ground surface. As the spring intercepts the Earth's surface, the groundwater is exposed to the surrounding atmosphere. As a gas, this atmospheric interaction causes the natural degassing of radon into the atmosphere, thus decreasing the radon activity in groundwater. It is thought to be for this reason that cold springs have low radon activities. Hot springs however, typically circulate at greater depths, usually in and around a fault or fault zone. Faults zones typically have elevated radon activities as they are zones of high mineralization of Uranium (Choubey et al., 2001) and areas of elevated temperatures and depths often have increased concentrations of uranium daughter products (Akawwi, 2014). The Montagu hot spring is known to be along an e-striking fault and the water sourced from depths of ~2000 m. This increased depth, elevated temperature (43°) and fault-hosted groundwater all contributed to the elevated radon activity. Similar observations and interpretations have been made on hot springs elsewhere in the world (Khan et al., 1979).

Figure *38* illustrates a summary of how the radon activity concentration in groundwater varies according to the host aquifer, the U concentration and the observed radon activity concentration differences between cold and hot springs.

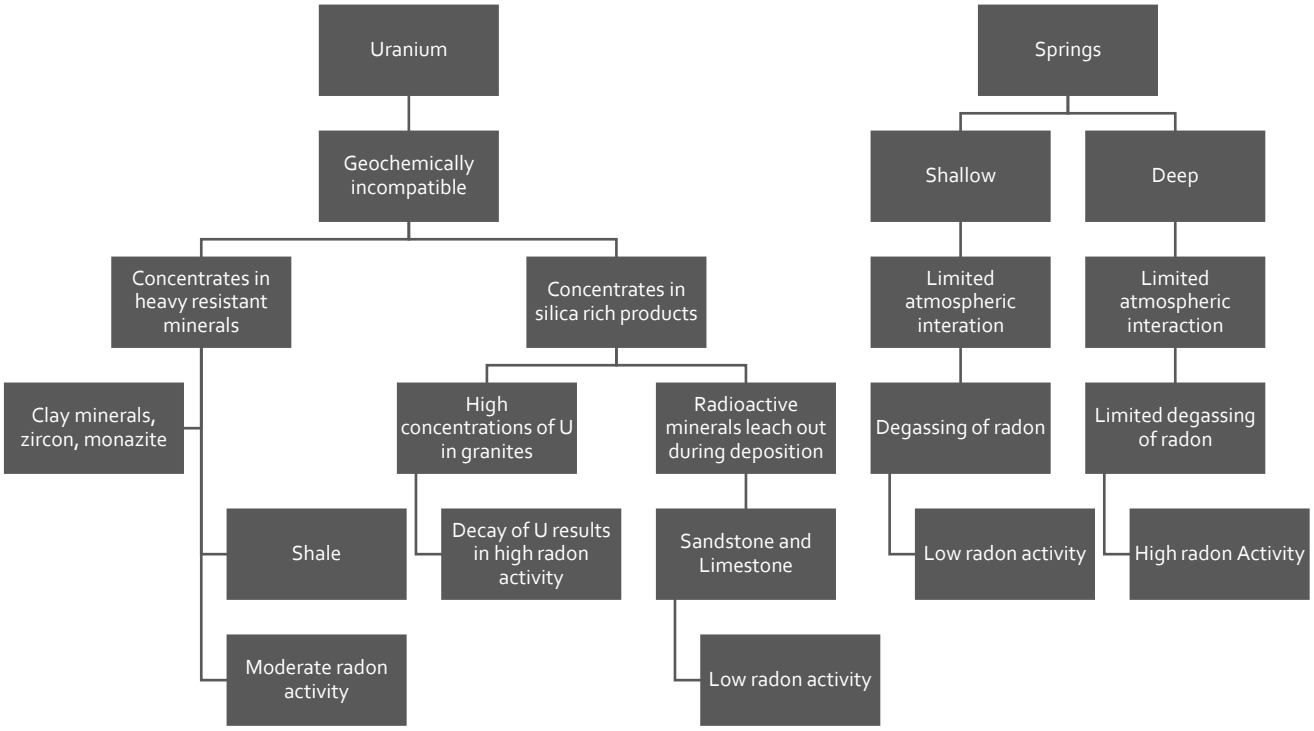

Figure 38 - *Summary of the radon activity in groundwater.*

4.4.2. Temporal Variation in Radon Activity

Due to the Mediterranean climate that dominates the Western Cape, the region experiences wet and cold winters and hot and dry summers. Sampling during the first sampling season was done during the winter, but due to the drought was a dry winter. With limited atmospheric interaction and prolonged groundwater wall rock interaction, the radon activities in the groundwater naturally accumulated. Within an enclosed system such as an aquifer, the input of radon is dominated by one variable, the presence and radioactive decay of U and Th. After 25-30 days secular equilibrium of the radon activity in groundwater will be reached and the radon activity should remain constant (Grolander, 2009), unless disturbed by atmospheric interaction and groundwater recharge.

The second sampling season commenced during the summer months; however, this sampling season was preceded by large rainfall events. With sufficient precipitation that was able to infiltrate and intercept the water table, groundwater recharge was noted by a significant drop in the radon activity concentration. As rainwater contains negligible amounts of radon, rainwater infiltration into the aquifer will cause a dilution in the radon activity. The observed activity differences in samples taken during the first and second sampling season indicated how the radon activity in groundwater remained at its original radon activity concentration until influenced by groundwater recharge, in both winter and summer (Fig. 39). As these samples were collected during two different seasons (winter

and summer), it was noted that the radon activity concentrations in groundwater was not affected by changes in seasonality but rather affected by recharge patterns.

`

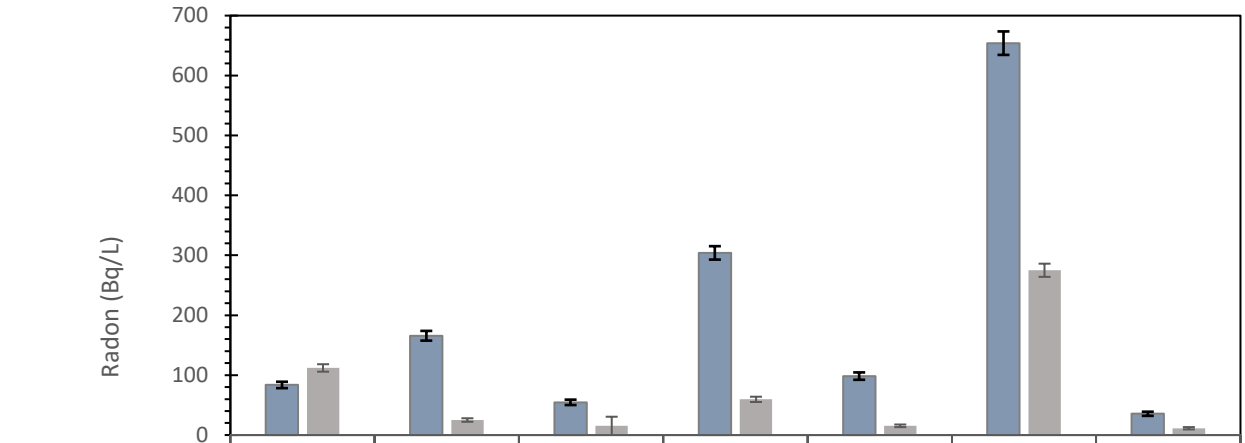

	Paarl Cape Granite	Paarl Malmesbury	Paarl Malmesbury	Somerset West Cape Granite	Stellenbosch Quaternary sediments	Stellenbosch Quaternary sediments	Stellenbosch Quaternary sediments
Aug (Winter) 2018	83,6	165,7	54,6	304	98,4	654	35,5
Apr (Summer) 2019	112	25,1	15,3	59,6	15,4	275	11,3

Figure 39 - *Temporal and spatial variation in Radon*

The results obtained from these two data sets introduced a hypothesis that centred on the noticeable differences observed in radon activity concentrations in both surface and groundwaters. Based on this hypothesis it was believed that in the presence of modern recharge, the radon activity concentration in groundwater would be diluted and therefore would drop from its original radon activity concentration. Based on the response of radon to groundwater recharge, three aquifer behavioural characteristics were identified: (1) aquifers where the radon activity concentration in groundwater dropped immediately implying a rapid response to recharge; (2) aquifers where the radon activity concentration dropped only after a few days to a week, implying a delayed response to recharge; and (3) aquifers that had a stable radon activity concentration irrespective of rainfall received in the immediate area, implying little or no direct recharge.

It is clear that groundwater samples collected from the Quaternary sediments recorded a rapid drop in the radon activity concentrations after rainfall events and that this represented a response to rapid direct recharge in line with the first radon activity concentration trend described above (Fig. 31 and Fig. 33). A groundwater sample obtained from Stias (Quaternary sediments) exhibited this trend. Howevever, this sample had a very high radon activity concentration and thus changes in this value were clear to see. At this location, the radon activity concentration dropped from 654 ± 20 Bq/L to

275 ± 11 Bq/L in April 2019 and to as low as 147 ± 7.4 Bq/L in August 2019 (Fig. 40). This site was close to a river and thus the rapid drop in radon activity concentration may be linked with surface water runoff and percolation towards the river facilitated by high hydraulic conductivities. Groundwaters with young residence times such as the TMG (Miller et al., 2017) likewise recorded immediate drops in the radon activity concentration, suggesting direct and immediate recharge taking place (Fig. 40).

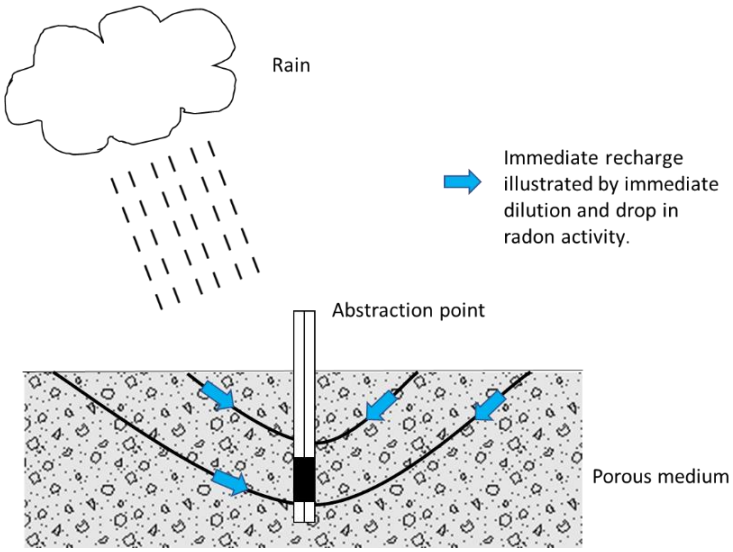

Figure 40 - An example of immediate groundwater recharge signified by an immediate dilution in radon activity. Flow arrows indicate proposed groundwater flow.

Samples obtained from the Malmesbury Group and Cape Granite Suite illustrated a delayed drop in the radon activities in response to recharge. This was marked by the initial radon activity concentration persisting over a few days and then dropping to lower activity concentrations (Fig.32). This trend was not completely uniform in an aquifer as in some cases the radon activity concentration would drop multiple times within a single aquifer. The groundwater associated with the Malmesbury Group (Durr Bottling site) is interpreted to be influenced by multiple injections of recharge owing to repeated drops in the radon activity concentration (Fig. 35). This could be explained by multiple packages of recharge water moving along different flow paths and reaching the borehole at different times with different radon activity concentrations. Although these radon activity concentrations will all be higher than rainwater (the recharge source), they will be variably lower than groundwater that has already been sitting in the aquifer (Fig. 41). This pattern characterised the second radon activity concentration trend indicated above.

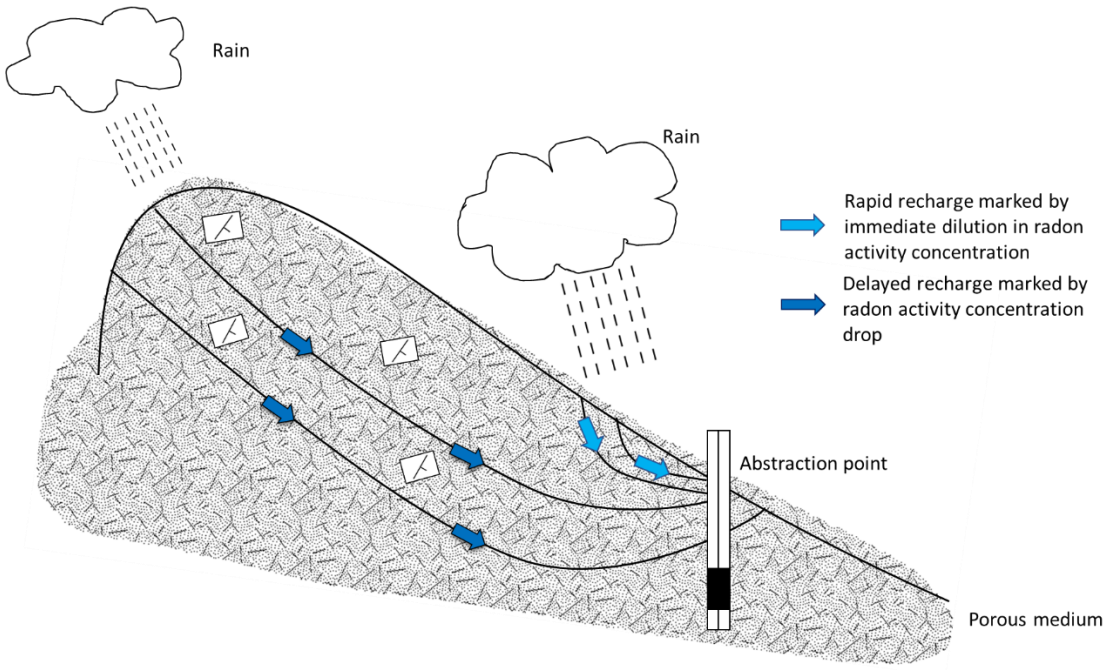

Figure 41 - An example of groundwater piston flow. This subsequently resulted in a delayed recharge in the Malmesbury Group aquifer. Flow arrows indicate proposed groundwater flow.

The third radon activity concentration trend is characterised by little or no variation in the radon activity concentration and this was characteristic of groundwater hosted by fractures in the Cape Granite Suite. Groundwater sampled once a week recorded stable radon activity concentrations. Slight changes in the radon activity concentration were noted, however these changes were not significant (change ≤ 40 Bq/L between analysis times) and were interpreted to represent no significant groundwater recharge (Fig.42). However, it is important to recognise that one of the limitations with radon is that after 20-25 days the radon activity concentration will equilibrate between the recharge water and the groundwater. Hence if recharge takes longer than this to reach the sampling point that there will be no discernible different in the radon activity concentration.

One location in Franschhoek (Nutfield Stud farm - Cape Granite Suite) recorded ambiguous behaviour in the radon activity concentrations. This site was sampled twice and exhibited different behaviour the two times. The first-time groundwater recorded a delayed drop in its radon activity concentration consistent with a delayed response to recharge (Fig.32). The second time it maintained its high radon activity concentrations implying no direct response to recharge (Fig.33). The granitic host of this aquifer and the deeper depth of the borehole is thought to be a contributing factor to the observed aquifer behavioural characteristics. During periods of higher precipitation (greater than 20 mm per week) the radon activity concentrations are diluted as a consequence of recharge percolating into the aquifer. During periods of lower precipitation (less than 10 mm per week), limited percolation and the

increased ingrowth of radon into the groundwater causes the radon activity concentration to remain stable.

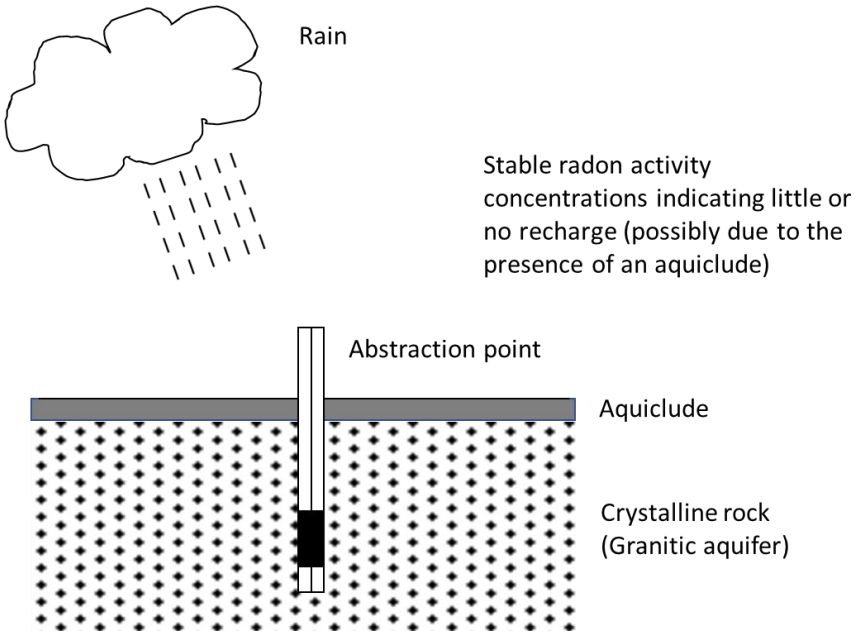

Figure 42 – An example of sample sites that illustrated little or no change recharge as the radon activity remained constant.

4.4.2.1. Groundwater recharge and its relationship to groundwater residence time

Radon activity concentrations were compared to groundwater residence times estimated from ^{14}C concentrations in groundwater (Harilall, 2020) from the same or similar boreholes. The assumption here was that if there was no dilution in the radon activity concentration, this would equate to no or little recharge and therefore longer residence times (older groundwater). On this basis, it is proposed that the three radon activity concentration trends described above, can be linked to different groundwater residence times. Based on the ^{14}C activities, groundwaters with ^{14}C activities ≥ 100 pMC (such as groundwater associated with the TMG and Quaternary sediments) corresponded with a rapid drop in the radon activity concentrations interpreted to represent rapid recharge. This was evident in groundwater samples obtained from Stias and Somerset West (103 pMC and 102 pMC respectively) (Harilall, 2020) (Fig.43). Groundwaters where the ^{14}C activity was between 80 – 90 pMC corresponded with a lag in the radon activity concentration drop in response to recharge. These groundwaters are young to moderately aged groundwaters and therefore are not recharged as rapidly as the groundwaters with ^{14}C activities ≥ 100pMC. This was observed in Franschhoek (Nutfield Stud Farm), where groundwater had a ^{14}C activity of 83.5 pMC (Harilall, 2020). Groundwater samples where the ^{14}C activity was ≤ 70pMC, corresponded with stable radon activity concentrations suggesting little to no direct recharge (Fig.43).

Groundwater residence times are often overestimated due to mixing between groundwater and surface water. Using radon to delineate patterns of modern groundwater recharge, these groundwater mixing relationships can be better defined. The application of radon in delineating zones of recent groundwater recharge enables us to evaluate the sustainability of the respective aquifer. Groundwaters with rapid changes in their radon activity concentrations due to rapid recharge (the ^{14}C activity was ≥ 100pMC) should be utilised at a rate that is proportional to or less than the rate of recharge. These groundwaters are vulnerable during periods of little or no precipitation due to their dependence on rain and thus should be used sparingly. The same can be said for groundwaters that record a delay in the decrease in radon activity concentration in response to a delay in recharge to the aquifer (^{14}C activity between 80 - 90 pMC).

Changes in precipitation patterns linked to climate change could impact how groundwater recharge takes place and thus could change the variation in radon activity concentrations in groundwater. Irrespective of this, older groundwater (^{14}C values of ≤ 70pMC) with stable radon activity concentrations should not be utilised without a better understanding of the aquifer is recharged. The observed stable radon activity concentration is linked to the secular equilibrium of ^{222}Rn in the aquifer. After 20-25 days (5 half-lives) the radon activity concentration in the aquifer becomes constant as the production and decay of radon is in equilibrium (Blackburn and Al-Masri, 1993) and is not disturbed by atmospheric interaction. In these aquifers the recharge rates may be very slow and longer than 20 – 25 days, hence there would be no detectable change in the radon activity concentration (Fig. 43). These groundwaters require thus isotopic tracers with longer half-lives to determine their residence time and thus their sustainability as only zones of direct and active groundwater circulation are zones of interest in radon studies.

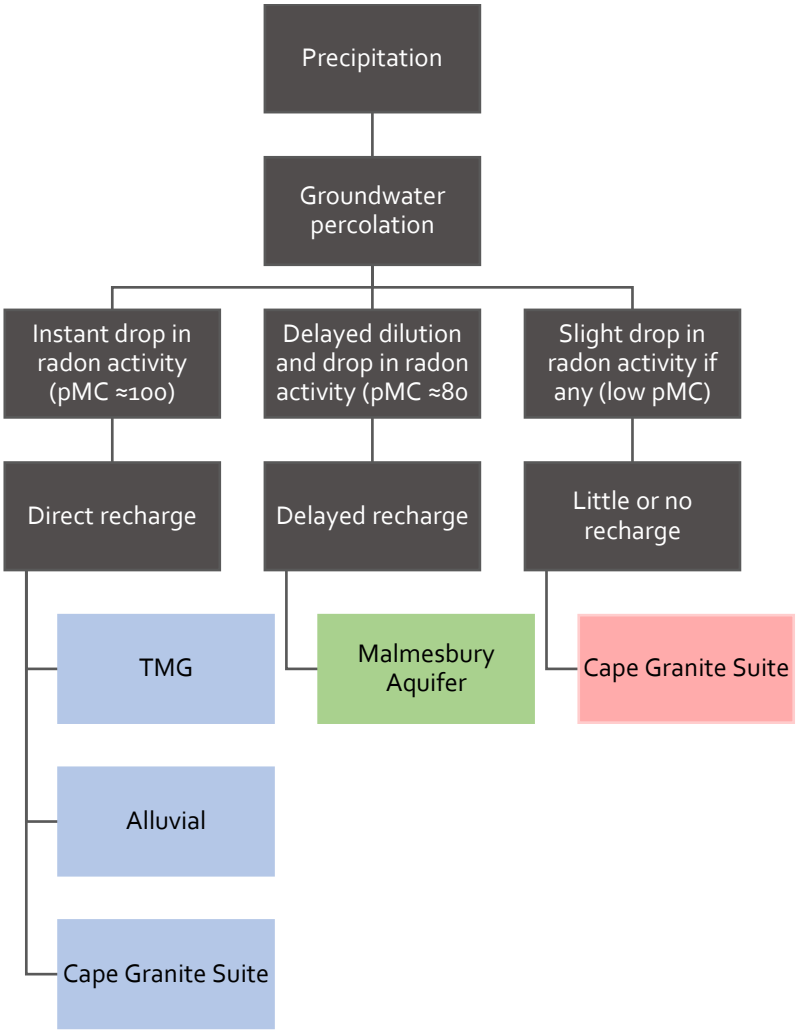

Figure 43 - Summary of three scenarios observed during recharge within the respective aquifers.

4.4.3. Recommendations for Future Study

Due to the pronounced radon activity concentration differences between surface water and groundwater, the application of radon in identifying zones of recent groundwater recharge and how the aquifer responds to the recharge is useful. The application of radon in identifying recent groundwater recharge may be improved by studying a single catchment and coupling it with another physical tracer (organic dyes) to observe the flow path of the recharge through the aquifer. Furthermore, rainfall gauges should be set up in order to quantify the amount of rainfall within a given area. The radon activity concentration varied substantially both between the different aquifers and within each aquifer (3 – 653 Bq/L Quaternary sediments) examined in this study and may be a function of the limited number of samples analysed. Therefore, additional analyses of radon in groundwater are required. Daily analyses may prove to be challenging, however twice a week or weekly analyses over a longer period (6 months) may give additional insight to the variability of radon in groundwater.

4.5. CONCLUSIONS

The radon activity concentration range for each aquifer was evaluated in order to delineate rapid and direct groundwater recharge patterns. Observed changes in the radon activity concentrations could be explained by three scenarios: (1) immediate drop in the radon activity concentrations due to direct recharge; (2) delayed drop in the radon activity concentration in response to delayed recharge; and (3) stable radon activity concentrations reflecting little or no recharge. These scenarios linked well to 14C concentration ranges suggesting that scenario [1] is modern or young groundwater, whilst scenario [3] is older possibly fossil groundwater. However, the significant difference in the half-life of ^{222}Rn (3.82 days) compared to ^{14}C (5730 years) means that additional isotope tracers should be used to fill in the middle range to better constrain the older but not necessarily fossil groundwater.

Knowledge of the radon activity concentration in groundwater provides us with a useful indicator for identifying the sustainability of the groundwater. Radon studies on groundwater have not been done in this way before in South Africa and represent an important advance in how recharge to the main aquifer systems can be tracked. The results also show how sensitive some aquifers are to direct recharge and hence modern precipitation patterns that are changing in response to climate variability (Şen, 2009). Thus, the results presented are of vital importance in understanding the recharge dynamics in groundwater in South Africa and for further highlighting the capabilities of radon as a tracer in groundwater

CHAPTER 5: CONCLUSIONS AND FUTURE RECOMMENDATIONS

5.1. GENERAL CONCLUSIONS

The principal aim of this project was to quantify the radon activity concentration in groundwater and to identify how it may be used in delineating zones of rapid groundwater recharge. Before doing so, a hydrochemical characterisation of all the groundwater sampled in this study was required to contextualise the radon activity concentrations. The entire database contained 48 groundwater samples which were characterised into six aquifers systems, the Malmesbury Group, the Cape Granite Suite, the TMG, Bokkeveld Group, Witteberg Group and the Quaternary sediments aquifer. Below each objective is presented and the findings of the objective summarised.

Key Objective One: To identify and delineate the different aquifer types represented by the existing boreholes sampled in this study, using hydrochemistry and stable isotopes.

Using existing literature, geology and hydrochemistry of the groundwater, 48 groundwater samples were characterised. The hydrochemistry within each aquifer varied as a consequence of host lithology, surface water groundwater mixing relationships and height above sea level. The TMG was the main focus of the study and the distinct hydrochemical character of the TMG groundwater, including very low EC and alkalinity values combined with a Na-Cl hydrofacies type and acidic pH range, facilitated identification of samples that belonged to the TMG aquifer. Groundwaters without these distinctive traits were then assigned to the other five aquifers depending on hydrochemical character.

Six samples with highly elevated EC values and alkalinities (in excess of 1000 µS/cm and 100 mg/L respectively) were identified as being groundwater derived from the Malmesbury Group aquifer. Seven samples with slightly acidic waters and variable but elevated ionic concentrations were associated with the Cape Granite Suite. Three samples with an average pH of 6.5 and elevated HCO_3^-

concentrations were identified as being groundwater associated with the Bokkeveld Group aquifer. One sample had elevated EC and alkalinity with slightly elevated Mg^{2}+ concentrations and low Cl^{-} concentrations and was classified as groundwater from the Witteberg Group. Nine samples with variable hydrochemical characteristics and alkalinities, in part resembling groundwater associated with the TMG, were identified as groundwater associated with the Quaternary sediments. There was no single unique parameter that allowed different groundwater samples to be assigned to a specific aquifer. Generally, two or more parameters were needed to assign groundwater samples where the aquifer host was unknown, to an aquifer system.

It is worth noting that the $\delta^{18}O$ and $\delta^{2}H$ values were not particularly useful in assisting with the assignment of aquifer systems to the sampled groundwaters. $\delta^{18}O$ and $\delta^{2}H$ values showed the most distinct variation when plotted as a function of elevation and this is likely to do with typical modelled Rayleigh fractionation affects. However, since the TMG aquifer tends to be dominate at higher elevations that was a correlation between higher $\delta^{18}O$ and the TMG groundwater

Key Objective Two: To quantity the ^{222}Rn activity concentration in groundwater in the greater Cape Town region.

Radon activity concentrations ranged between 1.04 ± 0.7 Bq/L (obtained on Table Mountain) and 653 ± 20 Bq/L (obtained in Stellenbosch). From previous literature, it was noted that the radon activity concentration in groundwater was directly linked to (1) the presence of U and Ra within the surrounding wall rock, (2) host rock lithology, (3) the presence of faults and folds, and (4) changes in temperature and depth (Akawwi, 2014; Virk and Singh, 1993; Voronov, 2003). The radon activity concentration data obtained in this study was consistent with these previous findings. Groundwaters hosted in the Cape Granite Suite rocks, which contain elevated U and Th concentrations, recorded the highest average radon activity concentrations found in this study. Furthermore, deeper boreholes/springs sampled in and around faults and fractures recorded elevated radon activity concentrations within the range of 120 Bq/L to 300 Bq/L (Montagu springs and Franschhoek – Nutfield stud farm). Variations in the radon activity concentration in a single aquifer were noted as well as between aquifers, and associated with borehole depth, fractures and faulting and different lithological properties in the aquifer host rock. The Quaternary sediments had very variable radon activity concentration data considered to be linked to the variable origin of the source sediments. In general, the TMG aquifer had low radon activity concentrations, but the other five aquifer systems did not have unique radon activity concentrations and hence a clear radon baseline for each of the different aquifer systems around Cape Town could not be easily defined.

As the radon activity concentration in surface water is negligible, whilst radon activity concentrations in groundwater tends to be higher due to radon-in-growth from the host rocks, this large difference was suitable to use as a tracer of rapid recharge. The reasoning was that direct recharge of a low radon water ("the recharge") would result in a dilution of the groundwater radon (Fukui, 1985). The radon in groundwater would then steadily increase back to an equilibrium concentration due to radon-in-growth before being diluted again in response to the next recharge event. Three aquifer behavioural characteristics were defined and differentiated based on the rate at which groundwater is recharged from the surface water. Where the measured radon activity concentration dropped rapidly after a rainfall event, this was interpreted as rapid and direct recharge. These groundwaters are considered sustainable so long as the current rainfall patterns (amount and distribution) remains constant and does not change in response to climate change. Older groundwaters require the application of additional isotopic tracers to identify the sustainability of the aquifer. As radon reaches secular equilibrium after 20-25 days, only zones of active groundwater circulation and regular atmospheric interaction are zones of interest in radon studies (Grolander, 2009).

Key Objective Three: To understand the relationship between groundwater ^{222}Rn activity and recharge and its bearing on sustainable groundwater management.

With a short half-life of 3.8 days, the decay and production of ^{222}Rn reaches an equilibrium state after around 20 - 25 days. This implies that groundwater being directly recharged by individual precipitation events, will see a drop in the radon activity concentration but that after ~ a month, this signal will have been removed. Therefore, where recharge takes longer than ~ one month to reach a sampling location, no change in radon activity concentration would be detected. However, it was found that groundwater that responded rapidly to recharge was associated with high ^{14}C activities implying young residence times, whilst groundwater that did not respond to recharge and had stable radon activity concentrations was associated with much lower ^{14}C activities implying older residence times. Although ^{14}C activities provide a reasonably clear indication of whether groundwater is young (actively recharged) or old (not actively recharged), the acquisition of ^{14}C data is time-consuming, expensive and not easily accessible. The data presented here on radon activity concentrations suggests that determining radon activity concentrations in groundwater before and after precipitation events may be a viable proxy for 14C and hence the residence time of the groundwater. Thus, radon activity concentrations can be used to assess residence times and hence groundwater sustainability. The application of radon in groundwater has not been applied in groundwater in this way in South Africa. The results presented here are of vital importance in understanding the recharge dynamics in groundwater especially in an arid country such as South Africa where the groundwater systems are

not fully understood. The application of radon in groundwater introduces a new approach to groundwater management.

5.2. FURTHER RECOMMENDATIONS

The hydrochemical characterisation of groundwater samples may have been improved by boreholes having a take-off point for sampling, prior to the water going into the water storage tanks and the irrigation system. Furthermore, the groundwater hydrochemical characterisation may be improved by utilising an EC profiling and borehole screening process in order to obtain the information about the aquifer under investigation. Borehole parameters such as depth and surrounding geology should be recorded and easily recoverable.

The application of radon for delineating groundwater recharge may be improved by a number of factors. In this study, no precipitation samples were taken to assess atmospheric radon concentrations. Radon was assumed to be negligible based on atmospheric data from Cape Point (Botha et al., 2018). However, for future work, setting up rainfall gauges to quantify radon in precipitation would help clarify the input radon associated with recharge. In this study, analyses were taken twice weekly. Although daily samples may help to evaluate finer temporal resolution, the 9-hour analysis window makes this challenging. However, twice a week or weekly measurements over a longer period (2-6 months) could be done to better quantify the variation in the radon activity. Pre-existing boreholes may be used, however an in-depth knowledge about the aquifer and the host lithology would contribute to the understanding the radon activities attained. For more conclusive results, a physical tracer (organic dyes) should be applied in conjunction with radon to observe the flow path of the recharge through the aquifer.

CHAPTER 6: REFERENCES

Adelana, S., Xu, Y., 2006. Contamination and protection of the Cape Flats Aquifer, South Africa, in: Groundwater Pollution in Africa. Taylor and Francis/Balkema, pp. 265–277.

Adelana, S., Xu, Y., Vrbka, P., 2010. A conceptual model for the development and management of the Cape Flats Aquifer, South africa. Water SA 36, 461–474.

Akawwi, E., 2014. Radon-222 Concentrations in the Groundwater along Eastern Jordan Rift. Journal of Applied Sciences 14, 309–316.

Akerblom, G., Lindgren, J., 1997. Mapping of groundwater radon potential. Uranium Exploration Data and Techniques Applied to the Preparation of Radioelement Maps (IAEA-TECDOC-980, IAEA, Vienna) 29, 237–255.

Belcher, R.W., Kisters, A.F.M., 2003. Lithostratigraphic correlations in the western branch of the Pan-African Saldania Belt, South Africa : the Malmesbury Group revisited. Geological Society of South Africa 106, 327–342.

Benhin, J.K.A., 2015. Climate change and South African agriculture: Impacts and adaptation options. Centre for Environmental Economics and Policy in Africa (CEEPA) 21, 1–114.

Blackburn, R., Al-Masri, M.S., 1993. Determination of radon-222 and radium-226 in water samples by Cerenkov counting. The Analyst 118, 873–876.

Blake, D., Mlisa, A., Hartnady, C., 2010. Large scale quantification of aquifer storage and volumes from the Peninsula and Skurweberg Formations in the southwestern Cape. Water SA 36, 177–184.

Booth, P.W.K., Brunsdon, G., Shone, R.W., 2004. A duplex model for the Eastern Cape Fold Belt? Evidence from the Palaeozoic Witteberg and Bokkeveld Groups (Cape Supergroup), near Steytlerville, South Africa. Gondwana Research 7, 211–222.

Botai, C.M., Botai, J.O., Adeola, A.M., 2018. Spatial distribution of temporal precipitation contrasts in South Africa. South African Journal of Science 114, 1–9.

Botha, R., Labuschagne, C., Williams, A.G., Bosman, G., Brunke, E.G., Rossouw, A., Lindsay, R., 2018. Characterising fifteen years of continuous atmospheric radon activity observations at Cape Point (South Africa). Atmospheric Environment 176, 30–39.

Bovolo, C.I., Parkin, G., Sophocleous, M., 2009. Groundwater resources, climate and vulnerability. Environmental Research Letters 4, 1–4.

Boyer, P., 2018. Geohydrology around the Breede River at the Witsand municipal water supply

borehole (Unpublished). Groundwater complete 1–10.

Brown, C., Colvin, C., Hartnady, C., Hay, R., le Maitre, D., Riemann, K., 2003. Ecological and Environmental Impacts of Large-scale Groundwater Development in the Table Mountain Group (TMG) Aquifer System. Report to Water Research Commission of South Africa K5/1327, 1–40.

Brunsdon, G., Booth, P.W.K., 2009. Faulting of the Witteberg Group Rocks, Steytlerville, Eastern Cape. 11th SAGA Biennial Technical Meeting and Exhibition 1, 500–505.

Cable, J.E., Burnett, W.C., Chanton, J.P., Weatherly, G.L., 1996. Estimating groundwater discharge into the northeastern Gulf of Mexico using radon-222. Earth and Planetary Science Letters 144, 591–604.

Calow, R.C., Robins, N.S., Macdonald, A.M., Macdonald, D.M.J., Gibbs, B.R., Orpen, W.R.G., Mtembezeka, P., Andrews, A.J., Appiah, S.O., Robins, N.S., Macdonald, A.M., Macdonald, D.M.J., 1997. Groundwater Management in Drought-prone Areas of Africa. Water resources development 13, 241–261.

Celle-Jeanton, H., Gonfiantini, R., Travi, Y., Sol, B., 2004. Oxygen-18 variations of rainwater during precipitation: Application of the Rayleigh model to selected rainfalls in Southern France. Journal of Hydrology 289, 165–177.

Choubey, V.M., Bartarya, S.K., Saini, N.K., Ramola, R.C., 2001. Impact of geohydrology and neotectonic activity on radon concentration in groundwater of intermontane Doon Valley, Outer Himalaya, India. Environmental Geology 40, 257–266.

Colvin, C., Riemann, K., Brown, C., Maitre, D. Le, Mlisa, A., Blake, D., Aston, T., Maherry, A., Engelbrecht, J., Pemberton, C., Magoba, R., Soltau, L., Prinsloo, E., 2003. Ecological and Environmental Impacts of Large-scale Groundwater Development in the Table Mountain Group (TMG) Aquifer System. Report to Water Research Commission of South Africa K5/1327, 170.

Conrad, J., Smit, L., Murray, K., van Gend-Muller, J., 2019. The Malmesbury Group - an aquifer of surprising significance. Geological Society of South Africa 122, 331–342.

Cook, P.G., Favreau, G., Dighton, J.C., Tickell, S., 2003. Determining natural groundwater influx to a tropical river using radon , chlorofluorocarbons and ionic environmental tracers. Journal of Hydrology 277, 74–88.

Cotter, E., 2000. Depositional setting and cyclic development of the lower part of the Witteberg Group (Mid- to Upper Devonian), Cape Supergroup, Western Cape, South Africa. South African Journal of Geology 103, 1–14.

Coursol, N., Lagoutine, F., Duchemin, B., 1990. Evaluation of non-neutron nuclear data for the uranium-238 decay chain. Nuclear Inst. and Methods in Physics Research 286, 589–594.

Craig, H., 1961. Isotopic Variations in Meteoric Waters. Science, New Series 133, 1702–1703.

Cumberland, S.A., Douglas, G., Grice, K., Moreau, J.W., 2016. Earth-Science Reviews Uranium mobility in organic matter-rich sediments : A review of geological and geochemical processes. Earth Science Reviews 159, 160–185.

Da Silva, L.C., Gresse, P.G., Scheepers, R., McNaughton, N.J., Hartmann, L.A., Fletcher, I., 2000. U-Pb SHRIMP and Sm-Nd age constraints on the timing and sources of the Pan-African Cape Granite Suite, South Africa. Journal of African Earth Sciences 30, 795–815.

De Beer, C., 2002. The stratigraphy, lithology and structure of the Table Mountain Group. A Synthesis of the Hydrogeology of the Table Mountain Group–Formation of a Research Strategy. WRC Report No. TT, 158(01), 9–18.

Diamond, R., 2014. Stable Isotope Hydrology of the Table Mountain Group. PhD. Unpublished.

University of Cape Town.

Diamond, R., 1997. Stable isotopes of the Thermal springs of the Cape Fold belt. MSc. Unpublished. University of Cape Town.

Diamond, R.E., Harris, C., 2000. Oxygen and hydrogen isotope geochemistry of thermal springs of the Western Cape , South Africa : recharge at high altitude? Journal of African Earth Sciences 31, 487–481.

Dickson, B.., 1990. Radium in groundwater. The environmental behaviour of radium 1, 335–365.

Du Toit, A.., 1954. The Geology of South Africa, in: 3rd Ed. Oliver and Boyd, Edinburgh, p. 611.

Duggal, V., Mehra, R., Rani, A., 2013. Determination of 222Rn level in groundwater using a RAD7 detector in the bathinda district of Punjab, India. Radiation Protection Dosimetry 156, 239–245.

Durridge, 2018. Electronic Radon Detector (Unpublished). p. 95.

DWAF, 2003. Breede river basin study, groundwater assesment. Department of Water Affairs and Forestry, South Africa. No. PH 00/, 103.

Edsfeldt, C., 2001. The radium distribution in some swedish soils and its effect on radon emanation. PhD. Unpublished. Royal Institute of Technology Stockholm, Sweden.

Fleischer, R., 1980. Isotopic Disequilibrium of Uranium : Alpha-Recoil Damage and Preferential Solution Effects. Science, New Series 207, 979–981.

Freyer, K., Treutler, H.C., Dehnert, J., Nestler, W., 1999. Determination of 222Rn in Groundwater - Recent Applications for the Investigation of River Bank Infiltration. International Symposium on Isotope Techniques in Water Resources Development and Management 29, 17–18.

Frimmel, H.E., Basei, M.A.S., Correa, V.X., Mbangula, N., 2013. A new lithostratigraphic subdivision and geodynamic model for the Pan-African western Saldania Belt, South Africa. Precambrian Research 231, 218–235.

Fukui, M., 1985. 222Rn concentrations and variations in unconfined groundwater. Journal of Hydrology 79, 83–94.

Gat, J.R., 1996. Oxygen and Hydrogen Isotopes in the Hydrologic Cycle. Annual Review of Earth and Planetary Sciences 24, 225–262.

Gerber, A., 1981. A digital model of groundwater flow in the Cape Flats. CSIR Contract Report C WaT 46, 1–10.

Gleeson, T., Befus, K.M., Jasechko, S., Luijendijk, E., Cardenas, M.B., 2015. The global volume and distribution of modern groundwater. Nature geoscience 9, 161–167.

Grolander, S., 2009. Radon as a groundwater tracer in Forsmark and Laxemar. Swedish Nuclear Fuel and Waste Management Co Box 41, 55.

Hälbich, I.W., Fitch, F.J., Miller, J.A., 1983. Dating the Cape orogeny. The Geological Society of South Africa; Johannesburg (South Africa) 17, 184.

Harilall, Z., 2020. Noble gas and radiocarbon constraints on the residence times of the groundwater in and around the City of Cape Town. MSc. Unpublished. Stellenbosch University.

Hartnady, C., Hay, R., 2002a. Potential of TMG Aquifers and Integration Into Catchment Water Management. A Synthesis of the Hydrogeology of the Table Mountain Group-formation of a Research Strategy. WRC report. No. TT 158, 242.

Hartnady, C., Hay, R., 2002b. Groundwater Prospecting on Verlorenvalley 334, Between Ceres and Touws River, Western Cape, South Africa. The need for Appropriate Research of the Table Mountain Group Aqufer systems 158, 188.

Hay, R., Mcgibbon, D., Botha, F., Riemann, K., 2015. Cape Flats Aquifer and False Bay - Opportunities to change (Unpublished). Umvoto Africa 1–16.

Hazen, R.., Ewing, R.., Sverjensky, D.A., 2009. Evolution of uranium and thorium minerals. American Mineralogist, 94, 1293–1311.

Herczeg, A.L., Simpson, J.H., Anderson, R.F., Trier, R.M., Mathieu, G.G., Deck, B.L., 1988. Uranium and Radium mobility in groundwaters and brines within the Delaware basin, southeastern New Mexico. Chemical geology 72, 181–196.

Higgins, F.B., Grune, W.N., Smith, B.M., James, G., Jr, T., Journal, S., Water, A., Association, W., January, N., Jr, F.B.H., Grune, W.N., 1961. Methods for Determining Radon-222 and Radium-226. American Water Works Association 53, 63–74.

Hiller, N., Dunlevey, J.N., 1978. The Bokkeveld-Witteberg boundary in the Montagu-Touws River area, Cape Province. Transactions of the Geological Society of South Africa 81, 101–104.

Hobbs, P.., Lindsay, R., Maherry, A., Matshaya, M., Newman, R.T., Talha, S.., 2010. The use of 222Rn as a hydrological tracer in Natural and polluted enviroments. WRC Report 1685, 1–96.

Hoehn, E., Von Gunten, H.R., 1989. Radon in groundwater: A tool to assess infiltration from surface waters to aquifers. Water Resources Research 25, 1795–1803.

Hounslow, A., 1995. Water Quality Data Analysis and interpretation, in: Press, C. (Ed.), . p. 416.

Jaffey, A.H., Flynn, K.F., Glendenin, L.E., Bentley, W.C., Essling, A.M., 1971. Precision measurement of half-lives and specific activities of U235 and U238. Physical Review C 4, 1889–1906.

Jia, H., 2007. Groundwater Resource Evaluation in Table Mountain Group Aquifer Systems. PhD. Unpublished. The University of the Western Cape.

Johnson, M.., Anhaeusser, C.R., Thomas, R.J., 2006. The Geology of South Africa. Council for Geoscience.

Jolly, L., 2002. “Sustainable use of Table Mountain Group aquifers and problems related to scheme failure.” A synthesis of the hydrogeology of the table mountain group–formation of a research strategy. WRC Report No. TT 158, 108–11.

Jolly, L., Kotze, J.C., 2002. The Klein Karoo rural water supply scheme. A Synthesis of the Hydrogeology of the Table Mountain Group-formation of a Research Strategy. WRC report. No. TT 158, 198.

Jones, J.A.A., 1999. Climate change and sustainable water resources : placing the threat of global warming in perspective. Hydrological Sciences Journal 44, 541–557.

Kahinda, J.M., Taigbenu, A.E., Boroto, R.J., 2010. Domestic rainwater harvesting as an adaptation measure to climate change in South Africa. Physics and Chemistry of the Earth 35, 742–751.

Khan, R.., Khazanchi, B., Miglani, T., Mahadevan, T., 1979. Regional hydrogeochemical investigations for uranium in the Siwalik belt of Himachal Pradesh and Punjab. Himal Geol 9, 773–785.

Kingsley, C.S., 1969. A new stratigraphic classifcation implying a lithofacies chnage in the Table Mountain sanstine in southern Natal. Transactions of the Geological Society of South Africa 78, 43–55.

Kisters, A., Belcher, R.W., Scheepers, R., Rozendaal, A., Jordaan, L.S., 2002. Timing and kinematics of the Colenso Fault: The Early Paleozoic shift from collisional to extensional tectonics in the Pan-Africa. South African Journal of Geology 105, 257–270.

Kisters, A.F.M., Agenbach, C., Frei, D., 2015. Age and tectonic significance of the volcanic Bloubergstrand member in the pan-African Saldania Belt, South Africa. South African Journal of Geology 118, 213–224.

Konikow, L.F., Kendy, E., 2005. Groundwater depletion: A global problem. Hydrogeology Journal 13, 317–320.

Kortatsi, B.K., 2006. Hydrochemical characterization of groundwater in the Accra plains of Ghana. Environmental Geology 50, 299–311.

Kotze, J.C., 2002. Hydrogeology of the Table Mountain sandstone aquifer - Klein karoo. PhD. Unpublished. University of the Free State, Bloemfontein.

Kraemer, T.F., Genereux, D.P., 1998. Applications of Uranium- and Thorium-Series Radionuclides in Catchment Hydrology Studies, in: Isotope Tracers in Catchment Hydrology. Elsevier, pp. 679–722.

Kulongoski, J.T., Hilton, D.R., Selaolo, E.T., 2004. Climate variability in the Botswana Kalahari from the late Pleistocene to the present day. Geophyscial research letters 31, 1–5.

Kundzewicz, Z.W., Döll, P., 2009. Will groundwater ease freshwater stress under climate change? Hydrological Sciences Journal 54, 665–675.

Lin, L., Lin, H., Xu, Y., 2014. Characterisation of fracture network and groundwater preferential flow path in the Table Mountain Group (TMG) sandstones , South Africa. Water SA 40, 263–272.

Loomis, D.P., 1987. An Investigation of Radon in North Carolina Groundwater and Its Relationship to Rock Type. Groundwater monitoring and redediation 7, 1–49.

Loucks, D.P., 2000. Sustainable water resources management. Water International 25, 3–10.

Mæller, D., 1990. The Na/CL ratio in rainwater and the seasalt chloride cycle. Tellus B: Chemical and Physical Meteorology 42, 254–262.

Mason, B., Moore, C.B., 1982. Principles of geochemistry. Wiley; 4th edition, p. 344.

Meyer, P., Jonck, F., 2001. An explanation of the 1:500 000 hydrogeological map of Cape Town 3317. Department of Water Affairs and Forestry, South Africa. Water Research Commission 517, 59.

Miller, J.A., Dunford, A.J., Swana, K.A., Palcsu, L., Butler, M., Clarke, C.E., 2017. Stable isotope and noble gas constraints on the source and residence time of spring water from the Table Mountain Group Aquifer, Paarl, South Africa and implications for large scale abstraction. Journal of Hydrology 551, 100–115.

Molinari, J., Snodgrass, W., 1990. The chemistry and radiochemistry of radium and the other elements of the uranium and thorium natural decay series. International Atomic Energy Agency, Vienna (Austria); Technical Reports Series; No. 310 1, 11–59.

Mook, W.G., 2000. Environmental Isotopes in the Hydrological Cycle. Principles and applications. Technical Documents in Hydrology IAEA report 3, 1–164.

Moore, W.S., 1999. The subterranean estuary : a reaction zone of ground water and sea water. Marine Chemistry 65, 111–125.

Netili, K.., 2007. A preliminary understanding of deep groundwater flow in the Table Nountain Group (TMG) aquifer system. MSc. Unpublished. University of Western Cape.

Newton, A.., Shone, R.., Booth, P.W.., Johnson, M.., Anhaeusser, C.., 2006. The Cape Fold Belt., in: The Geology of South Africa, Johannesburg. pp. 521–528.

Pavlidou, S., Koroneos, A., Papastefanou, C., Christofides, G., Stoulos, S., Vavelides, M., 2006. Natural radioactivity of granites used as building materials. Journal of Environmental Radioactivity 89, 48–60.

Postel, S.L., 2000. Entering an era of water scarcity: The challenges ahead. Ecological Applications 10, 941–948.

Rama, Moore, W., 1984. Mechanism of transport of U-Th series radioisotopes solids into ground water. Geochimica et Cosmochimica Acta 48, 395–399.

Rosewarne, P., 2002. Hydrogeological characteristics of the Table Mountain Group aquifers. A Synthesis of the Hydrogeology of the Table Mountain Group-formation of a Research Strategy. WRC report. No. TT 158, 33–44.

Rozendaal, A., Gresse, P.G., Scheepers, R., Le Roux, J.P., 1999. Neoproterozoic to early Cambrian crustal evolution of the Pan-African Saldania Belt, South Africa. Precambrian Research 97, 303–323.

Rust, I.C., 1977. Evidence of shallow marine and tidal sedimentation in Ordovician Graafwater Formation, Cape Province,South Africa. Sediment Geology 18, 123–133.

Rust, I.C., 1973. The evolution of the Palaeozoic Cape Basin, southern margin of Africa. Nairn, A.E.M. & Stehli, F.G. (eds.) The Ocean Basins and Margins 1, 247-276.

Rust, I.C., 1967. On the sedimentation of the Table Mountain Group in the Western Cape Province. D.Sc. Unpublished. Stellenbosch University.

Saidian, M., Godinez, L.J., Prasad, M., 2016. Effect of clay and organic matter on nitrogen adsorption specific surface area and cation exchange capacity in shales (mudrocks). Journal of Natural Gas Science and Engineering 33, 1095–1106.

Schalke, H.J.W.., 1973. The upper Quaternary of the Cape Flats area, Cape Province, South Africa. Scripta Geol 15, 1–57.

Scheepers, R., 1990. Magmatic association and radioelement geochemistry of selected Cape granites with special reference to subalkaline and leucogranitic phases. PhD. Unpublished. Stellenbosch University.

Scheepers, R., Nortjé, A.N., 2000. Rhyolitic ignimbrites of the Cape Granite Suite, southwestern Cape province, South Africa. Journal of African Earth Sciences 31, 647–656.

Schumann, R.R., Gundersen, L.C.S., 1997. Geologic and climatic controls on the radon emanation coefficient. Environment International 22, 439–446.

Seckler, D., Barker, R., Amarasinghe, U., 1999. Water scarcity in the twenty-first century. International Journal of Water Resources Development 15, 29–42.

Şen, Z., 2009. Global warming threat on water resources and environment: a review. Environmental Geology 57, 321–329. https://doi.org/10.1007/s00254-008-1569-5

Siegel, M.D., Bryan, C.B., 2003. Environmental Geochemistry of Radioactive Contamination. Sandia Report 39, 114.

Skeppström, K., Olofsson, B., 2007. Uranium and radon in groundwater. European Water 17, 51–62.

Smart, M.C., Tredoux, G., 2002. Groundwater quality and fitness for use. A Synthesis of the Hydrogeology of the Table Mountain Group-formation of a Research Strategy. WRC report. No. TT 158, 118–123.

SRK, 2009. Preliminary Assessment of Impact of the Proposed Riviera Tungsten Mine on Groundwater Resources.

Steube, C., Richter, S., Griebler, C., 2009. First attempts towards an integrative concept for the ecological assessment of groundwater ecosystems 23–35. https://doi.org/10.1007/s10040-008-0346-6

Stites, J.., 1950. Separation of Radium from Uranium residues. Chemistry-radiation and radiochemistry 3, 1–35.

Stuyfzand, P.J., 2014. Predicting the effects of sea spray deposition and evapoconcentration on shallow coastal groundwater salinity under various vegetation types. Proceedings of the 23rd Salt Water Intrusion Meeting 1, 401–404.

Swana, K., 2016. Application of hydrochemistry and residence time constraints to distinguish groundwater systems in the Karoo Basin prior to shale-gas exploration. (Unpublished) MSc.

Tankard, A.J., Jackson, M.P.A., Eriksson, K.A., Hobday, D.K., Hunter, D.R., Minter, W.E.L., 1982. 3.5 Billion years of Crustal Evolution in Southern Africa. Springer Science & Business Media.

Telahigue, F., Agoubi, B., Souid, F., Kharroubi, A., 2018. Groundwater chemistry and radon-222 distribution in Jerba Island, Tunisia. Journal of Environmental Radioactivity 182, 74–84.

Thamm, A.G., Johnson, M.R., Anhaeusser, C.R., Thomas, R.J., 2006. The cape supergroup. The Geology of South Africa, 443-460.

Theron, J, N., 1972. The stratigraphy and sedimentation of the Bokkeveld Group. (Unpublished) MSc, in: Stellenbosch University. pp. 1–278.

Tye, A.M., Milodowski, A.E., Smedley, P.L., 2017. Distribution of natural radioactivity in the environment., British Geological Survey Internal Report.

UNESCO, 1998. Sustainability criteria for water resource systems. Cambridge University Press M.VI.

United Nations, U., 2018. World Urbanization Prospects. Demographic Research 12, 197–236.

Uosif, M.A.M., Issa, S.A.M., Abd El-Salam, L.M., 2015. Measurement of natural radioactivity in granites and its quartz-bearing gold at El-Fawakhir area (Central Eastern Desert), Egypt. Journal of Radiation Research and Applied Sciences 8, 393–398.

USDA, 2011. Soil Health Quality Indicators: chemical Properties- EC (Unpublished). p. 3.

Vaux, H., 2011. Groundwater under stress : the importance of management. Environmental Earth Sciences 62, 19–23.

Virk, H.., Singh, B., 1993. Radon anomalies in soil gas and groundwater as a earthquake precursor phenomena. Tectonophysics 227, 215–224.

Visser, J.N.J., 1974. The Table Mountain Group: A study in the deposition of quartz arenites on a stable shelf. Transactions of the Geological Society of South Africa 77, 229–237.

Voronov, A.N., 2003. Radon-rich waters in Russia. Environmental Geology 46, 630–634.

Vorosmarty, C.J., Leveque, C., Revenga, C., Bos, R., Caudill, C., 2005. Fresh Water, in: In Terrestrial Environments. pp. 171–186.

Wanty, R.B., Nordstrom, D.K., 1993. Natural radionuclides., in: Regional Ground-Water Quality: New York, Van Nostrand Reinhold. pp. 423-441.

Weaver, J.. M.., 2002. Hydrogeology of the Table Mountain Group. A Case Study at Botrivier. Water Research Commission 155–160.

Weaver, J.M.C., Talma, A.S., Cave, L.C., 1999. Geochemistry and isotopes for resource evaluation in the fractured rock aquifers of the Table Mountain Group. Water Research Commission 481, 1–121.

Whittingham, J.K., 1987. Palaeozoic geology of Steytlerville- Klipplaat-Kirkwood-Paterson area, Eastern Cape. Geological Survey South Africa Report 198, 37.

Xu, Y., Lin, L., Jia, H., 2009. Groundwater Flow Conceptualization and Storage Determination of the Table Mountain Group (TMG) Aquifers. Water Research Commission 9, 1–268.

CHAPTER 7: APPENDICES

7.1. APPENDIX 1

Table 10 - Summary of all the replicated data sets during 12-week resampling season.

	Day	Date	Sample Number	Location	222Rn (Bq/L)	222Rn Uncert.
Rainfall on the 29th-31st of July (38mm) 5th-7th August (35 mm) -Stellenbosch-						
WEEKONE						
Sample collected just after rainfall, rest of the week no rain	Tuesday	13 08 2019	YAD19SVRD001	Paarl	6.45	0.9
		13 08 2019	YAD19SWRD001	Somerset W	97.3	5.8
		13 08 2019	YAD19OHRD001	Stellenbosch	12.5	1.7
		13 08 2019	YAD19StiasRD001	Stellenbosch	147	7.4
	Wednesday	14 08 2019	YAD19RVRD001	Paarl	208	9.1
		14 08 2019	YAD19DBRD001	Paarl	248	10
	Thursday	15 08 2019	YAD19SVRD002	Paarl	5.10	0.7
		15 08 2019	YAD19SWRD002	Somerset W	150	7.5
		15 08 2019	YAD19OHRD002	Stellenbosch	120	6.6
		15 08 2019	YAD19StiasRD002	Stellenbosch	542	17
WEEK TWO						
No rain	Tuesday	20 08 2019	YAD19SVRD003	Paarl	2.89	0.3
		20 08 2019	YAD19SWRD003	Somerset W	221	9.9
		20 08 2019	YAD19OHRD003	Stellenbosch	101	6.3
		20 08 2019	YAD19StiasRD003	Stellenbosch	525	18
		20 08 2019	YAD19DBRD002	Paarl	50.5	4.0
No rain	Thursday	22 08 2019	YAD19SVRD004	Paarl	75.3	5.1
		22 08 2019	YAD19SWRD004	Somerset W	206	9.3
		22 08 2019	YAD19OHRD004	Stellenbosch	105	6.3
		22 08 2019	YAD19StiasRD004	Stellenbosch	611	18
		22 08 2019	YAD19DBRD003	Paarl	149	7.6
No rainfall	Friday	23 08 2019	YAD19RVRD002	Paarl	47.9	3.8
WEEK THREE						
No rainfall	Tuesday	27 08 2019	YAD19SVRD005	Paarl	24.7	2.6
		27 08 2019	YAD19SWRD005	Somerset W	211	9.3
		27 08 2019	YAD19OHRD005	Stellenbosch	125	7.0

	Day	Date	Sample Number	Location	222Rn (Bq/L)	222Rn Uncert.
		27 08 2019	YAD19StiasRD005	Stellenbosch	776	21
		27 08 2019	YAD19DBRD004	Paarl	48.8	3.9
		27 08 2019	YAD19RVRD003	Paarl	212	9.9
No rainfall	Thursday	29 08 2019	YAD19SVRD006	Paarl	21.7	2.6
		29 08 2019	YAD19SWRD006	Somerset W	171	8.2
		29 08 2019	YAD19OHRD006	Stellenbosch	109	6.3
		29 08 2019	YAD19StiasRD006	Stellenbosch	606	18.6
		29 08 2019	YAD19DBRD005	Paarl	159	7.7
Pre-Rain Samples						
No rainfall	Tuesday	10 09 2019	YAD19SWRD007	Somerset W	217	9.2
		10 09 2019	YAD19NFSRD001	Franschhoek	291	12
No rainfall	Wednesday	11 09 2019	YAD19DBRD006	Paarl	122	6.5
		11 09 2019	YAD19LMRD002	Franschhoek	15.5	2.3
		11 09 2019	YAD19COETRD001	Stellenbosch	55.4	2.9
		11 09 2019	YAD19RVRD4	Paarl	134	7.0
Heavy rainfall Thursday (12 Sept 2019)						
WEEKONE						
No rainfall	Monday	16 09 2019	YAD19LMRD003	Franschhoek	92.8	5.6
		16 09 2019	YAD19NFSRD002	Franschhoek	329	12
		16 09 2019	YAD19SWRD008	Somerset W	314	10
		16 09 2019	YAD19RVRD005	Paarl	163	7.3
		16 09 2019	YAD19DBRD007	Paarl	158	7.1
No rainfall	Wednesday	18 09 2019	YAD19LMRD004	Franschhoek	112	6.2
		18 09 2019	YAD19NFSRD003	Franschhoek	271	11
		18 09 2019	YAD19CoetRD002	Stellenbosch	88.5	6.0
		18 09 2019	YAD19DBRD008	Paarl	141	7.4
		18 09 2019	YAD19SWRD009	Somerset W	265	9.3
Rainfall on the 21th September (8mm) -Stellenbosch-						
WEEKTWO						
No rainfall	Monday	23 09 2019	YAD19LMRD005	Franschhoek	57.3	4.3
		23 09 2019	YAD19NFSRD004	Franschhoek	329	12
		23 09 2019	YAD19SWRD010	Somerset West	161	7.9
		23 09 2019	YAD19CoetRD003	Stellenbosch	81.5	5.1
		23 09 2019	YAD19DBRD009	Paarl	126	6.3
No rainfall	Wednesday	25 09 2019	YAD19LMRD006	Franschhoek	105	6.0
		25 09 2019	YAD19NFSRD005	Franschhoek	278	11
		25 09 2019	YAD19SWRD011	Somerset W	262	9.3
		25 09 2019	YAD19CoetRD004	Stellenbosch	79.9	5.1
		25 09 2019	YAD19DBRD010	Paarl	118	6.1
	Friday	27 09 2019	YAD19RVRD006	Paarl	119	6.5
WEEK THREE						
No rainfall	Monday	30 09 2019	YAD19LMRD007	Franschhoek	102	5.9
		30 09 2019	YAD19NFSRD006	Franschhoek	267	9.3
		30 09 2019	YAD19SWRD012	Somerset W	350	11
		30 09 2019	YAD19CoetRD005	Stellenbosch	102	5.8
		30 09 2019	YAD19DBRD011	Paarl	161	7.1
No rainfall	Wednesday	02 10 2019	YAD19LMRD008	Franschhoek	185	8.3
		02 10 2019	YAD19NFSRD007	Franschhoek	353	11
		02 10 2019	YAD19SWRD013	Somerset W	369	11
		02 10 2019	YAD19CoetRD006	Stellenbosch	99.2	5.7

	Day	Date	Sample Number	Location	222Rn (Bq/L)	222Rn Uncert.
		02 10 2019	YAD19DBRD012	Paarl	158	7.1
WEEK FOUR						
No rainfall	Wednesday	09 10 2019	YAD19DBRD013	Paarl	144	6.6
		09 10 2019	YAD19LMRD009	Franschhoek	119	6.1
		09 10 2019	YAD19NFSRD008	Franschhoek	340	11
		09 10 2019	YAD19SWRD014	Somerset W	299	10
No rainfall	Thursday	10 10 2019	YAD19RVRD007	Paarl	171	7.3
		10 10 2019	YAD19CoetRD007	Stellenbosch	87.5	5.2
	Tuesday	15 10 2019	YAD19RVRD008	Paarl	152	6.6
Rainfall on the 25th October(32mm) -Stellenbosch-						
WEEK ONE						
No rainfall	Tuesday	22 10 2019	YAD19DBRD014	Paarl	168	7.2
		22 10 2019	YAD19NFSRD009	Franschhoek	364	11
		22 10 2019	YAD19Aquelle001	Franschhoek	58.2	4.4
		22 10 2019	YAD19CoetRD009	Stellenbosch	87.9	5.2
		22 10 2019	YAD19StiasRD007	Stellenbosch	561	14
WEEK TWO						
Rainfall on the 25th October (34.5mm) and 27-28 Oct (39 mm)- Stellenbosch -	Tuesday	29 10 2019	YAD19CoetRD010	Stellenbosch	84.1	5.1
		29 10 2019	YAD19StiasRD008	Stellenbosch	389	11
		29 10 2019	YAD19DBRD015	Paarl	156	7.0
		29 10 2019	YAD19NFSRD010	Franschhoek	394	12
		29 10 2019	YAD19Aquelle002	Franschhoek	40.7	3.7
No rainfall	Friday	01 11 2019	YAD19DBRD016	Paarl	164	7.2
		01 11 2019	YAD19NFSRD011	Franschhoek	348	11
		01 11 2019	YAD19Aquelle003	Franschhoek	28.1	3.0
		01 11 2019	YAD19CoetRD011	Stellenbosch	81.8	5.0
		01 11 2019	YAD19StiasRD009	Stellenbosch	431	12
WEEK THREE						
No rainfall	Tuesday	05 11 2019	YAD19DBRD017	Paarl	178	7.7
		05 11 2019	YAD19NFSRD012	Franschhoek	342	11
		05 11 2019	YAD19Aquelle004	Franschhoek	30.1	3.1
		05 11 2019	2YAD19CoetRD011	Stellenbosch	79.0	4.9
		05 11 2019	YAD19StiasRD010	Stellenbosch	565	14
No rainfall	Friday	08 11 2019	YAD19DBRD018	Paarl	159	7.0
		08 11 2019	YAD19NFSRD013	Franschhoek	349	11
		08 11 2019	YAD19Aquelle005	Franschhoek	30.8	3.4
		08 11 2019	2YAD19CoetRD012	Stellenbosch	90.5	5.3
		08 11 2019	YAD19StiasRD011	Stellenbosch	698	16
WEEK THREE						
No rainfall	Tuesday	12 11 2019	YAD19DBRD018	Paarl	162	7.1
		12 11 2019	YAD19NFSRD014	Franschhoek	339	11
		12 11 2019	YAD19Aquelle005	Franschhoek	26.5	3.0
		12 11 2019	YAD19CoetRD014	Stellenbosch	111	6.1
		12 11 2019	YAD19StiasRD012	Stellenbosch	626	15

7.2. APPENDIX 2

Table 11 - pMC for groundwater samples presented in this study, plot derived from Harilall (2020)

Sample number	Lithology	pMC	Std dev	Corrected pMC
YAD018Ra222-01	Quarternary	110	0.35	119
YAD018Ra222-02	Quarternary	103	0.35	105
YAD018Ra222-04	Quarternary			
YAD018Ra222-05	Quarternary			
YAD018Ra222-06	Quarternary			
YAD19TK001	Quarternary			
YAD19TK002	Quarternary			
YADKR001	Quarternary	84	0.50	102
YAD18Cer001	Bokkeveld	23.1	0.11	80.0
YAD18BD001	Bokkeveld	62.1	0.19	86.1
YAD18MON001	Bokkeveld	55.5	0.18	54.1
YAD18RivFarm001	Granite	101.	0.36	101
YADKB001	Granite	93.6	0.35	105
YADKB002	Granite			
YAD18SW001	Granite	102	0.24	103
YAD18SW002	Granite	102	0.25	102
YAD19Frans003	Granite	86.6	0.21	102
YAD18Frans002	Granite	26.7	0.11	30.1
YAD18SVL001	Malmesbury	32.6	0.22	25.0
YAD18PV001	Malmesbury	59.6	0.18	60.8
YAD18ROB002	Malmesbury	39.9	0.17	40.8
YAD18DB001	Malmesbury			
YAD18DB005	Malmesbury			
YAD19PAA001	Malmesbury	31.3	0.17	30.8
YAD18DB002	TMG			
YAD18DB003	TMG			
YAD18DB004	TMG			
YAD19Cer002	TMG	94.3	0.22	102
YAD18JH001	TMG			
YAD18JH002	TMG			
YAD18DD001	TMG	100	0.23	101
YAD18DD002	TMG	99.5	0.24	99.5
YAD18BD002	TMG	91.8	0.21	100
YAD18Vill001	TMG	97.4	0.22	101
YAD18Frans001	TMG	96.6	0.23	100
YAD19MP001	TMG			
YAD19NW001	TMG			
YAD19TM001	TMG			
YAD19SprFrans001	TMG			
YAD19Vills002	TMG	93.2	0.22	106
YAD19Vills003	TMG	81.4	0.29	81.7
YAD19GB001	TMG			
YAD19KM001	TMG			
YAD19KM002	TMG	99.4	0.49	115
YAD19Kmond001	TMG			
YAD19Kmond002	TMG			
YAD19Kmond003	TMG			
YAD18ROB001	Witteberg	11.4	0.09	43